UNIVERSITÁ DEGLI STUDI DI PADOVA

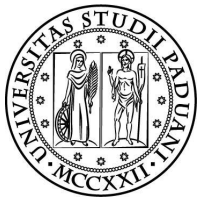

DIPARTIMENTO DI FISICA E ASTRONOMIA
"GALILEO GALILEI"
Corso di Laurea in Fisica

Tesi di Laurea Magistrale

Primordial Non-Gaussianity and Cosmic Microwave Background Anomalies

Relatore
Dr. Nicola Bartolo

Laureando
Lorenzo Bordin

Anno Accademico 2013/2014

Primordial non-Gaussianity and Cosmic Microwave Background Anomalies

Abstract: The analyses of the recent *Planck* satellite data have confirmed some of the (large-scale) "anomalies" in the Cosmic Microwave Background observed by the WMAP satellite at a similar level of significance (while others have been strongly constrained). Among these anomalies there is the so called hemispherical asymmetry in power between the "northern" and "southern" hemispheres. The *Planck* satellite has provided also the tightest constraints on primordial non-Gaussianity predicted by various early universe (inflationary) models. The goal of this Thesis is to investigate possible connections between CMB anomalies and primordial non-Gaussianity from various points of view, ranging from models of the early Universe with non-Gaussian signatures which can give rise to such anomalies, to new predictions for the models already proposed.

Notation and convention

In this thesis we work in natural units

$$\hbar = c = 1.$$

Our metric signature is $(-+++)$. Greek indices take the values $\mu, \nu = 0, 1, 2, 3$ and Latin indices stand for $i, j = 1, 2, 3$. For conformal time we use the letter τ and derivatives with respect to conformal time are indicated with a prime '. The conformal time is related to cosmic time t by $dt = a\, d\tau$ where a is the scale factor. Our convention for the Fourier transform is

$$f(\mathbf{x}) = \int \frac{d^3k}{(2\pi)^3} e^{-i\mathbf{kx}} f(\mathbf{k}).$$

Repeated indices are always summed over, unless otherwise specified. Newton gravitational constant G is used to define the reduced Planck mass $M_{Pl} = (8\pi G)^{-1/2}$.

Contents

Introduction

The birth of modern cosmology was possible only with the coming of the 20^{th} century, when Einstein formulated the theory of General Relativity. This is because through such a theory the laws of gravity can be properly accommodated within a cosmological context. Together with Einstein equations of gravity another ingredient upon which cosmological inferences are based on is the *cosmological principle*, which states that the Universe looks the same in all directions and in every place. Starting from them, cosmologists were able to build up the modern cosmological model, the so called Inflation+ΛCDM (Lambda Cold Dark Matter) model which provides the best description of the history of the Universe up to now.

In the ΛCDM model the content of the Universe is dominated at the present epoch by Dark Energy, parametrized as a cosmological constant Λ and Cold Dark Matter (CDM). Moreover the model assumes General Relativity as the correct theory of gravity valid on cosmological scales.

The Dark Energy component is commonly associated with a vacuum energy that explains the present accelerating expansion of the Universe against the attractive effects of gravity as confirmed by various cosmological observations. A cosmological constant has negative pressure, $P = -\rho$, which contributes to the total stress-energy tensor that, according to General Relativity, causes an accelerating expansion, [19]. At present, Dark Energy should dominate the energy density of the Universe being 67% of the total energy density.

The other main component of the current Universe is the Cold Dark Matter (CDM), a form of pressureless matter introduced in order to account for gravitational effects observed in the cosmological structures that cannot be accounted by the quantity of observed (baryonic) matter. Dark matter is described as being cold [1], non-baryonic and at most weakly interacting and should constitute 26% of the total energy density.

Ordinary matter which includes all the observable structures of the Universe fills almost all the remaining fraction of the Universe content (including baryons, photons[2] and neutrinos).

[1] Namely the CDM particles are non-relativistic at the epoch of its decoupling from ordinary matter.

[2] Mainly from the Cosmic Microwave Background.

This model provides a very good account of the observed properties of the Universe on cosmological scales, like the temperature and polarization anisotropies of the Cosmic Microwave Background (CMB), the Large Scale Structures (LSS) in the distribution of galaxies, the abundances of light elements (Hydrogen, Helium, and Lithium), and the accelerating expansion of the Universe. All the structures of the Universe arose from the initial conditions of the ΛCDM model. Inflation provides an explanation for the generation of the primordial density perturbations, namely the initial conditions.

The ΛCDM model is characterized by just six parameters. Four of them describe the "late time" evolution of the Universe. They can be taken as the value of the sound horizon at recombination time ($\Delta\theta^*$), the baryon density Ω_B and the CDM density Ω_c. The fourth suitable parameter is the optical depth τ , such that $e^{-\tau}$ is the probability that a photon emitted before reionization (but after photon decoupling) re-scatters. To describe the primordial perturbations (the initial seeds) we need two more parameters, specifying the normalization of the power spectrum A_s of the primordial density perturbations and the spectral index n_s (which describes the shape of the power spectrum).

Parameters	*Planck* (CMB + lensing)
$\Omega_b h^2$	0.02205 ± 0.00028
$\Omega_c h^2$	0.1199 ± 0.0027
$100\Delta\theta_*$	1.04147 ± 0.00062
$\ln(10^{10} A_s)$	$3.089^{+0:024}_{0.027}$
n_s	0.9585 ± 0.0070
τ	0.089 ± 0.032
H_0 $(Km\,s^{-1}\,Mpc^{-1})$	67.3 ± 1.2
Ω_Λ	0.639 ± 0.019
z_*	1090.43 ± 0.54
t_0 (Gyr)	13.796 ± 0.058
z_{eq}	3391 ± 60

Table 1: Above: the values of the 6 cosmological parameters obtained fitting the *Planck* data [69] with the ΛCDM model. Below: other cosmological parameters derived from the six parameters: H_0 is value the Hubble rate at present time, Ω_Λ the ratio of the cosmological density to the total energy density, z_* the redshift at recombination in the inflationary scenario (when CMB photons decoupled from ordinary matter), t_0 the age of the Universe and z_{eq} the redshift at the time of equivalence, namely when the density the matter energy density became equal to the radiation energy density.

At very early times a quasi-de Sitter accelerated expansion, driven by a

scalar field, solves the open problems left by the Hot-Big-Bang model, namely the horizon, the flatness and the magnetic monopole problems. However inflation has become so crucial in modern cosmology because it gives a natural explanation of the origin of both the CMB and the LSS.

Because of the accelerated expansion, during inflation, the causal horizon [3] decreases, then, when inflation ends it starts to grow. In fact, during the inflationary epoch some quantum fluctuations, with proper length λ, are produced on microscopic scales. These primordial perturbations are then stretched on cosmological scales, in this way, the accelerated expansion and primordial density fluctuations of all sizes, also grater than the causal horizon are generated. After inflation, the inflaton decays into relativistic particles and the usual radiation and matter dominated epochs take place. In particular the Universe contains CMB photons and baryons tightly coupled together by Compton scattering. Before recombination epoch the primordial density fluctuations that are still super-horizon are frozen, while the sub-horizon ones oscillates because of the opposing action of the fluid pressure and self-gravity. Such oscillations are named CMB *acoustic oscillations*. This phenomenon continues until recombination time occurs, when electrons and protons combine together to form neutral atoms of hydrogen. Has a consequence, CMB photons decouples from ordinary matter and can travel until us. Moreover, at this epoch, begin the gravitational collapse in the matter fluid that has originated the LSS and in general all the cosmological objects we observe today.

The CMB represents one of the most important observables on the early Universe. According to the standard cosmological model its photons were created shortly after inflation when the Universe was very hot and dense. Then, until the Universe was hot enough to be ionized the photons generated at very early time were thermalized by the Compton and Thompson scattering [4]. In this way their spectrum became a perfectly blackbody one. Finally, during recombination, the Universe became transparent to photons and thus they were free to travel without significant interactions from the so called last scattering surface to us, carrying a snapshot of the primordial phases of the Universe. With the Universe expansion, the blackbody spectrum did not change its shape, anyway the photons suffered a redshift z that lowered their temperature. So the early dazzling light in the sky became a faint microwave background radiation. It bring us fundamental clues about the composition, the geometry and the evolution of the early Universe.

Many observations have been made to study the CMB, most of them focused on the detection of the temperature anisotropies, which can be linked to the primordial quantum fluctuations occurred during inflation. The first measurement of the temperature CMB anisotropies of cosmological origin

[3] The causal horizon is the maximum distance travelled by light at the considered epoch.
[4] The Thompson scattering is the non-relativistic limit of the Compton scattering.

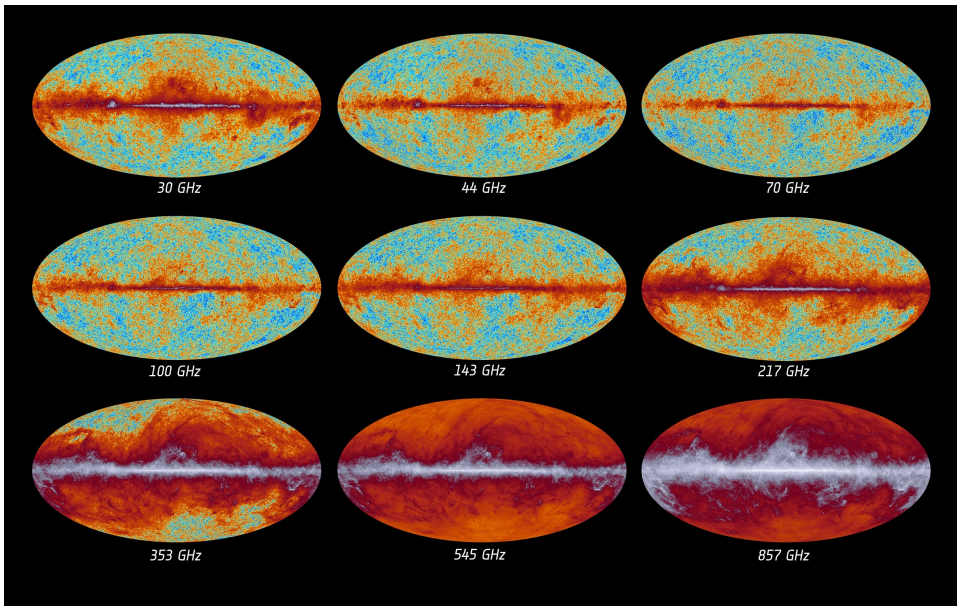

Figure 1: All-sky maps recorded by *Planck* at nine different frequencies during its first 15.5 months of observations. The Cosmic Microwave Background is most evident in the frequency bands between 70 and 217 GHz. Observations at the lowest frequencies are affected by foreground radio emission from the interstellar material in the Milky Way, which is mostly due to synchrotron radiation emitted by electrons that spiral along the lines of the Galactic magnetic field, but also comprises bremsstrahlung radiation, emitted by electrons that are slowed down in the presence of protons, as well as emission from spinning dust grains. Observations at the highest frequencies are affected by foreground emission from interstellar dust in the Milky Way.

were made by the COBE satellite [59] which recorded the first full sky map of the CMB temperature anisotropies. After it WMAP [11], [12], and finally *Planck*, [65], [66], [67], [68], [69], probed the CMB temperature anisotropies with an extremely high level of accuracy and precision. According to the theoretical predictions, all the surveys found a perfect CMB blackbody spectrum characterized by a mean temperature $T \simeq 2.7\ K$ and with very small temperature fluctuations of order $\langle \Delta T \rangle / T \sim 10^{-5}$. Such fluctuations are randomly distributed with a nearly gaussian statistics and with an high level of homogeneity and isotropy, thus confirming the predictions of inflation.

On the other hand, some "anomalous" features in the angular CMB power spectrum of the temperature anisotropies, have been observed by WMAP [11] and then confirmed by *Planck* [67], suggesting a possible violation of the symmetries of the cosmological principle (breaking of statistical homogeneity and isotropy). Various anomalies were observed: cold spots, a low quadrupole amplitude, the alignment between the quadrupole and

octupole moments and a hemispherical power asymmetry between to opposite hemispheres (the "northern" and the "southern" celestial hemispheres). These features suggest a possible violation of homogeneity and/or isotropy symmetries.

In fact, the so called *Hemisperical Power Asymmetry* (HPA), is one of the most statistically significant among these "anomalies". It consists in a different amplitude of the CMB temperature fluctuations between the "northern" and the "southern" celestial hemispheres. Such asymmetry can be modelled on the largest angular scales as a dipolar modulation of an otherwise statistically isotropic distribution

$$\frac{\Delta T}{T}(\hat{\mathbf{n}}) \equiv \theta(\hat{\mathbf{n}}) = \theta_{iso}(\hat{\mathbf{n}})\,(1 + A\hat{\mathbf{p}} \cdot \hat{\mathbf{n}})\,,$$

in which $\hat{\mathbf{p}}$ is the preferred direction in the sky, $\hat{\mathbf{n}}$ is the direction of the line of sight and A is the amplitude of asymmetry with the best fit value $A = 0.072 \pm 0.022$ for $l < 64$, [67] .

Motivated by these observations this Master thesis was born with the idea to investigate the theoretical issues implied by HPA, considering some of the early-Universe models proposed to explain an eventual HPA and trying to obtain new predictions for some of the models proposed.

The thesis is structured as follows:

- Chapter 1 contains a review of the inflationary paradigm. More in detail it describes the basics of inflation as driven by a real scalar field and the description of the origin and evolution of the quantum fluctuations that originated the primordial density perturbations.

- Chapter 2 explains the theory of cosmological perturbations in General Relativity which is a fundamental background to deal with the study of the evolution of the Universe. We paid particular attention to the study of the generation and the evolution of the curvature and the tensor perturbation fields. In fact, during inflation, primordial gravitational waves (tensor modes) are inevitably generated.

- Chapter 3 introduces briefly the study of the CMB anisotropies. We describe some basics of the analysis that is made on the most important CMB observables, namely the map of the temperature fluctuations and the polarization map. We make also a brief review of the most relevant anomalies found in the CMB temperature fluctuations maps by the WMAP and *Planck* satellites.

- Chapter 4 focuses on the *Hemispherical Power Asymmetry* (HPA). A phenomenological model that describes the primordial curvature field and could explain the HPA is derived. It is based upon super-horizon curvature fluctuations that modulates the amplitude of temperature fluctuations inside the observable Universe.

- Chapter 5 contains the application of the formalism developed in Chap. 4, to some concrete models of inflation. First we apply it to the simplest model of single-field slow-roll inflation, then we turn our attention to the *Curvaton model*, that is slightly more complicated.

- Chapter 6 contains an extension of the idea developed in Chap.4. We applied the formalism of Chap.4 also to tensor perturbations of primordial gravitational waves that are inevitably generated during inflation. We explain several applications of this formalism: first we calculate some *consistency relations* that holds for any single-field inflationary model; then we discuss on a mechanism that could alleviate the possible tension that could exist between the measurements made by *Planck* and BICEP2 on the amount of primordial gravitational waves from inflation.

- Chapter 7 summarises the results of the thesis and mentions some futures prospects.

Chapter 1

The inflationary paradigm

The inflationary paradigm is one of the basis of modern cosmology. It is widely believed that before the beginning of the so called standard Universe at early epoch, there was a time in which the Universe expansion was accelerated. This scenario was thought first by Guth in 1981, [31], to solve some of the problems of the standard cosmological Hot-Big-Bang model, like the horizon, and the flatness problems.

The horizon problem arises because, in the standard cosmology framework the Cosmic Microwave Background (CMB) arose at the time when photons decoupled from matter. This happened at a redshift of about $z \sim 1100$. Since from that epoch photons free-streamed, this means that when we detect CMB photons it is equivalent to take a snapshot of the Universe when it was about $300,000\ yrs$ old. A problem arises because at that time the volume, that now correspond to our causal horizon, contained about 10^6 causally disconnected regions. However all the CMB experiments reveals that photons, independently from their incoming direction, have nearly the same characteristics, with a precision of 10^{-5}. However the probability that about 10^6 causally disconnected regions experienced the same identical history is infinitesimal.

The flatness problem is associated to a problem of fine tuning. In fact at present time the Universe is known to be almost flat. Experimental measurements states $K_0 \lesssim 10^{-2}$, where K is the curvature parameter defined in the metric (1.2) and the subscript 0 denotes the present time. However, the standard Hot-Big-Bang predicts that at early times the Universe was flatter than now, more in detail, to explain the current value K_0 one finds that immediately after the Big-Bang it must be be $K \sim 10^{-60}$. We then see that to explain the current value K_0 we should know the early value of K with an unacceptable level of precision.

During the years, the importance of inflation has increased, because it provides a compelling description of how the the Large-Scale Structure (LSS) and the Cosmic Microwave Background (CMB) temperature anisotropies took place from quantum fluctuations that arose during inflation. In this

chapter we will briefly review some of the basics of inflation and we will introduce the theory of quantum fluctuations of a generic scalar field evolving in a fixed quasi de Sitter background.

Many books treat inflationary paradigm in detail e.g. [42] and [51]. For further information the reader is referred to some review papers: [45], [5], [61], [33], [10], [15] and [55]. The latter also discuss in detail issue of the primordial non-gaussianity, that it is introduced at the end of the chapter.

1.1 Basics of inflation

The Einstein equations link the space-time with the matter and the energy contained in the Universe. Their form is

$$R_{\mu\nu} + \frac{1}{2} g_{\mu\nu} R = 8\pi G T_{\mu\nu}, \tag{1.1}$$

where $R_{\mu\nu}$ and R are respectively the tensor and scalar Ricci, $g_{\mu\nu}$ the metric, G the Newtonian gravitational constant and $T_{\mu\nu}$ is the energy-momentum tensor of the fluid which describes the energy content of the Universe. This is a very complicated set of non-linear differential equations. For this reason, to deal with the study of the Universe, cosmologists assumed the so called *Cosmological Principle*. This principle states that, at large scales, the Universe looks same in all directions for all observers. This assumption is consistent with the observation of both Large-Scale Structures and temperature anisotropies of CMB. Using this symmetry argument one can derive a unique metric, the so called Friedmann-Robertson-Walker (FRW) metric. Its line element is

$$ds^2 = -dt^2 + a^2(t) \left[\frac{dr^2}{1 - Kr^2} + r^2 \left(d\theta^2 + \sin^2\theta \, d\phi^2 \right) \right], \tag{1.2}$$

where t is the cosmic time, r, θ, ϕ are the comoving (polar) adimensional coordinates, $a(t)$ is the scale-factor of the Universe[1], and K is the curvature parameter of 3-dimensional hypersurfaces. The latter parameter can assume only the values $K = \{0, \pm 1\}$.

We can describe the content of the universe as a perfect fluid with energy density and pressure, respectively ρ and P with 4-velocity $u_\mu := dx_\mu/d\lambda$ and λ some affine parameter. Its energy-momentum tensor, indeed, satisfies the same symmetries of the FRW metric (1.2):

$$T_{\mu\nu} = (\rho + P)\, u_\mu u_\nu - P g_{\mu\nu}. \tag{1.3}$$

[1] Note that since the polar coordinates are adimensional, the scale factor must has the dimension of a length.

Therefore, plugging this tensor and the metric (1.2) into Einstein equations (1.1), one finds the Friedmann equations

$$H^2 = \frac{8\pi G}{3}\rho - \frac{K}{a^2}, \tag{1.4}$$

$$\frac{\ddot{a}}{a} = -\frac{4\pi G}{3}(\rho + 3P); \tag{1.5}$$

where $H = \dot{a}/a$ is the Hubble rate and the dots denote differentiation with respect to the cosmic time t.

From Eq(1.5) we see that inflation can be reached if the fluid that fills the Universe has a negative pressure such that $P \leq -\rho/3$. For sake of simplicity, we set the value[2] $P = -\rho$. This particular case is called *de Sitter stage* though, usually, inflation is thought as a *quasi* de Sitter epoch. Thanks to the energy continuity equation written in the expanding background

$$\dot{\rho} = -3H(\rho + P) \tag{1.6}$$

we argue that ρ is constant in time [3]. Furthermore, Eq(1.4) tells us that the scale factor exponentially grows in time as $a(t) \sim e^{\lambda t}$, this means that, during inflation, the Hubble rate is fixed at constant value $H = H_I \equiv \dot{a}/a$.

A crucial quantity to study both the inflationary dynamics and the generation of the primordial density perturbations during inflation, is the Hubble horizon $R_H = H^{-1}$. The Hubble horizon represents a characteristic length scale beyond which causal processes cannot operate. During inflation R_H is almost constant but its comoving quantity, the comoving Hubble horizon, defined as $r_H = R_H/a = (aH)^{-1}$ decreases in time. Using this quantity we are able to explain how the horizon problem can be solved. In fact, during inflation the comoving length scales, which are at the beginning causally connected, gradually become larger than r_H and therefore leave the horizon. Then, during radiation and matter dominated era, r_H increases in time allowing these scale to reconnect themselves.

The last parameter we want to define, before talking about one of the physical processes that may led to inflation, consists in an estimate of the duration of the inflationary epoch. In fact, we need to ensure that the

[2] Obviously this is an idealized case.

[3] We can use the continuity equation (1.6) and the first Frieadmann equation (1.4) to compute the dependence of the scale factor $a(t)$ with respect to the cosmic time t also during radiation and matter dominated epochs. Let be

$$P = w\ \rho \tag{1.7}$$

the state equation for the fluid ($w = 1/3, 0$ respectively for radiation and mater), then the continuity equation can be easily solved. Furthermore, plugging the solution into Eq.(1.4) one finds easily

$$a(t) \propto t^{\frac{2}{3(1+w)}}. \tag{1.8}$$

.

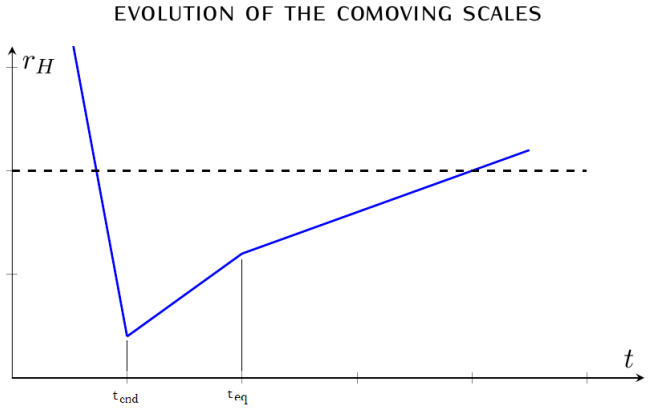

Figure 1.1: Cartoon which represents the evolution of the comoving hubble radius r_H during the history of the Universe (solid blue curve). The dashed black curve represents a comoving scale λ. It is causally connected in the others before inflation, then it becomes super-horizon until the matter-domination era. The end of the inflation is labelled with t_{end}, while t_{dec} labels the time of equivalence between matter and radiation.

inflationary epoch were long enough, such that all the currently observed comoving scales exited the Hubble horizon during inflation in such a way to solve the horizon problem. The number of *e-foldings* N, defined as

$$N = \ln\left(\frac{a(t_{end})}{a(t_{start})}\right) = \int_{t_{start}}^{t_{end}} H(t)dt. \tag{1.9}$$

provides an evaluation of the duration of inflation. Notice that in the above expression t_{start} and t_{end} are respectively the time in which inflation began and ended. To explain the smoothness at the largest observable scale one finds that$N$ must satisfies the constraint $N \gtrsim 50 - 60$.

1.2 The inflaton field

As pointed out by Guth, [31], the vacuum energy of a real scalar field $\varphi(t, \mathbf{x})$, called *inflaton* may be responsible for the primordial inflationary phase. Assuming that this field is minimally coupled to gravity, its action is given by

$$S = \int dtd^3x \ \sqrt{-g}\ \mathcal{L}(g_{\mu\nu}, \varphi, \partial_\mu\varphi), \tag{1.10}$$

where $g = \det(g_{\mu\nu})$ and $\mathcal{L}(g_{\mu\nu}, \varphi, \partial_\mu\varphi)$ is the Lagrangian associated with the scalar field. In the simplest model it assumes the form

$$\mathcal{L}(\frac{1}{2}g_{\mu\nu}, \varphi, \partial_\mu\varphi) = g^{\mu\nu}\partial_\mu\varphi\partial_\nu\varphi - V(\varphi). \tag{1.11}$$

Given the action S, the covariantly conserved energy-momentum tensor $T_{\mu\nu}$ in General Relativity is

$$T_{\mu\nu} = \frac{-2}{\sqrt{g}} \frac{\delta S}{\delta g^{\mu\nu}}. \tag{1.12}$$

Therefore, the tensor admitted by the theory (1.10) is given by

$$T_{\mu\nu} = -2\frac{\partial \mathcal{L}}{\partial g^{\mu\nu}} + g_{\mu\nu}\mathcal{L}. \tag{1.13}$$

Note that this tensor can be interpreted as an energy-momentum tensor of a prefect fluid with 4-velocity

$$u_\mu = \frac{\partial_\mu \varphi}{\sqrt{\partial_\nu \varphi \partial^\nu \varphi}} \tag{1.14}$$

and energy density and pressure respectively

$$\rho = -\frac{1}{2}(\partial_\mu \varphi)^2 + V(\varphi), \tag{1.15}$$

$$P = -\frac{1}{2}(\partial_\mu \varphi)^2 - V(\varphi). \tag{1.16}$$

Now let us look at the equation of the motion of the scalar field. They correspond to the Klein-Gordon equation defined on a curved space-time

$$\Box \varphi = \frac{\partial V}{\partial \varphi} \equiv V_\varphi \tag{1.17}$$

where the covariant D'Alembert operator is

$$\Box = (-g)^{-1/2}\, \partial_\nu(\sqrt{-g}\; g^{\mu\nu}\partial_\mu). \tag{1.18}$$

For a FRW (flat) metric described by (1.2), the equation of motion reads

$$\ddot{\varphi} + 3H\dot{\varphi} - \frac{\nabla^2 \varphi}{a^2} = -V_\varphi. \tag{1.19}$$

We want to point out the presence of the $3H\dot{\varphi}$ term that is typical of a curved space-time. This term does not appear in the "usual" Klein-Gordon equation defined in a Minkowskian space-time. It can be interpreted like a sort of friction which the field suffers during its motion, due to the expansion of the universe. To see how the field $\varphi(t, \mathbf{x})$ may led to inflation, it is convenient to split it into a background value plus fluctuations:

$$\varphi(t, \mathbf{x}) = \varphi_0(t) + \delta\varphi(t, \mathbf{x}). \tag{1.20}$$

Here, φ_0 is the classical value of the field evaluated in the vacuum state[4], $\varphi_0(t) = \langle 0|\varphi(t, \mathbf{x})|0\rangle$. The quantity $\delta\varphi(t, \mathbf{x}) = \varphi(t, \mathbf{x}) - \varphi_0(t)$, instead, represents the quantum fluctuations of the scalar field. In the following we will consider the quantum fluctuations as small perturbations of the background $|\delta\varphi| \ll \varphi_0$. This assumption is legitimate by the amplitude of the CMB temperature anisotropies which are very small ($\Delta T/T \sim 10^{-5}$).

[4]That is defined in the homogeneous and isotropic background.

1.2.1 Background dynamics

The background value $\varphi_0(t)$ acts as a perfect fluid that permeates the Universe with density and pressure respectively

$$\varrho = \frac{1}{2}\dot{\varphi}^2 + V(\varphi) \tag{1.21}$$

$$P = \frac{1}{2}\dot{\varphi}^2 - V(\varphi). \tag{1.22}$$

We can argue this by computing the energy-momentum tensor (1.13) in the vacuum state. Therefore, inflation can be obtained by the inflaton field if, at a certain epoch, it dominated the energy density of the Universe and if, during this epoch, its potential was much greater than its kinetic term. In this case it would be $P \approx -\rho \approx V(\varphi) \approx const.$ This requirement can happen if φ_0 is crossing an almost flat region of its potential, in this sense we can state that φ is *slow rolling* down its potential. We call *first slow roll condition* this requirement, namely that $V(\varphi) \ll 1/2\,\dot{\varphi}^2$. Such a requirement is not improbable. For instance we could assume that at the beginning, the energy density was dominated by the kinetic term, in such a way that $P \approx \rho$. But from the continuity equation (1.6), one finds that the kinetic energy density scales as a^{-6} while the potential energy remains constant in time. In conclusion, after an initial transient inflation would started in any case. In this sense the inflationary solution is called an *attractor*.

Let now concentrate on the dynamics of φ_0. Rewriting Eq(1.19) in terms of the background value[5] we get

$$\ddot{\varphi} + 3H\dot{\varphi} = -V_\varphi. \tag{1.23}$$

The first slow roll condition implies $V_\varphi(\varphi) \ll V(\varphi)$ ($\approx const.$). Then, with this assumption, the asymptotic solution of Eq(1.23) is

$$\dot{\varphi} \simeq -\frac{V_\varphi}{3H}. \tag{1.24}$$

This expression is called *second slow roll condition*. Differentiating it with respect to the cosmic time t we get

$$\ddot{\varphi} \approx -\frac{V_{\varphi\varphi}\,\dot{\varphi}}{3H} \ll 3H\dot{\varphi} \tag{1.25}$$

therefore the second derivative of φ can be neglected in Eq.(1.23), because it is one order of magnitude smaller than the $\dot{\varphi}$ term.

To test the features we outlined, one can define some *slow-roll parameters*. These quantities are useful to compare the theoretical predictions of

[5] Hereafter for simplicity we will neglect the subscript 0.

inflationary models with observations. The two most important parameters are, ϵ and η. They are respectively defined as

$$\epsilon := -\frac{\dot{H}}{H^2} \simeq \frac{3}{2}\frac{\dot{\varphi}^2}{V} \simeq \frac{{M_{Pl}}^2}{2}\left(\frac{V_\varphi}{V}\right)^2, \tag{1.26}$$

$$\eta := \frac{V_{\varphi\varphi}}{3H^2} \simeq M_{Pl}^2\left(\frac{V_{\varphi\varphi}}{V}\right), \tag{1.27}$$

where $M_{Pl} := \sqrt{8\pi/G}$ is the reduced Planck mass. The slow-roll motion states that during inflation $\epsilon, \eta \ll 1$, as a result, we can state that inflation ends when they reach the unity.

1.2.2 Quantum fluctuations of the inflaton field

Besides the background inflationary dynamics, it is of crucial importance to discuss the issue of the evolution of the quantum fluctuations of the *inflaton* field $\delta\varphi(t, \mathbf{x})$. We can interpret them as a random realization of a certain field. In the inflationary paradigm these quantum fluctuations were the origin of all the structures in the universe. It is believed that they arose on scales which were much smaller than the comoving Hubble radius r_H, then inflation strenched their wavelength to scales bigger than the horizon. On such scales the fluctuations are not causally connected and since in this regime microscopic physics does not affect the evolution of fluctuations, their amplitude remained almost constant in time. Therefore such frozen fluctuations appear as a realization of a classical random field that generated the density perturbations which were the origin of the all the structures in the universe.

To describe the evolution of the quantum fluctuations we perturb the equation of motion (1.19). At first order, we get

$$\ddot{\delta\varphi} + 3H\dot{\delta\varphi} - \frac{\nabla^2\delta\varphi}{a^2} = -V_{\varphi\varphi}\delta\varphi. \tag{1.28}$$

To study this equation it is convenient, first of all, to rewrite the quantum fluctuations as a function of the conformal time defined as $\tau = \int dt/a(t)$. Second, to avoid the friction term $3H\dot{\delta\varphi}$ to appear in the equation we make the following redefinition

$$\delta\hat{\varphi} = a\delta\varphi. \tag{1.29}$$

It is now quite simple to study the dynamics of $\delta\hat{\varphi}(\tau, \mathbf{x})$ in Fourier space. Its Fourier transform is

$$\delta\hat{\varphi}(\tau, \mathbf{x}) = \int \frac{d^3k}{(2\pi)^3} e^{-i\mathbf{kx}}\, \delta\hat{\varphi}(\tau, \mathbf{k}), \tag{1.30}$$

where the reality conditions requires $\delta\hat{\varphi}^*(\tau, \mathbf{k}) = \delta\hat{\varphi}(\tau, -\mathbf{k})$. We quantize this field by implementing the standard technique of second quantization,

which consists in introducing the creation and annihilation operators $a_{\mathbf{k}}$ and $a^{\dagger}_{\mathbf{k}}$ and therefore we promote $\delta\hat{\varphi}$ to an operator which can be decomposed as

$$\delta\hat{\varphi}(\tau,\mathbf{x}) = \int \frac{d^3k}{(2\pi)^3}\left[u_k(\tau)a_{\mathbf{k}}e^{-i\mathbf{kx}} + u^*_k(\tau)a^{\dagger}_k e^{i\mathbf{kx}}\right]. \tag{1.31}$$

The creation and annihilation operators obey the usual algebra

$$[a_{\mathbf{k}}, a^{\dagger}_{\mathbf{k}}] = \delta^3(\mathbf{k}-\mathbf{k}'); \quad [a_{\mathbf{k}}, a_{\mathbf{k}'}] = 0, \tag{1.32}$$

while the normalization of the modes $u_k(\tau)$ implies the condition

$$u^*_k u'_k - u_k u^{*\prime}_k = -i. \tag{1.33}$$

Note that here the symbol $'$ denotes the derivation respect to the conformal time[6]. In conclusion, in the new variable $\delta\hat{\varphi}$ Eq(1.28) simplifies, giving rise to

$$u''_k + \left(k^2 - \frac{a''}{a} + a^2 m^2_{eff}\right) u_k = 0. \tag{1.34}$$

Here $m^2_{eff} = V_{\varphi\varphi}$ is the effective mass of the inflaton. Eq(1.34) admits an exact solution in the case of a *de Sitter* stage, but it is more clear and instructive to solve the equation in an approximated way, focusing in the two opposite asymptotic regimes, when the dominant term is either k^2 or a''/a.

We assume that the effective mass of the field m_{eff} is negligible, we can made it because, during slow-roll, $m^2_{eff} = H^2_I$. During inflation, when $H = H_I$ is almost constant $\tau = \int dt/a = \int da(\dot{a}a)^{-1} = \int da(a^2 H_I)^{-1} \simeq -(aH_I)^{-1}$, and hence, deriving respect the conformal time, we find $a''/a = 2a^2H^2_I = 2r^2_H$. We can therefore distinguish two regimes the first, called sub-horizon regime in which the comoving wavelength k^{-1} of the fluctuation is smaller than r_H and the super-horizon regime that start when the mode k exits the Hubble radius.

In the *sub-horizon* regime the comoving wavenumber k is much greater than r_H, we can therefore neglect the term a''/a in Eq(1.34), then the equation of motion reduces to a simple harmonic oscillator equation

$$u''_k + k^2 u_k = 0. \tag{1.35}$$

The solutions approach plane waves of the form

$$u_k(\tau) = \frac{e^{-ik\tau}}{\sqrt{2k}}. \tag{1.36}$$

As expected in the small scales limit we got the standard treatment of quantum fluctuations. In fact we reduced to the quantum field theory in an ordinary flat space-time. To conclude, we remark that in this regime the

[6] $d\tau = a(t)dt \Rightarrow \frac{d}{d\tau} = \frac{1}{a(t)}\frac{d}{dt}$.

quantum fluctuations oscillate in time with a decaying amplitude $|\delta\varphi| = |u_k(\tau)|/a(\tau) = (a(\tau)\sqrt{2k})^{-1}$.

In the *super-horizon* regime, on very large scales, when $k \ll r_H$, Eq(1.34) becomes

$$u_k'' - \frac{a''}{a}u_k = 0. \tag{1.37}$$

The solution is polynomial in the scale factor $a(\tau)$. In particular it consists in a sum of a growing and a decaying mode

$$u_k(\tau) = B_+(k)a(\tau) + B_-(k)a^{-2}(\tau). \tag{1.38}$$

We are interested only in the growing mode. Therefore one can fix its initial amplitude by matching the amplitude of the plain wave solution (1.36) with the solution (1.38) at the time in which the mode k leaves the horizon. In this epoch the wavelength of the perturbation and the comoving Hubble radius have the same value $k = a_k H_k$, where the subscript $\mathbf{k}$ means that we evaluated a and H at the time in which the comving scale $\mathbf{k}$ left the horizon. As a result one finds $|B_+(k)|\, a(\tau)|_{k=a_k H_k} = [1/\sqrt{2k}\,]_{k=a_k H_k} = H_k/\sqrt{2k^3}$. Notice that for a pure de Sitter stage H_k takes the same value, H_I for all scales. In a quasi de Sitter, instead, H experiences a variation of the order of slow-roll parameter (see Eq(1.26)). In conclusion, during the super-horizon epoch as we have already anticipated the quantum fluctuations remains frozen at the constant value

$$|\delta\varphi(\mathbf{k})| = |B_+(k)| = \frac{H_k}{\sqrt{2k^3}}. \tag{1.39}$$

Fig.(1.2.2) shows the qualitative evolution of the primordial quantum fluctuations as function of the cosmic time t.

1.2.3 Statistics of the quantum fluctuations

In this section we briefly discuss about the statistics of the primordial quantum fluctuations. This is a crucial point, because their statistics will affect also the statistical distribution of other types of perturbations, including the CMB temperature anisotropies. In this way, probing for example the statistics of the CMB temperature anisotropies we could be able to infer some details about the physics of the early Universe.

For clarity, in the formalism of the perturbation theory described in details in the next chapter one can expand $\delta\varphi(t, \mathbf{x})$ in power series:

$$\delta\varphi(t, \mathbf{x}) = \sum_{k=1}^{\infty} \frac{\delta\varphi^{(k)}}{k!}. \tag{1.40}$$

Here with $\delta\varphi^{(1)}$, we refer to the linear (first-order) term in perturbation theory. Therefore this term is a gaussian random variable. It is important to

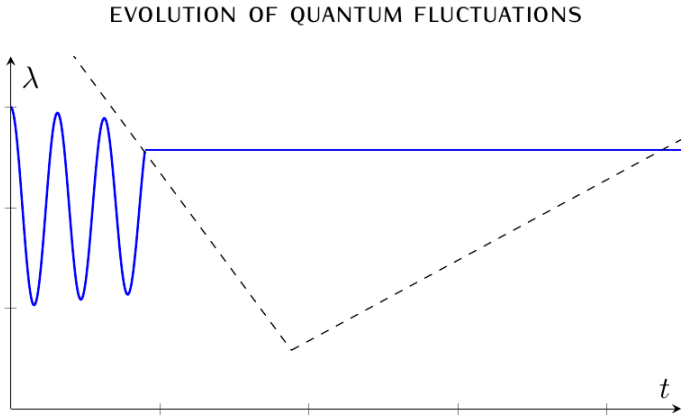

Figure 1.2: Cartoon of the evolution of the quantum fluctuations of a scalar field in a de-Sitter inflationary phase. The dashed curve represent the comving Hubble horizon during inflation (decaying line) and during the FRW Universe (growing line).

stress that this does not mean that the field $\delta\varphi(t,\mathbf{x})$ will be gaussian distributed too since in general it will contain higher-order perturbation terms in Eq(1.40). In fact a non-Gaussian statistics (i.e. *non-Gaussianity*) is generated as soon as the scalar field has some interactions with itself (or other fields). This amounts to saying that the potential contains some terms beyond the quadratic mass term.

To describe the statistics of a random field we can turn to the n-point correlation functions $\langle\delta\varphi(x_1)\dots\delta\varphi(x_n)\rangle$. For a gaussian field only the 2-point function (and hence its Fourier transform) is relevant. In fact all the odd correlation functions vanish, while the even ones can be simply expressed in terms of the 2-point function.

Since observations tells us that the statistics of $\delta\varphi(t,\mathbf{x})$ is mainly gaussian we turn our attention to the 2-point correlation function in Fourier space $\langle\delta\varphi(\mathbf{k})\delta\varphi^*(\mathbf{k}')\rangle$ and to the *power spectrum* $P(k)$. They are respectively defined as

$$\begin{aligned}\langle\delta\varphi(\mathbf{k})\delta\varphi^*(\mathbf{k}')\rangle &= \int d^3x\; d^3x'\; e^{i(\mathbf{kx}+\mathbf{k}'\mathbf{x}')}\langle\delta\varphi(\mathbf{x})\delta\varphi^*(\mathbf{x}')\rangle = \\ &= (2\pi)^3\delta^3(\mathbf{k}-\mathbf{k}')P_\phi(k). \qquad (1.41)\end{aligned}$$

To justify the last step, we assumed homogeneity and isotropy (so that $\langle\delta\varphi(\mathbf{x})\delta\varphi(\mathbf{x}')\rangle$ is a function only of $|\mathbf{x}-\mathbf{x}'|$) [7] . The power spectrum can be interpreted as the square of the average amplitude of $\delta\varphi(\mathbf{k})$. Treating the

[7] It is easy to show in Eq(1.41) that statistical homogeneity and isotropy are respectively guaranteed by $\delta^3(\mathbf{k}-\mathbf{k}')$ and by the fact that $P(k)$ does not depend on the direction of $\mathbf{k}$.

the quantum fluctuations $\delta\varphi(\mathbf{k})$ as operators, Eq(1.31), where the modulus of $u_k(\tau)$ is given by Eq(1.36), one can easily compute the 2-point function $\langle\delta\varphi(\mathbf{k})\delta\varphi^*(\mathbf{k}')\rangle$ and check that

$$P_{\delta\varphi}(k) = \frac{H_k^2}{2k^3}. \tag{1.42}$$

We can define also the dimensionless power spectrum as

$$\mathcal{P}(k) = (k^3/2\pi^2)P(k). \tag{1.43}$$

In case of primordial quantum fluctuations it corresponds to

$$\mathcal{P}_{\delta\varphi}(k) = \left(\frac{H_k}{2\pi}\right)^2. \tag{1.44}$$

The dimensionless power spectrum can be interpreted also as the logarithmic scale contribution to the variance of the fluctuations, indeed

$$\begin{aligned}\sigma^2_{\delta\varphi} = \langle\delta\varphi^2(\mathbf{x})\rangle &= \int \frac{d^3k}{(2\pi)^3}\frac{d^3k'}{(2\pi)^3}\langle\delta\varphi(\mathbf{k})\delta\varphi^*(\mathbf{k}')\rangle \\ &= \int \frac{d^3k}{(2\pi)^3}\frac{d^3k'}{(2\pi)^3}\delta^3(\mathbf{k}-\mathbf{k}')P_\varphi(k) = \\ &= \int \frac{dk}{k}\mathcal{P}_\varphi(k).\end{aligned} \tag{1.45}$$

Since the surveys about the statistics of the primordial fluctuations are increasingly precise, it is interesting to go beyond the 2-point function, looking for a deviation from a gaussian statistics. The first term that shows the eventual presence of non-Gaussianity is the 3-point function. For a homogeneous and isotropic field, its Fourier transform is

$$\begin{aligned}\langle\delta\varphi(\mathbf{k_1})\delta\varphi(\mathbf{k_2})\delta\varphi(\mathbf{k_3})\rangle &= (2\pi)^3\delta^3(\mathbf{k_1}+\mathbf{k_2}+\mathbf{k_3})\,F(k_1,k_2,k_3) = \\ &\equiv (2\pi)^3\delta^3(\mathbf{k_1}+\mathbf{k_2}+\mathbf{k_3})\,f_{_{NL}}\,\mathcal{B}(k_1,k_2,k_3).\end{aligned} \tag{1.46}$$

Here $f_{_{NL}}$ is a dimensionless parameter defining the amplitude of non-gaussianity, while the function $\mathcal{B}(k_1,k_2,k_3)$ is called *bispectrum* and captures the momentum dependence or the "shape" of non-Gaussianity. The parameter $f_{_{NL}}$ is (usually) defined in such a way that

$$f_{_{NL}} = \frac{F(k,k,k)}{6\ P^2(k)}. \tag{1.47}$$

Notice that isotropy requires that the bispectrum depends only on the modulus of the wavenumbers $\mathbf{k_i}$, $i = 1,2,3$ and that that the three arguments of the bispectrum can be exchanged between them. The amplitude and sign

of f_{NL}, as well as the shape of the bispectrum depend on the details of the interaction generating the primordial non-Gaussianity. It is important to notice that to compute the level of non-Gaussianity we have to go beyond the first order in perturbations theory, because, as we have already said, the first order can give rise only to a gaussian distribution.

Primordial non-Gaussianity is a fundamental probe of the early Universe since different inflationary models predict different amplitudes and shapes of non-Gaussianity [10], [15]. The most common shapes of non-Gaussianity are the *squeezed* (or *local*), the *equilateral* and the *folded* ones. The *squeezed* non-Gaussianity peaks in the limit $k_1 \ll k_2 \simeq k_3$, namely when one perturbation mode has a wavelength much greater than the others two. A bispectrum that peaks in the local configuration is expected in multi-fields inflationary models or in models in which non-linearities develop on super-horizon scales. The current bound on the local type of non-Gaussianity is $f_{NL}^{local} \lesssim 14$ (68% C.L.), [68] [8]. The *equilateral* shape peaks in configurations in which the three Fourier modes have nearly the same modulus $k_1 \simeq k_2 \simeq k_3$. This kind of non-Gaussianity is typical of single-field inflationary models in which the field has a non trivial kinetic term. The current upper bound on the equilateral shape is $f_{NL}^{equil.} \lesssim 195$ (68% C.L.), [68]. The *folded* shapes peaks in the configuration $k_1 \simeq k_2 + k_3$. Higher derivative interactions in the inflationary fields bring the signal to be maximal in the this limit (there is no published constraint on f_{NL}^{folded} at present).

[8] Notice that this and the other reported values on f_{NL} do not refer to the quantum fluctuations $\delta\varphi$ but to the non-Gaussianity of the curvature perturbations $\zeta(\mathbf{x})$, defined in Sec. 2.6.

Chapter 2

Cosmological perturbations

The study of the evolution of cosmological perturbations is of primary importance for understanding the origin of the CMB temperature anisotropies and LSS from the primordial quantum fluctuations of the field (or fields) present during inflation. In order to make a complete discussion of the primordial perturbations we need to study not only the quantum fluctuation of the inflaton field but also the perturbations of the metric. The reason is that, when the inflaton dominates the energy density of the Universe, any quantum fluctuation $\delta\varphi$ implies a perturbation of the energy-momentum tensor $\delta T_{\mu\nu}$, and a perturbation in the energy-momentum tensor implies, through the Einstein equations (1.1), a perturbation of the metric. On the other hand perturbations in the metric affects the evolution of $\delta\varphi$ through the perturbed Klein-Gordon equation trough the D'Alembert operator (1.18). Therefore perturbations of the inflaton field and perturbations of the metric are tightly coupled to each other and have to be studied together [1].

In this chapter we will give a short review about the theory of perturbations in General Relativity. We will start presenting the basics of this formalism providing a mathematical definition about gauges and perturbations and we will introduce the so called gauge problem that arises in General Relativity. Then we will see how we can split the metric and the energy-momentum tensor in a background value plus fluctuations, spending also some words about the calculation of the evolution of such perturbations. After this we shall discuss some relevant gauges and gauge invariant perturbations, focusing on the *gauge invariant* curvature perturbation ζ. This is the most relevant perturbation during the evolution of the early Universe, it is also related, through Bardeen's gravitational Φ, to the origin of the CMB anisotropies. Finally, we will briefly discuss how to extend the formalism in

[1] Notice that in the previous Chapter we perturbed the Klein-Gordon equation neglecting metric perturbations. We can do this because, it can be shown that the perturbed Klein-Gordon equation written in Fourier space and in the spatially flat gauge (defined in Sec. 2.5) has the same form as Eq.(1.34) and thus we can just follow the same procedure described in Sec. 1.2.2, simply replacing m^2_{eff} with $\mathcal{M}^2_{eff}$, that is an effective mass of the inflaton field in that gauge, [10]

the case in which more than one field is present during inflation. We will find that we have to introduce another type of fluctuation called *isocurvature perturbation*, S_{IJ}.

Some useful references about the topics discussed in this chapter are, about gauges in General Relativity, Refs [3], [14] and [58], while one can turn at Ref.[57] and [7] if one is interested in a detailed study about the evolution of perturbations and gauge invariant perturbations in cosmology. Finally, regarding to isocurvature perturbations we refer to [56], while [71], [49], [15] and [49] are suitable references about the δN formalism, discussed a the end of the chapter.

2.1 Perturbations in General Relativity

The idea underlying the theory of space-time perturbations is the same that we have in any perturbative formalism: we search approximate solutions of some field equations, regarding them as "small" deviations from a known exact background solution. The basic difference arising in General Relativity, is that we have to deal with perturbations not only of fields in a given geometry, but of the geometry itself.

The main hypothesis consists in assuming the existence of a parametric family of solutions of the field equations, to which the unperturbed background space-time belongs. We can label each of these solutions with a parameter $\lambda \in \mathbb{R}$ such that $\lambda = 0$ represent the background solution. In this formalism the physical quantities are represented by tensor fields T_λ. They are defined on the real Universe $\mathcal{M}_\lambda$ that is different from the idealized $\mathcal{M}_0$ of the background solution. With $\mathcal{M}_0$ we refer to a manifold with a FRW metric ($g_{\mu\nu} = a\,\eta_{\mu\nu}$), where the observables are homogeneous and isotropic tensors T_0. The aim of perturbations theory is to construct an approximate theory for $\mathcal{M}_\lambda$ and to do this we shall assume that the parameter λ differs slightly from 0 (and hence $\lambda \ll 1$). In this sense we can state that the real universe $\mathcal{M}_\lambda$ is close to the unperturbed background manifold.

To relate the unperturbed background $\mathcal{M}_0$ with $\mathcal{M}_\lambda$ we use diffeomorphisms which are one-to-one correspondences between points of $\mathcal{M}_0$ and points of $\mathcal{M}_\lambda$. Such a maps, that are function of the parameter λ, define a *gauge* choice. Hereafter, with a little abuse of notation we will call the map itself a gauge. The gauges help us to relate the physical quantities with the the one built on $\mathcal{M}_0$. In fact when we measure an observable we make a measurement of T_λ and since our purpose consists in comparing it with its unperturbed quantity T_0 defined on $\mathcal{M}_0$, [2] we have to define some representative of T_λ in the unperturbed background.

A problem that arises in this theory is that we can define an indefinite number of gauges between $\mathcal{M}_0$ and $\mathcal{M}_\lambda$. Suppose that the coordinates x^μ

[2] In such a way we can define the perturbations of T_λ.

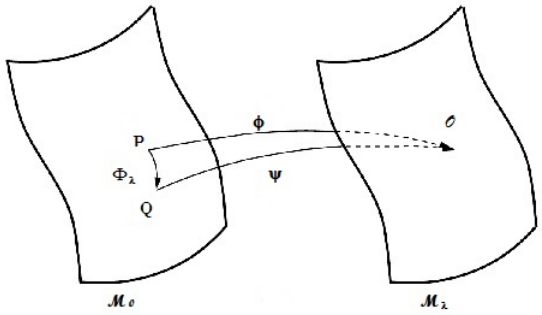

Figure 2.1: Gauge transformation. The diffeomorphism Φ_λ maps $\mathcal{M}_0$ into itself.

have been assigned to the points of the background $\mathcal{M}_0$. Let now φ_λ and ψ_λ be two different gauges and suppose further that at the given points of $\mathcal{M}_0$, p and q, $\varphi_\lambda(p) = \psi_\lambda(q) = \mathcal{O} \in \mathcal{M}_\lambda$. Therefore we can define the map $q = \Phi_\lambda(p) := \varphi_\lambda^{-1}(\psi_\lambda(p))$, which is a one-to-one correspondence between points in $\mathcal{M}_0$. The map $\Phi_\lambda(p)$ is called *gauge transformation*. Such a transformation, that in one given coordinate system moves each point to another, is often called active coordinate transformation.

Let's now look at the tensors T_λ. Thanks to the gauges we can define representations of them on $\mathcal{M}_0$, let us call them $T(\lambda)$. We can choose infinite gauges and then we can define infinite representations $T(\lambda)$. What we find is that such $T(\lambda)$, for a given T_λ, assume different values in different gauges. Therefore, when we deal with tensor perturbations it is essential to be able to distinguish between physical inhomogeneities and gauge artefacts. Moreover, since General Relativity is invariant under coordinate reparametrization, we are free to pick the coordinate system best adapted to the problem at hand. This is both a blessing and a curse, because in this way we also obtain apparently different results depending upon this arbitrary choice of coordinates. This is the so called gauge issue.

To see how the gauge choice affects the physical quantities we have to understand what we mean with perturbation. Given a representation $T(\lambda)$ and its corresponding background value T_0, we call perturbation the quantity

$$\Delta T(\lambda) = T(\lambda) - T_0. \tag{2.1}$$

Recall that we are thinking at the real space $\mathcal{M}_\lambda$ as slightly different from the unperturbed background. This means $\lambda \ll 1$ and then we can expand the physical $T(\lambda)$ in power series of λ. Then the perturbation $\Delta T(\lambda)$ can be

written as

$$\Delta T(\lambda) = \sum_{k=1}^{\infty} \frac{\lambda^k}{k!} \delta T^{(k)}; \tag{2.2}$$

where $\delta T^{(k)}$ represents the perturbation at the k^{th} order.

Now we concentrate on a gauge transformation. Let us suppose there are two representations $T(\lambda)$ and $\tilde{T}(\lambda)$ defined through two different gauge transformations, respectively φ_λ and ψ_λ. To relate the two representations we exploit the gauge transformation $\Phi_\lambda = \varphi_\lambda^{-1}(\psi_\lambda(\tilde{x^\mu}))$. We expand Φ_λ in Taylor series at first order in λ:

$$\tilde{x}^\mu(\lambda) = x^\mu + \lambda\xi^\mu + \mathcal{O}(\lambda^2). \tag{2.3}$$

This is often called an "infinitesimal point transformation". A result of differential geometry is that, under a gauge transformation[3], tensors transforms as $\tilde{T}(\lambda) = e^{\mathcal{L}_\xi} T$, where $\mathcal{L}_\xi$ denotes the Lie derivative with respect the field ξ^μ. Therefore at first order we get:

$$\tilde{T} = T_0 + \lambda\, \mathcal{L}_\xi\, T_0 + \mathcal{O}(\lambda^2), \tag{2.4}$$

and therefore taking into account also the perturbations, the physical quantities transform, at first order, as:

$$\tilde{T} = T_0 + \Delta\tilde{T} = T_0 + \lambda\Delta T + \lambda\, \mathcal{L}_\xi\, T_0. \tag{2.5}$$

Finally, we find that at first order the perturbations are affected by the gauge transformations in the following way:

$$\Delta\tilde{T} = \Delta T + \mathcal{L}_\xi\, T_0. \tag{2.6}$$

From the above expression, we see explicitly what we are stressing in this section, namely that the choice of the gauge affects physical quantities at the same order of the perturbations. As a result a crucial issue concerning perturbation theory in general relativity consists in distinguishing between the physical perturbation and the part arising from its gauge dependence. We can perform this erasing the gauge dependence, this can be done following two paths: or we completely fix the coordinate system (thus we make a gauge choice), or we use gauge invariant approach. In the following we will see both these approaches.

To conclude the section let us give the formulae of the Lie derivative that must be used to explicitly compute the transformation of the perturbations. The physical quantities, according to their transformation proprieties, can

[3]Notice that, at first order, a gauge transformation is fully specified by the choice of the 4-vector ξ^μ.

be scalars (S), vectors (V_μ) and tensors (T^μ_ν) of the manifold $\mathcal{M}_\lambda$. For them the Lie derivative acts as

$$\mathcal{L}_\xi S = \partial_\lambda (S\ \xi^\lambda), \tag{2.7}$$
$$\mathcal{L}_\xi V_\mu = V_\lambda\ \mathcal{D}_\mu \xi^\lambda + \mathcal{D}_\mu V_\lambda\ \xi^\lambda, \tag{2.8}$$
$$\mathcal{L}_\xi T^\mu_\nu = -T^\lambda_\nu\ \mathcal{D}_\lambda \xi^\mu + T^\mu_\lambda\ \mathcal{D}_\nu \xi^\lambda + \mathcal{D}_\lambda T^\mu_\nu\ \xi^\lambda; \tag{2.9}$$

where the symbol $\mathcal{D}$ denotes the covariant derivative.

Let us now show which perturbations affect the metric $g_{\mu\nu}$ and the energy momentum tensor of a general fluid $T_{\mu\nu}$ which is supposed to fill the Universe.

2.2 Metric perturbations

It is convenient to slice the space-time manifold into a one-parameter family of spatial hypersurfaces of constant conformal time τ. Having done this, we can split the metric tensor $g_{\mu\nu}(x)$ into background plus fluctuations:

$$g_{\mu\nu}(\tau, \mathbf{x}) = g^{(0)}_{\mu\nu} + \delta g_{\mu\nu}(\tau, \mathbf{x}), \tag{2.10}$$

here the background is $g^{(0)}_{\mu\nu} = a^2(\tau)\eta_{\mu\nu}$. It then turns out to be useful to split the metric perturbation into different parts, according to their transformation properties on the background spatial hypersurfaces. We define, indeed, scalar, vector and tensor perturbations, that can be expanded into first and higher order parts using Eq(2.2). The perturbed part of the metric at first order is

$$\delta g_{00} = -2a^2\phi, \tag{2.11}$$
$$\delta g_{0i} = a^2 B_i, \tag{2.12}$$
$$\delta g_{ij} = C_{ij}. \tag{2.13}$$

Here, ϕ is called the lapse function, it can be interpreted as the Newtonian gravitational potential. The lapse function plays an important role in determining the CMB temperature anisotropies, as we will seen later. The vector perturbation B_i is called shift vector. It can be further splitted into a curl-free part plus a divergence-free part

$$B_i = \partial_i B + S_i, \quad \text{with} \quad \partial_i S_i = 0, \tag{2.14}$$

where the indexes are raised and lowered with the Kronecker symbol δ_{ij}. Also the spatial part of the metric can be further splitted into

$$C_{ij} = a^2 \left[-2\psi\delta_{ij} + \partial_i\partial_j E + \partial_{(i}F_{j)} + 2h_{ij} \right]. \tag{2.15}$$

With $\partial_{(i}F_{j)}$ we mean the symmetric derivative $\frac{1}{2}(\partial_i F_j + \partial_j F_i)$. Because the symmetric tensor h_{ij} is transverse (i.e. $\partial_i h_{ij} = 0$) and traceless (i.e. $h_{ii} = 0$), it does not contain any pieces which transform as scalars or vectors.

To summarize we list the different type of perturbations of the FRW metric. We have:

i. 4 scalars ϕ, ψ, E, and B;

ii. 2 vectors S_i and F_i with 3 components each but it has to satisfy 2 constraints;

iii. 1 symmetric tensor h_{ij}, it has 6 components but has to satisfy 4 constraints, so it has only 2 degrees of freedom.

In total we have 10 degrees of freedom, that is the number of independent components of $\delta g_{\mu\nu}$. We can use the gauge freedom, that consists at first order to set the 4-vector ξ^μ to eliminate 4 degrees of freedom. In this way the total degrees of freedom reduces at 6.

Let us stress that the metric perturbations (2.11), (2.12) and (2.13) still include all orders, for example $\phi = \phi^{(1)} + \frac{1}{2}\phi^{(2)} + \dots$. In his thesis, for simplicity, we will overview the theory of perturbations only at first order, therefore, hereafter, with ϕ we shall refer only to first order perturbations.

To conclude this section we will give some results on how the metric perturbations (2.11), (2.12) and (2.13) change under a gauge transformation. To derive these results, thanks to Eq(2.3), we fixed the gauge transformation through

$$\xi^\mu := (\alpha, \beta^i), \tag{2.16}$$

where the vector β^i is splitted into a curl and divergence-free part

$$\beta^i = \partial^i \beta + \gamma^i \quad \text{with} \quad \partial_i \gamma^i = 0, \tag{2.17}$$

and then we use Eqs(2.7), (2.8) and (2.9) to see how scalars, vectors and tensors perturbations respectively transform. We found that the scalar perturbations of the metric transform as

$$\tilde{\phi} = \phi + \mathcal{H}\alpha + \alpha', \tag{2.18}$$
$$\tilde{\psi} = \psi - \mathcal{H}\alpha, \tag{2.19}$$
$$\tilde{E} = E + \beta, \tag{2.20}$$
$$\tilde{B} = B - \alpha + \beta; \tag{2.21}$$

while for vector perturbations we get

$$\tilde{S}^i = S^i - \gamma^{i\prime} \tag{2.22}$$
$$\tilde{F}^i = \tilde{F}^i + \gamma^{i\prime}. \tag{2.23}$$

Finally, regarding tensor perturbation h_{ij} one finds that it is invariant up to first order.

2.3 Energy-momentum tensor

Together with metric perturbations we have to study also the perturbations in the matter content of the Universe in order to understand how these perturbations affect the metric.

2.3.1 Single fluid

We start assuming that a single fluid dominates the energy density of the Universe. The most general energy-momentum tensor covariantly conserved for such fluid is

$$T_{\mu\nu} = (\rho + P)u_\mu u_\nu + P g_{\mu\nu} + \pi_{\mu\nu}. \tag{2.24}$$

where ρ and P are respectively the energy density and pressure, u_μ the fluid 4-velocity and $\pi_{\mu\nu}$ is the anisotropic part of the stress. We split the quantities into a background part and perturbations around it. The energy density and the pressure are:

$$\rho = \rho_0 + \delta\rho, \tag{2.25}$$
$$P = P_0 + \delta P. \tag{2.26}$$

The 4-velocity, is defined by $u^\mu = dx^\mu/d\lambda$, where λ is some affine parameter. It subjects to the constraint

$$u_\mu u^\mu = -1. \tag{2.27}$$

Using this, we split u_μ as

$$u_0 = \frac{dx_0}{d\tau} = -a(1+\phi), \tag{2.28}$$
$$u_i = \frac{dx_i}{d\tau} = a(v_i + B_i), \tag{2.29}$$

where as usually, v_i is splitted into a scalar part v plus a vector $v^\perp$ part. Note that ϕ and B_i are metric perturbations defined in Eqs (2.11) and (2.12). Let us stress that while the temporal component of the 4-velocity has a non-vanishing background value, its spatial part takes a non zero value only at first order. The same holds also for the tensor $\pi_{\mu\nu}$. It must obey at the constraints

$$\pi_{\mu\nu}u^\nu = 0, \qquad \pi^\mu_{\ \mu} = 0 \tag{2.30}$$

We follow Ref.[40] in defining the proper energy density as the eigen-value of the energy momentum tensor, and the 4-velocity u^μ as the corresponding eigenvector

$$T^\mu_{\ \nu}u^\nu = -\rho u^\mu. \tag{2.31}$$

This lead to the fact that the "00" component of $\pi_{\mu\nu}$ is null at first order [40]. Then we consider only the spatial part π_{ij} which we split into a trace-free scalar part Π, a vector part Π_i and a tensor part Π_{ij}, getting

$$\pi_{ij} = a^2 \left[\left(\partial_i \partial_j - \frac{1}{3} \nabla^2 \right) \Pi + \frac{1}{2} \partial_{(i} \Pi_{j)} + \Pi_{ij} \right]. \tag{2.32}$$

In conclusion, plugging Eqs (2.25), (2.28) and (2.29) into the energy-momentum tensor (2.24) we get at first order

$$T^0_{\ 0} = -(\rho_0 + \delta\rho), \tag{2.33}$$
$$T^0_{\ i} = (\rho_0 + P_0)(v_i + B_i), \tag{2.34}$$
$$T^i_{\ j} = (P_0 + \delta P)\delta^i_{\ j} + a^{-2}\pi^i_{\ j}\,. \tag{2.35}$$

We can compare the above results with the energy-momentum tensor of a real scalar field minimally coupled with gravity which obeys the Lagrangian (1.11):

$$\mathcal{L}(g_{\mu\nu},\, \varphi,\, \partial_\mu \varphi) = \frac{1}{2} g^{\mu\nu} \partial_\mu \phi \partial_\nu \phi - V(\varphi). \tag{2.36}$$

According to Eq(1.13), the explicit expression for the energy-momentum tensor is

$$T^{\varphi}_{\mu\nu} = \partial_\mu \varphi \partial_\nu \varphi + g_{\mu\nu} \left(\frac{1}{2} g^{\mu\nu} \partial_\mu \varphi \partial_\nu \varphi - V(\varphi) \right), \tag{2.37}$$

that is equivalent with to the energy-momentum tensor of a fluid with 4-velocity

$$u_\mu = \frac{\partial_\mu \varphi}{\left(\partial_\alpha \varphi\, \partial^\alpha \varphi\right)^{1/2}}. \tag{2.38}$$

We see that $T^{\varphi}_{\mu\nu}$ is equivalent to the tensor of a perfect fluid (and so with $\pi_{ij} = 0$). Moreover, splitting φ and $g^{\mu\nu}$ into a background value plus a perturbation we get at first order

$$T^{0\,\varphi}_{\ 0} = -a^{-2}\frac{1}{2}\varphi'^2 - V(\varphi) + a^{-2}\varphi'(\phi\varphi' - \delta\varphi') - V_\varphi \delta\varphi, \tag{2.39}$$
$$T^{0\,\varphi}_{\ i} = -a^{-2}\varphi' \partial_i \delta\varphi, \tag{2.40}$$
$$T^{i\,\varphi}_{\ j} = \left[a^{-2}\frac{1}{2}\varphi'^2 - V(\varphi) - a^{-2}\varphi'(\phi\varphi' - \delta\varphi') - V_\varphi \delta\varphi \right] \delta^i_{\ j}. \tag{2.41}$$

Thus, comparing Eq(2.41) with Eq(2.35) we conclude that at first order a scalar fields does not support vector and tensor perturbations.

Finally, as we have already done in previous section we give the transformation under a gauge changing defined in (2.16) of the perturbations that we have just defined. For our purpose is sufficiently to give the transformation of the energy density perturbation under the gauge transformation (2.16). Thanks to Eq(2.7) we find

$$\widetilde{\delta\rho} = \delta\rho + \rho_0' \alpha. \tag{2.42}$$

2.3.2 Multiple fluids

Now we want to extend our formalism assuming the existence of more than one fluid that permeate the space-time. This extension of primary importance when we are dealing with the *curvaton model*, a particular model of inflation in which there are two scalar fields that fill the Universe during inflation [47], [8].

More in general, let us assume that the Universe is filled with n different interacting fluids. We can still define an energy-momentum tensor for each fluid. In addition we can construct the total energy-momentum tensor as the sum of the energy-momentum tensors of each individual fluid $T^{(I)}_{\mu\nu}$:

$$T_{\mu\nu} = \sum_I T^{(I)}_{\mu\nu}, \tag{2.43}$$

Only this sum is covariantly conserved while for each fluid holds

$$\mathcal{D}^\mu T^{(I)}_{\mu\nu} = Q^{(I)}_\nu, \tag{2.44}$$

where $Q^{(I)}_\nu$ is the energy-momentum transfer 4-vector relative to the I^{th} fluid. The covariant conservation of $T_{\mu\nu}$ constrains

$$\sum_I Q^{(I)}_\nu = 0. \tag{2.45}$$

A final remark: under a gauge transformation (2.16) the perturbations for each fluid, in general, transform in a different way respect to case of a single fluid. Anyway, since the total density perturbation $\delta\rho$ is the the sum of the density perturbation for each fluid $\delta\rho_I$, we see that $\delta\rho = \sum_I \delta\rho_{(I)}$ and $\delta\rho_{(I)}$ transform in the same way according to eq.(2.42).

2.3.3 Non adiabatic pressure

In general the pressure P is a function of 2 quantities: the energy density ρ and the entropy S. Fluctuations in the pressure are then given by

$$\delta P = \frac{\partial P}{\partial \rho}\delta\rho + \frac{\partial P}{\partial S}\delta S. \tag{2.46}$$

We call (squared) *sound of speed* the quantity $c_s^2 := (\partial P/\partial\rho)_S$, and respectively adiabatic and non-adiabatic pressure perturbation δP_{nad} the fluctuations

$$\delta P_{nad} = \frac{\partial P}{\partial S}\delta S, \tag{2.47}$$

$$\delta P_{ad} = \frac{\partial P}{\partial \rho}\delta\rho. \tag{2.48}$$

The non adiabatic pressure perturbation arises only in presence of entropy perturbations. This latter is sourced either by anisotropic stress which is the signature of an imperfect fluid or by the presence of more fluids. Assuming that the early Universe was dominated by scalar fields, since they behave each one as a perfect fluid, we conclude that non adiabatic pressure perturbations arise only from the relative interaction between the fluids.

2.4 Dynamics

Now that we have defined the perturbations of both the metric and the fluid we can study their coupled evolution. In this way we can understand how the primordial perturbations evolved until now to form the current Universe. Furthermore the dynamics of the perturbations allows us to derive some key properties of the perturbation variables. The dynamics of the perturbations can be derived by perturbing at the desired order the Einsteinequations (1.1)

$$R_{\mu\nu} + \frac{1}{2} g_{\mu\nu} R = 8\pi G T_{\mu\nu}, \tag{2.49}$$

and the continuity equation of the energy-momentum tensor of the fluid(s) which fills the Universe

$$\mathcal{D}^{\mu} T_{\mu\nu} = 0. \tag{2.50}$$

Here we give the expression of the perturbed Einstein equation relative to the scalar perturbations, at fist order, without have specified the gauge. The 00 Einstein equation is

$$3\mathcal{H}(\psi' + \mathcal{H}\phi) - \nabla^2(\psi + \mathcal{H}\sigma) = -4\pi G a^2 \delta\rho, \tag{2.51}$$

where $\sigma = E' - B$ is called shear. The $0i$ Einstein equation is

$$\mathcal{H}\phi + \psi' = -4\pi G a^2 (\rho + P)(v + B) \tag{2.52}$$

the of trace equation is

$$\sigma' + 2\mathcal{H}\sigma + \psi - \phi = 8\pi G a^2 \Pi, \tag{2.53}$$

and the trace is

$$\psi'' + 2\mathcal{H}\psi' + \mathcal{H}\phi' + (2\mathcal{H}' + \mathcal{H}^2)\phi = 4\pi G a^2 \left(\delta P + \frac{2}{3}\nabla^2 \Pi\right) \tag{2.54}$$

Finally the evolution equation for the tensor perturbaion is

$$h_{ij}'' + 2\mathcal{H} h_{ij}' - \frac{\nabla^2 h_{ij}}{a^2} = 8\pi G a^2 \Pi_{ij}^{(TT)}, \tag{2.55}$$

Notice that we do not write the equations for the vector perturbations because we do not care about them. In fact the first order vector perturbations have decreasing amplitudes and are not generated in the standard scenarios, namely in presence of scalar fields [4]. This argument allows us to conclude

[4] Vector perturbations may be generated in exotic scenarios in which inflation is driven by a vector scalar field [76], but in this thesis we will not consider such scenarios.

that they can be safely disregarded, [10].

2.5 Gauge choices and gauge invariant cosmological perturbations

The problem associated with perturbations is that the notion of density perturbations, for example, loses its direct physical significance due to the presence of coordinate gauge freedom inherent in general relativistic perturbation theories. Indeed, one can assign practically any value to a given perturbation by a suitable gauge transformation. For this, when one deals with perturbations in General Relativity it is of primary importance to avoid the perturbation gauge dependence and isolate the gauge artefacts. Otherwise, unphysical gauge modes would dominate over physical modes and lead to an incorrect conclusion.

To solve this problem we can either choose a gauge and write all perturbations in such gauge, or work with the so called gauge invariant perturbations. These quantities are particular combinations of scalar perturbations that remain unchanged under a gauge transformation. Let us stress that we can construct gauge invariant combinations, which may be referred to as the gauge invariant curvature perturbation ζ (defined eq(2.60), but it only correspond with the curvature perturbation in one particular gauge (the uniform density one).

In the following we define some gauges which will be used in this thesis, i.e. the conformal Newtonian gauge, the uniform density gauge and the spatially flat gauge. We will define also some gauge invariant quantities necessary to the study of the origin of the CMB temperature fluctuations.

Conformal Newtonian gauge. The longitudinal or conformal Newtonian gauge is the gauge in which the Bardeen potentials Φ and Ψ, defined as [7]

$$\Phi := \phi + \mathcal{H}(B - E') + (B - E')', \tag{2.56}$$

$$\Psi := \psi - \mathcal{H}(B - E'), \tag{2.57}$$

turn out to coincide with the scalar metric perturbations ϕ and ψ in the slices with zero-shear, namely such that $\sigma = (E' - B) = 0$. Notice that Φ and Ψ are gauge invariant quantities [7].

To set a gauge one has to set the coefficient α, β_i defined in Eq(2.16), which represent the gauge choice. As one can easily check, according to the transformations of B and E, respectively Eqs(2.21) and (2.20), to set the longitudinal gauge (labelled with l) one must require $(\alpha)_l = B - E'$. There are still 3 degrees of freedom, i.e. one could set $(\gamma_i)_l = S_i$ and $(\beta)_l = -E$, where β and γ_i are defined in Eq(2.17). In this way according to Eq(2.22), $(S_i)_l$ vanishes. Therefore the metric in this gauge results

$$ds^2 = a^2(\tau)\left\{-(1-2\Phi)d\tau^2 + [(1+2\Psi)\delta_{ij} + 2h_{ij}]\, dx^i dx^j\right\}. \tag{2.58}$$

Studying the dynamics of Φ and Ψ in the longitudinal gauge one finds (see [54], [51] and [57])

$$\Psi - \Phi = 8\pi G a^2 \Pi, \tag{2.59}$$

where Π is the trace-free scalar part of the anisotropic stress defined in (2.32). Indeed, in absence of anisotropic stress we have $\Phi = \Psi$ [5]. This means that there is only one variable required to describe all scalar metric perturbations.

UNIFORM DENSITY GAUGE. The uniform density gauge (u) is identified by requiring the energy density perturbation $(\delta\rho)_u = 0$. Thus the transformation equation (2.42) for $\delta\rho$ implies $(\alpha)_u = -\delta\rho^{(1)}/\rho_0'$. Notice that there are still 4 degrees of freedom that can be arbitrarily fixed.

A relevant quantity is the curvature perturbation in the uniform density hypersurfaces ζ that consists in the value of the curvature of the uniform density 3-dimensional slices [6] . In this gauge

$$\zeta := -(\psi)_u = -\left(\psi + \mathcal{H}\frac{\delta\rho}{\rho_0'}\right). \tag{2.60}$$

The curvature perturbation ζ is a very useful quantity, first of all because it is a gauge invariant variable. It is often used to study the evolution of the primordial density perturbations during inflation. We will discuss further about this quantity in the next section.

SPATIALLY FLAT GAUGE. An alternative gauge choice is the spatially flat or off diagonal gauge. In this gauge one selects spatial hypersurfaces on which the induced 3-metric on the three-dimensional hypersurfaces is left unperturbed by scalar, vector or tensor perturbations. Therefore one has to require $(\psi)_{flat} = (E)_{flat} = (F_i)_{flat} = 0$. Using Eqs (2.19), (2.20) and (2.23) this corresponds to a gauge transformation (2.16) where $(\alpha)_{flat} = \psi/\mathcal{H}$, $(\beta)_{flat} = -E_1$ and $(\gamma^i)_{flat} = -F^i$. Then the curvature of the three-dimensional slices is, according to Eq(2.19),

$$(\psi)_{flat} = \psi - \mathcal{H}(\alpha)_{flat} = 0. \tag{2.61}$$

The quantity ζ, in this gauge, depends only on the density perturbation, as one can easily see from Eq(2.60):

$$\zeta = -\mathcal{H}\frac{\delta\rho_{flat}}{\rho_0'}. \tag{2.62}$$

[5] This is satisfied in many cases of physical interest, for instance during an inflationary epoch driven by a single scalar field. In fact, in this latter epoch only neutrinos species contributes to the anisotropic stress but with a negligible supply (see again [51]).

[6] Strictly speaking the definition the curvature of a 3-dimensional slice is ${}^{(3)}R = \frac{4}{a^2}\nabla^2\psi$ and hence in the uniform density gauge ζ is the value of the curvature times k^2 in Fourier space.

2.6 Curvature and isocurvature perturbations

The gauge invariant curvature perturbation ζ is usually adopted to characterize the so called adiabatic perturbations. In fact the adiabatic perturbation is such that a net perturbation in the total energy density and in the intrinsic spatial curvature are produced. However, as we have seen, neither the energy density nor the curvature perturbation are gauge invariant, hence the utility of using the variable ζ.

A crucial result about the dynamics of the curvature perturbation is that under a quite wide range of situations ζ is constant on super-horizon scales. In fact, one can easily check that the perturbed continuity equation, derived from Eq(2.50) and written in the uniform density gauge gives an equation for ζ

$$\zeta' = -\mathcal{H}\frac{\delta P_{nad}}{\rho_0 + P_0} - \frac{1}{3}\nabla^2(v - E'). \tag{2.63}$$

From this equation we can clearly see that, on scales larger than the comoving Hubble horizon r_h, since the Laplacian rewrites in Fourier space as $k^2 \ll r_H$, the term $\nabla^2(v - E)$ is negligible and hence ζ is conserved if $\delta P_{nad} = 0$.

2.6.1 Single scalar field

Let's focus now on the case in which inflation is driven by a single scalar field the "inflaton" field $\varphi(t, \mathbf{x})$. Since such a field behaves like a perfect fluid no non-adiabatic fluctuations are created. This means that during inflation (and on super-horizon scales) ζ is the only scalar perturbation that we need. In fact, quantum fluctuations of the field are generated during inflation. Since gravity acts on any component of the Universe, the quantum fluctuations gives rise to perturbations of the curvature ζ. The physical wavelengths of these perturbations grow exponentially leaving the horizon. On super-horizon scales, curvature fluctuations are frozen in and considered as classical. Finally, when these fluctuations re-enters the horizon, during radiation or matter dominated epoch, the curvature perturbation gives rise to temperature and matter perturbations.

Let us sketch how density perturbations are generated during inflation. Since in this model the potential $V(\varphi)$ have to dominate the energy density, the primordial density perturbation is given by

$$\delta\rho \approx \frac{\partial V}{\partial \varphi}\delta\varphi. \tag{2.64}$$

This gives rise in turn to a curvature perturbation that we compute, for simplicity, in the spatially flat gauge:

$$\zeta = -\mathcal{H}\frac{\delta\rho_{flat}}{\rho_0'} = -H\frac{\delta\rho_{flat}}{\dot{\rho}_0} = -H\left(\frac{\delta\varphi}{\dot{\varphi}}\right)_{flat}. \tag{2.65}$$

To justify the last passage we recall that during inflation $\rho \simeq V(\varphi) = -3H\dot{\varphi}$ where we used the from the slow roll condition (1.24). Deriving this expression we find also $\delta\rho = -3H\dot{\varphi}\delta\varphi$. Finally, thanks to continuity equation (1.6) we find $\dot{\rho} = -3H(1/2\dot{\varphi}^2 + V(\varphi) + 1/2\dot{\varphi}^2 - V(\varphi)) = -3H\dot{\varphi}^2$. The result in Eq(2.65) is then straightforward to reach.

Let us now compute the power spectrum of the curvature perturbations is straightforward: remembering eqs (1.41) and (1.42) we find

$$\langle\zeta(\mathbf{k})\zeta^*(\mathbf{k}')\rangle = (2\pi)^3\delta^3(\mathbf{k}-\mathbf{k}')P_\zeta(k), \tag{2.66}$$

or, remembering the definition (1.43) of the dimensionless power spectrum:

$$\langle\zeta(\mathbf{k})\zeta^*(\mathbf{k}')\rangle = (2\pi)^3\delta^3(\mathbf{k}-\mathbf{k}')\frac{k^3}{2\pi^2}\mathcal{P}_\zeta(k), \tag{2.67}$$

with $\mathcal{P}_\zeta(k)$ that is

$$\mathcal{P}_\zeta(k) = \left(\frac{H^2}{2\pi\dot{\varphi}}\right)^2_k. \tag{2.68}$$

The amplitude of $\mathcal{P}_\zeta(k)$ gives an estimate of the amplitude of the CMB temperature anisotropies. It can be shown, indeed, [7] that at the time the temperature fluctuations froze in (the recombination time), the Bardeen's potential Φ is related to ζ by

$$\Phi = -\frac{3}{5}\zeta. \tag{2.69}$$

In turn, as we will see later in Chap.3, the Bardeen gravitational potential Φ, is one of the main sources of the CMB anisotropies (For example through the so called Sachs-Wolfe effect $\Delta T/T = \Phi/3$. Therefore any particular feature of $\mathcal{P}_\zeta(k)$ like its scale dependence, is reflected in the CMB power spectrum.

Let us study the shape of the primordial power spectrum $\mathcal{P}_\zeta(k)$. Since inflation in general predicts a non scale invariant spectrum, we define the *spectral index* n_s which quantify the departure of scale invariance of $\mathcal{P}_\zeta(k)$ through the relation

$$(n_s - 1) = \frac{d\ln\mathcal{P}_\zeta(k)}{d\ln k}. \tag{2.70}$$

Eq(2.68) allows us to write $\mathcal{P}_\zeta(k)$ as a power law in k:

$$\mathcal{P}_\zeta(k) = A_s\left(\frac{k}{k_0}\right)^{n_s-1}, \tag{2.71}$$

where k_0 is some pivot scale and A_s a normalization. Note that the value $n_s = 1$ denotes a scale invariant spectrum. The predicted departure from

[7] See [51] Chap.8.4

scale invariant in general is very small: in the case of a single scalar field n_s in terms of the slow-roll parameters (1.26) and (1.27) is given by

$$n_s - 1 = -6\epsilon + 2\eta. \tag{2.72}$$

The explicit calculation of the spectral index can be found in AppendixA. Observations confirmed this prediction; the last measurement about n_s was provided by *Planck* [66] which measured $n_s = 0.9624 \pm 0.0075$, a more than 5-sigma deviation from scale invariance.

2.6.2 Multiple fields: isocurvature perturbations

The presence of more than one scalar field during inflation causes the increase of the degrees of freedom and as a result we have to consider also other primordial perturbations in addition of ζ: we have to take into account also the *isocurvature* perturbations modes S.

Let us assume that at early times, during inflation, there were n real scalar fields. We describe them as n interacting fluids. Let ρ_I be the energy density of the I^{th} fluid and $\delta\rho_I$ its density fluctuation. We can still construct the gauge invariant curvature perturbation for each fluid

$$\zeta_I = -\psi - \mathcal{H}\frac{\delta\rho_I}{\rho_I'} \tag{2.73}$$

which represents the the curvature of the uniform I^{th}-fluid density hypersurfaces. More in general we can use such gauge invariant quantities to construct the total curvature ζ in the uniform total density gauge; but, in addition to ζ, we have to define $n-1$ isocurvature perturbations S_{IJ} that are relative density perturbations between the different components of the fluid. Thus we define

$$\zeta = -\psi - \mathcal{H}\frac{\delta\rho}{\rho'} = \sum_I \frac{\rho_I'}{\rho'}\zeta_I, \tag{2.74}$$

$$S_{IJ} = -3(\zeta_I - \zeta_J). \tag{2.75}$$

We can also compare the relative density fluctuation of the I^{th} fluid with the total density perturbation. We label with S_I this kind of isocurvature perturbations

$$S_I = -3\mathcal{H}\ (\zeta_{tot} - \zeta_). \tag{2.76}$$

In conclusion we saw that in presence of n fluids we have to consider n types of perturbations: the adiabatic curvature perturbation ζ and the entropy or isocurvature one S_I. We will use this formalism in Chap.5 when we will discuss an alternative model of inflation the so called *curvaton model* based on two real scalar fields.

2.6.3 The δN formalism

To conclude this section we introduce the so called δN formalism which, in some cases, is a powerful technique to calculate the primordial curvature power spectrum and non-Gaussianity in presence of more than one fields, [71].

In the uniform density gauge $\zeta(t, \mathbf{x})$ affects the spatial part of the squared line element ds^2, adding a factor $e^{2\zeta(t,\mathbf{x})}$. We can therefore interpret this field as the perturbed scale factor $a'(t, \mathbf{x}) = a(t)\, e^{\zeta}(t, \mathbf{x})$,

$$ds^2 = -dt^2 + a^2(t) e^{2\zeta(t,\mathbf{x})} dx^i dx_j \equiv -dt^2 + a'^{\,2}(t, \mathbf{x})\; dx^i dx_j. \tag{2.77}$$

For super-horizon modes, ζ is frozen and if we look at the different regions of the Universe separated by a super-horizon distance, they are causally disconnected from each other. So they evolve independently and locally in space. Therefore, in the uniform density gauge, different regions experience a different scale factor. This is also called the separate universe picture. In conclusion the primordial curvature perturbations manifest themselves as the different number of e-foldings δN, at different positions [8]. Since different regions experiences a slightly different different expansion we can split N into a background value N_0 plus fluctuations. They are function of the primordial density perturbation which in turn depends on the quantum fluctuations of the fields $\phi_I(t, \mathbf{x})$ during inflation. As a result we can write

$$\delta N(\phi_{0\,I}) = N(\phi_{0\,I}) - N_0(\phi_0). \tag{2.78}$$

so we can expand δN in power series:

$$\delta N = N_I \delta\varphi_I + \frac{1}{2} N_{IJ} \delta\varphi_I \delta\varphi_J + \dots, \tag{2.79}$$

where the subscript I denotes the partial derivatives with respect to I^{th} fluid and the sum over the repeated indices is understood.

Notice that the perturbation of δN coincides with the curvature perturbation ζ. In fact, differentiating the definition (1.9) of N, we get $\delta N = H\delta t$. Now, the equation of the dynamics of the quantum fluctuations $\delta\varphi(t, \mathbf{x})$, Eq(1.28), on super-horizon scales, when the term $\nabla^2\delta\varphi/a^2 \approx 0$, is the same equation obeyed by $\dot{\varphi}$, the derivative of the background value. We get its evolution equation by deriving the equation of motion of φ_0, (1.23):

$$(\dot{\varphi})^{\cdot\cdot} + 3H(\dot{\varphi})^{\cdot} = -V_{\varphi\varphi}\dot{\varphi}. \tag{2.80}$$

This allows us to write that, on large scales, $\delta\varphi(t, \mathbf{x}) = -\delta\varphi(\mathbf{x})\dot{\varphi}(t) \equiv -\delta t(\mathbf{x})\dot{\varphi}(t)$. This means that the scalar field, in each region of the Universe,

[8] Let us stress that the number of e-foldings N, defined in Eq(1.9), provides an evaluation of the duration of inflation and the expansion of the Universe during inflation.

evolves in the same way but at different times, because of the presence of the quantum fluctuations which give the term $\delta t(\mathbf{x})$. Then, we can write

$$\delta N = H\delta t = -H\frac{\delta\varphi}{\dot{\varphi}} = -H\frac{\delta\rho_{flat}}{\dot{\rho}}, \tag{2.81}$$

where the last step is justified by Eq(2.65). In conclusion, if we compute $\delta\rho$ in the uniform density gauge we get

$$\delta N = -H\frac{\delta\rho_{flat}}{\dot{\rho}} = \zeta, \tag{2.82}$$

as we stated.

Thanks to Eq(2.79) it is straightforward to calculate formally any n-point correlation function of the curvature perturbation ζ and its Fourier transform. As example we compute the the 2-point correlation function in Fourier space:

$$\langle\zeta(\mathbf{k})\zeta^*(\mathbf{k}')\rangle = N_I N_J\langle\delta\varphi_I k\delta\varphi_J^* k'\rangle = (2\pi)^3\delta^3(\mathbf{k}+\mathbf{k}')\frac{k^3}{2\pi^2}\mathcal{C}_{\phi_I\phi_J}, \tag{2.83}$$

where $\mathcal{C}_{IJ}$ is the correlation function between the fields I and J, which reduces to $\mathcal{P}_{\delta\varphi_I}$ in the case $I = J$

Another important parameter which in some cases [9] can be calculated using the δN formalism is the level of non-gaussianity f_{NL} of the curvature perturbation [10]. We can calculate the parameter f_{NL} by directly calculating the bispectrum of curvature perturbation using the δN expansion (2.83). What we find is

$$\begin{aligned}\langle\zeta(\mathbf{k})\zeta(\mathbf{k}')\zeta(\mathbf{k}'')\rangle &= \delta^3\left(\sum\mathbf{k}\right)\frac{N_I N_J N^{IJ}}{(N_K N_K)^2}\left[P_\zeta(k)P_\zeta(k') + \text{"}cyclic\text{"}\right] \\ &\equiv f_{NL}\left[P_\zeta(k)P_\zeta(k') + \text{"}cyclic\text{"}\right],\end{aligned} \tag{2.84}$$

while we call bispectrum the quantity $\mathcal{B}_\zeta(k,k',k'') = [P_\zeta(k)P_\zeta(k') + \text{"}cyclic\text{"}]$. In conclusion we find

$$f_{NL} = \frac{N_I N_J N^{IJ}}{(N_K N_K)^2}. \tag{2.85}$$

Let us consider the inflaton field slow-rolling down its potential. The above expression for f_{NL} reduces to $f_{NL} = N_{\varphi\varphi}/N_\varphi^2$. Remembering that ζ is equal to δN, thanks to Eq(2.79) we can expand the curvature perturbation as

$$\delta N = N_I\delta\varphi_I + \frac{1}{2}N_{IJ}\delta\varphi_I\delta\varphi_J + \dots. \tag{2.86}$$

[9] This formalism applies only on cases in which one is interested on perturbations present on scales much greater than the Hubble horizon, therefore one can compute only the non-gaussianity in this case.

[10] Note that here the f_{NL} parameter is different from the one defined in Chap.1, in fact here we are referring to the non-gaussianity ot curvature perturbation while in the previous chapter were dealing with primordial quantum fluctuations. The full calculation of the parameter f_{NL} which takes into account also the sub-horizon evolution can be found in [40] and [7].

Then, Eq(2.65) tells us

$$N_\varphi = \frac{H}{\dot{\varphi}} \approx \frac{1}{\sqrt{2}M_{pl}} \frac{1}{\sqrt{\epsilon}}. \tag{2.87}$$

and hence from this we can derive the second derivative $N_{\varphi\varphi}$ which, after some algebra results

$$N_{\varphi\varphi} \approx -\frac{1}{2} \frac{\eta - 2\epsilon}{M_{Pl}^2 \, \epsilon}. \tag{2.88}$$

In conclusion, we argued that the level of non-gaussianity generated during the standard inflation is typically [20]

$$f_{_{NL}} \approx \mathcal{O}(\epsilon, \eta). \tag{2.89}$$

2.7 Tensor perturbations

Besides scalar perturbations, also tensor perturbations are inevitably generated during inflation. Tensor perturbations are generated with the same mechanism in which scalar perturbations were generated. They arose from the quantum fluctuations of the inflaton field which affects the metric causing the generation of tensor perturbations. Then the fluctuations in the gravitational field get pushed outside the horizon during inflation where they remain as classical gravitational waves [1].

In fact the perturbed Einstein's equations reduces for tensor perturbations to

$$h_{ij}'' + 2\mathcal{H}h_{ij}' - \frac{\nabla^2 h_{ij}}{a^2} = 8\pi G a^2 \Pi_{ij}^{(TT)}, \tag{2.90}$$

where $\Pi_{ij}^{(TT)}$ is the transverse and trace-free part of the anisotropic stress (2.32). We want to study this equation in Fourier space, then we write the tensor perturbation as

$$h_{ij}(\tau, \mathbf{x}) = \int \frac{d^3k}{(2\pi)^3} \, e^{-ikx} \sum_{s=+,\times} \epsilon_{ij}^s(\tau, \mathbf{k}) \; h^s(\mathbf{k}), \tag{2.91}$$

where the subscript s states for the two possible polarization states: $+$ and $\times$, while $\epsilon_{ij}^s(\mathbf{k})$ is the polarization tensor. It obeys the conditions

$$\epsilon_{ii}^s(\mathbf{k}) = k_i \, \epsilon_{ij}^s(\mathbf{k}) = 0 \qquad \text{and} \qquad \epsilon_{ij}^s(\mathbf{k}) \, \epsilon_{ij}^{s'}(\mathbf{k}) = 2\delta_{ss'} \, . \tag{2.92}$$

Assuming the inflation was driven by a single scalar field $\varphi(t, \mathbf{x})$ we have $\Pi_{ij}^{(TT)} = 0$ and hence, Eq(2.90), in Fourier space, rewrites as

$$h_s{}'' + 2\mathcal{H}h_s{}' + \frac{k^2}{a^2} h_s = 0. \tag{2.93}$$

Notice that $h^s(\tau, \mathbf{k})$ obeys the same equation obeyed by a massless scalar field (1.28) in an unperturbed FRW flat metric. As a result tensor perturbations experience the same evolution of the quantum fluctuations $\delta\varphi$: their amplitude oscillates at sub-horizon scales then, at horizon crossing, it freezes at the value

$$|h^s| = \sqrt{32\pi G}\frac{H_k}{\sqrt{2k^3}}, \tag{2.94}$$

and then the perturbations reach the super-horizon regime.

Following the same steps as for the scalar perturbations we find that the 2-point correlation function in Fourier space which is

$$\langle h^s(\mathbf{k}) h^{s'}(\mathbf{k}')\rangle = (2\pi)^3\ \delta^{ss'}\ \delta^3(\mathbf{k}+\mathbf{k}')\ \frac{2\pi^2}{k^3}\ \mathcal{P}_h(k), \tag{2.95}$$

where $\mathcal{P}_h(k)$ is the dimensionless power spectrum, which thanks to Eq.(2.94) results

$$\mathcal{P}_h(k) = \frac{H_k^2}{\pi^2 M_{Pl}^2}. \tag{2.96}$$

This latter is usually parametrized as

$$\mathcal{P}_h(k) = A_t\left(\frac{k}{k_0}\right)^{n_t}, \tag{2.97}$$

where n_t, is defined as

$$n_t = \frac{d\ln\mathcal{P}_h}{d\ln k}. \tag{2.98}$$

In the case of the single-field models of inflation holds [11]

$$n_t = -2\epsilon. \tag{2.99}$$

An other important cosmological parameter is the so called tensor-to-scalar *ratio*, r, defined as

$$r = \frac{2\mathcal{P}_h(k)}{\mathcal{P}_\zeta(k)}. \tag{2.100}$$

where the factor 2 takes into account the two states of polarization of the tensor perturbations. From Eqs(2.96) and (2.68) one finds that in the case of single-field inflation holds

$$r = 16\epsilon. \tag{2.101}$$

Notice that a measurement of r would allow us to quantify $\mathcal{P}_h(k)$. We want to point out that the tensor power spectrum (2.96) depends only on the value of the inflationary Hubble rate, which in turn is proportional to the energy density ρ. Therefore with a measure of r we could infer the energy scale of inflation.

[11] The expression of n_t is explicitly computed in AppendixA.

Moreover, the ratio r defines also an important *consistency relation*, which holds for every model of inflation driven by a single scalar field. Such consistency relation relates the tensor-to-scalar-ratio r with the scale dependence coefficient n_t of is $\mathcal{P}_h(k)$. Comparing Eq(2.99) with Eq(2.101), it reads

$$r = -8\, n_t. \tag{2.102}$$

Chapter 3

The Cosmic Microwave Background

The inflation, was introduced to solve some problems of the standard cosmological model. But the theory of inflation did not exhaust in this. At the present day, its most important success consists the compelling description of the origin of the temperature anisotropies of the Cosmic Microwave Background (CMB), that the inflationary paradigm gives. The CMB is a thermal radiation which is assumed to be left over from an epoch in which the Universe was very hot [42], [51]. Although predicted by earlier theories, the CMB was first found accidentally in 1964 by A. Penzias and R. Wilson. They found a low, steady, mysterious noise evenly spread over the sky that persisted in their receiver. Were R. Dicke, P. Peebles, P. Roll and D. Wilkinson that interpreted this radiation as a signature of the primordial hot phase of the Universe.

The CMB radiation is characterized by a blackbody spectrum at a temperature $T_0 = 2.725\ K$. A crucial observable quantity related to the CMB is the angular temperature fluctuations between different patches of the sky. The mean amplitude of such fluctuations is very small ($\Delta T/T_0 \sim 10^{-5}$), however their detailed study, have led to a stunning confirmation of the Inflation+ΛCDM: what we can call now the standard model of cosmology. The satellite probe COBE [59] was the first survey which mapped the CMB temperature anisotropies of cosmological origin. After COBE, the great technological progresses have allowed the lunch of the WMAP satellite, [11],[12] which scanned the sky with an angular resolution of 1°. Anyway, is the *Planck* satellite, [65], [66], [67], [69], the ultimate survey on the temperature anisotropies. Whose angular resolution was about 0.07°, nearly a hundred times the resolution of COBE. Planck is testing theories of the early Universe and the origin of cosmic structure and providing a major source of information relevant to many cosmological and astrophysical issues.

In this chapter we will study some features regarding the CMB, focusing mainly on its temperature fluctuations. We are going to illustrate their origin, from the quantum fluctuations of the inflaton field, to the time of recombination, when the photons were free to propagate until us. Then we

will mention how the study of CMB anisotropies can be carried out. We will highlight the agreement between observations and the predictions of the standard cosmological model. However, despite this extremely accurate agreement, some observed features seem to depart from this concordance scenario. In particular some of these features seem to suggest a possible deviation from statistical isotropy, which is one of the building blocks of modern cosmology, and one of the prediction of the simplest models of inflation. For these reasons such features have been dubbed "anomalies". We will therefore discuss some basics of the observational aspects of these anomalies. A large part of this thesis is about the so called *Hemispherical Power Asymmetry*, one of the most important anomalies.

Also, throughout the chapter we will mention the polarized component of the CMB, an important observable which is focusing the attention of the cosmological community because it can still gives us a lot of informations, for instance about the existence and the features of the primordial gravitational waves. Moreover the knowledge of the CMB polarization map could allow us to infer more about the statical significance of the founded anomalies in the CMB temperature anisotropies.

3.1 The CMB temperature anisotropies and the polarized component

In the standard scenario, inflation ends when the inflaton (o an another field) falls into and starts to oscillates around the minimum of its potential. During this phase, called *reheating*, the field acquires a non-negligible mass m_{eff} and behaves like pressureless matter (see [42] Ch.8.3). Since $m_{eff} \neq 0$, interactions between the inflaton and other fields becomes relevant. Therefore the inflaton starts to decay into radiation and relativistic particles, repopulating the otherwise cold and empty Universe. It is after this epoch, when the inflaton is completely decayed, that begins the usual FRW Universe first radiation and then matter dominated.

At these early epochs photons and baryons are tightly coupled. We can describe the Universe content as a relativistic fluid with density ρ and pressure $P \simeq \rho/3$. More in detail, since the scattering cross section between a charged particle and a photon is $\sigma \propto m^{-1}$, where m is the particle mass, the electrons, the lightest interacting particles, are the ones that mainly interact with photons. In turn, electrons scattering with baryons via electromagnetic scattering. The main interaction between electrons and photons is the Compton scattering

$$e^- + \gamma \rightarrow e^- + \gamma,$$

that reduces to Thompson scattering when electrons are no longer relativistic. Anyway it is thanks to all the interactions with matter that the fluid is

characterized by a blackbody spectrum [1].

Photons and baryons remains tightly coupled until the *recombination* or *decoupling* epoch which happened when the Universe was matter-dominated. At that epoch the temperature of the Universe has cooled enough to allow the formation of the hydrogen atoms. Since electrons and protons are bounded together, the Thompson cross section decrease by almost 2000 times and, as a result, this scattering is no longer efficient. For this reason matter decouples from radiation and therefore photons are free to propagate until us. Assuming that recombination occurs at the same time, t_{rec}, in each region of the Universe, the photons that travel until us comes from the same spherical hypersurface called *last scattering surface* and placed at redshift $z_{rec} \approx 1100$ [2].

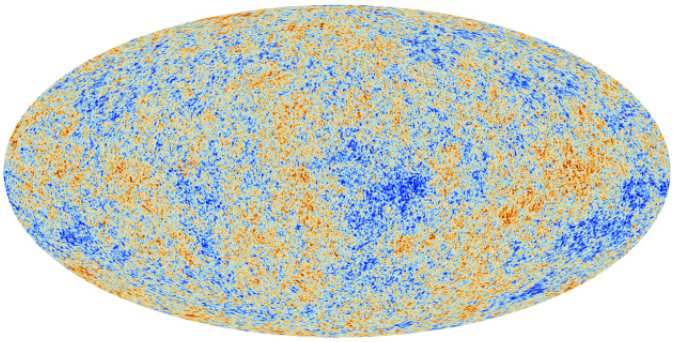

Figure 3.1: The anisotropies of the Cosmic Microwave Background as observed by Planck, [65].

Let us now focus on how CMB cosmological fluctuations arise from the primordial curvature perturbations. We choose to work in the Newtonian conformal gauge defined in Sec.2.5. In such a gauge, to describe all the scalar perturbations we need only the gauge invariant Bardeen potential, Φ (Eq.(2.56)), which during matter domination is proportional to the curvature perturbation ζ through Eq(2.69). Let us stress that Φ (on very large scales) corresponds to the primordial gravitational potential that arose from the inflaton primordial density perturbation. We call gravitational wells the regions in which Φ is more intense. Photons are not much attracted by these wells, but this is not the case for baryons that are massive: they fall down dragging with them the photons. Because of the fluid pressure, which contrasts this falling, the gravitational collapse does not occur but, rather the fluid starts to oscillate. Studying the relativistic fluid in Fourier space

[1] Notice that until now, no deviations from the blackbody shape were found in the CMB spectrum.

[2] Obviously the instantaneous recombination is only an approximation. This means that the last scattering surface is not a properly surface but there is an optical depth Δz in which recombination occurs. However $\Delta z \ll z_{rec}$, [36]

one can argue the presence of the so called *acoustic oscillations*. They are generated by the mechanism of compression and rarefaction caused by the contrast between the gravitational force and the fluid pressure. Because of these oscillations we expect that the CMB spectrum acquires a sinusoidal shape. An important feature is that the acoustic oscillations propagate in the fluid with a finite velocity, that in units of c is $c_s \simeq 1/\sqrt{3}$.

At recombination time photons are free to exit from the gravitational wells so they propagate almost undisturbed to us. Notice that it is at this time that the Universe, becomes transparent to the CMB photons. To calculate the temperature of the CMB photon that reach us, we split their temperature into the mean value T_0 [3] plus fluctuations ΔT. In dimensionless units the latter are $(\Delta T/T)_*$, where by the subscript $*$ we mean the fluctuations of CMB photons evaluated at time of decoupling. At this value we have to add another term, acquired when the photons get out from the graviational wells from the last scattering surface.Indeed, they experience a gravitational shift of magnitude Φ. In conclusion the effective temperature anisotropy that is measured is:

$$\left(\frac{\Delta T}{T}\right) = \left(\frac{\Delta T}{T}\right)_* + \Phi_*. \tag{3.1}$$

To compute the initial temperature fluctuations which are related to the primordial ones from inflation, we use the relation between the temperature T of the Universe and the scale factor a ($T \propto a^{-1}$, [42]). This relation says that $\delta T/T = -\delta a/a$, so when the Universe is matter dominated, thanks to Eq(1.8),

$$a \propto t^{2/3} \;\Rightarrow\; \frac{\delta a}{a} = \frac{2}{3}\frac{\delta t}{t} = \frac{2}{3}\Phi; \tag{3.2}$$

where the last step is justified by the gravitational redshift. Indeed, since Φ affects the $_{00}$ component of the metric tensor, it affects also the proper time τ of the photons:

$$d\tau = \sqrt{g_{00}}\, dt \simeq (1+\Phi)dt, \tag{3.3}$$

and hence

$$\frac{\Delta t}{t} \equiv \frac{\tau - t}{t} \simeq \Phi. \tag{3.4}$$

In conclusion the total temperature fluctuations are related to the gravitational potential through the relation

$$\frac{\Delta T}{T} = \frac{\Phi_*}{3}. \tag{3.5}$$

The physical process described here to compute the CMB temperature anisotropies, is called Sachs-Wolfe effect, it holds on large angular scales, the ones

[3] Hereafter we drop the subscript 0.

larger than the sound horizon s_* [4] computed at t_{rec} and hence that had not been influenced by the oscillations of the relativistic fluid. Therefore this result does not take into account any other process that occurs in the relativistic fluid like the acoustic oscillations on small scales [36].

These are the basic facts about the origin of the temperature fluctuations field $\Delta T/T$. For a more detailed discussion the reader is referred to [37] and [24] (Chapters. 7-8).

Before concluding this section we give some information about the formation of the CMB polarized component. The radiation in the CMB is expected to be polarized because of Thompson scattering at the time of decoupling. To understand how it happens let us consider the scattering between a photon and an electron. The latter is placed in the origin of the axes while the photon in incoming from the $-\mathbf{x}$ direction, with polarization vector $\hat{\epsilon}'$. Let us assume that the photon is scattered into the direction $\mathbf{z}$ with a new polarization vector $\hat{\epsilon}$. Heuristically, incoming radiation shakes the electron in the direction of its electric field vector $\hat{\epsilon}'$ causing it to radiate with an outgoing polarization $\hat{\epsilon}$ parallel to that direction. However outgoing polarization must be orthogonal to $\mathbf{z}$ the outgoing direction and so there is only one allowed polarization state, the one such that $\hat{\epsilon} \parallel \mathbf{y}$.

Let us consider now the primordial fluid of photon and electrons. Given an electron, if the photon distribution surrounding it is isotropic, Thompson scattering cannot generate a net polarization. In this case in fact, radiation coming along the *y–axis* would provide the polarization state that is missing from that coming along *x–axis* and so on. Anyway, an isotropic distribution might generate a net polarization.

The simplest example of anisotropy is a dipole pattern. Let us assume that its axis coincides with the x-axis, in the $+\mathbf{x}$ direction there is the cold spot while the hot spot is in the $-\mathbf{x}$ direction. Now the outgoing intensity along the x-axis comes from the $\pm\mathbf{y}$ incident radiation, which has the average temperature. The outgoing intensity along the y-axis is also neither hot nor cold because it comes from a cold spot (the $\mathbf{x}$ direction) and a hot spot (the $-\mathbf{x}$ direction). In conclusion the dipole pattern leads only to cancellations and unpolarized outgoing radiation.

To produce polarized radiation, the incoming radiation must have a nonzero quadrupole. Figure 3.2 illustrates the polarization produced by an incoming quadrupole. The hotter (colder) radiation incident from the $\mathbf{x}$ ($\mathbf{y}$) direction produces higher (lower) intensity along the $\mathbf{y}$ ($\mathbf{x}$) axis for the outgoing wave. Therefore, the intensity of the outgoing wave is greater along the $\mathbf{y}$-axis than along the $\mathbf{x}$-axis: the outgoing radiation is polarized.

The fact that Thompson scattering produces polarization only when the

[4] The sound horizon s is the maximum distance trvelled by the acoustic oscillations, $s(t) = \int_{t_0}^{t} c_s dt$.

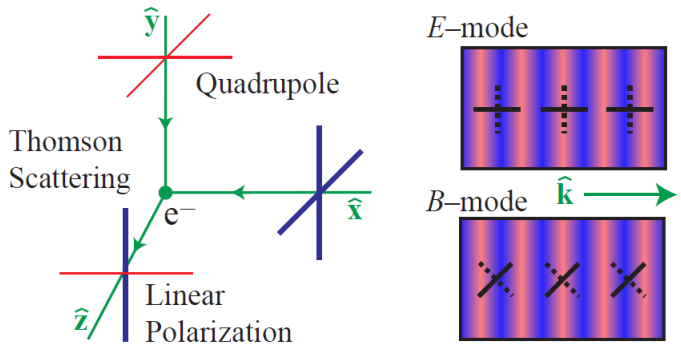

Figure 3.2: Polarization generation and classification, [37]. Left: Thomson scattering of quadrupole temperature anisotropies (depicted here in the $x-y$ plane) generates linear polarization. Right: polarization in the $x-y$ plane along the outgoing z axis. The component of the polarization that is parallel or perpendicular to the wavevector $\mathbf{k}$ is called the E-mode and the one at 45° angles is called the B-mode.

incident field has a quadrupole moment has important ramifications for cosmology. First of all we need Thompson scattering to produce the polarization, so we need to focus on the epoch before electrons and photons have completely decoupled from each other. However, in this epoch electrons and photons are tightly coupled, which leads to a very small quadrupole. Therefore, we expect polarization from the standard decoupling epoch to be smaller than the anisotropies. For this reason the polarization spectrum should be smaller than the temperature spectrum at recombination. As a final remark notice that the quadrupole moment in the photon distribution around an electron can be generated by both scalar and tensor perturbation but with specific distinctions that we will show later.

3.2 Basics of CMB angular power spectrum

3.2.1 Temperature anisotropies

Since the observed CMB comes from the spherical last scattering surface located at redshift $z_* \approx 1100$, the temperature anisotropies are usually expressed by using a spherical harmonic expansion of the CMB sky:

$$\theta(\hat{\mathbf{n}}) := \frac{\Delta T}{T}(\hat{\mathbf{n}}) = \sum_{l,m} a_{lm} Y_{lm}(\hat{\mathbf{n}}). \tag{3.6}$$

Since a single spherical harmonic $Y_{lm}(\hat{\mathbf{n}})$ corresponds to angular variation of $\Delta\theta \sim \pi/l$, the a_{lm} coefficients contain anisotropy information from the size

of the CMB map with angular aperture equal to $\Delta\theta$. The above expansion starts from the quadrupole $l = 2$: the monopole is just the mean temperature $T_0 = 2.725\ K$ while the second term, the dipole, is by far dominated by the result of the Doppler shift caused by the motion of the Earth relative to the nearly isotropic blackbody field. For this reason only the higher multipoles ($l \geq 2$) are considered to study the perturbations in the energy density of the early Universe.

The a_{lm} coefficients are the projection of the field $\theta(\hat{\mathbf{n}})$ into the sphere. On the other hand $\theta(\hat{\mathbf{n}})$ depends on $\Phi(t, \mathbf{x})$ which is directly related to the inflaton fluctuations, it is expected that they are almost gaussian distributed. Assuming that only the Sachs-Wolfe effect contributes to generate $\theta(\hat{\mathbf{n}})$, their explicit form is

$$\begin{aligned} a_{lm}^{SW} &= \int d\Omega_{\mathbf{n}} \theta(\hat{\mathbf{n}}) Y_{lm}^*(\hat{\mathbf{n}}) = \\ &= \frac{1}{3} \int d\Omega_{\mathbf{n}} \Phi_*(\hat{\mathbf{n}}) Y_{lm}^*(\hat{\mathbf{n}}) = \\ &= \frac{1}{3} \int d\Omega_{\mathbf{n}}\ Y_{lm}^*(\hat{\mathbf{n}}) \int \frac{d^3k}{(2\pi)^3} e^{-i\mathbf{kx}} \Phi_*(\mathbf{k}). \end{aligned} \tag{3.7}$$

Notice that in the last step we write Φ_* [5] in Fourier space. Now the exponential $e^{-i\mathbf{kx}}$ can be expanded into a sum of spherical Bessel functions $j_l(k\, x_{dec})$:

$$e^{-i\mathbf{kx}} = 4\pi \sum_{l,m} (-i)^l j_l(k\, x_{dec}) Y_{lm}^*(\hat{\mathbf{k}}) Y_{lm}(\hat{\mathbf{n}}), \tag{3.8}$$

where x_{dec} is the distance from the last scattering surface. Plugging the above expression in Eq(3.7) we get

$$\begin{aligned} a_{lm}^{SW} &= \frac{4\pi}{3} \int \frac{d^3k}{(2\pi)^3}\ d\Omega_{\mathbf{n}}\ \Phi_*(\mathbf{k}) \sum_{l'm'} (-i)^{l'}\ j_{l'}(k\, x_{dec})\ Y_{l'm'}^*(\hat{\mathbf{k}}) \\ &\qquad \times Y_{l'm'}(\hat{\mathbf{n}}) Y_{lm}^*(\hat{\mathbf{n}}) = \\ &= \frac{4\pi}{3} \int \frac{d^3k}{(2\pi)^3} \Phi_*(\mathbf{k}) \sum_{l'm'}\ j_{l'}(k\, x_{dec})\ Y_{l'm'}^*(\hat{\mathbf{k}}). \end{aligned} \tag{3.9}$$

Notice that in the second step we used the orthonormality of the spherical harmonics $\int d\hat{\mathbf{n}}\, Y_{lm}^*(\hat{\mathbf{n}})\, Y_{l'm'}(\hat{\mathbf{n}}) = \delta_{l\,l'}\, \delta_{mm'}$. Notice also that the above expression the term $j_{l'}(k\, x_{dec})/3$ takes into account for the Sachs-Wolfe effect and for the projection of the plane waves into the spherical surface. In general, if we consider all the physical processes that occur in the CMB (like the acoustic oscillations) we generalize $j_{l'}(k\, x_{dec})/3$ with $\Delta_l(k)$ that takes into

[5] We stress that here with the subscript $*$ we mean the potential Φ evaluated at decoupling time.

account of both the relation between Φ and θ and the projection of Φ into the spherical surface. Therefore in general the a_{lm} coefficients are given by

$$a_{lm} = 4\pi \int \frac{d^3k}{(2\pi)^3} \, (-i)^l \Phi(\mathbf{k}) \Delta_l(k) Y^*_{lm}(\hat{\mathbf{k}}). \tag{3.10}$$

To compute the correlation matrix $\langle a_{lm} a^*_{l'm'} \rangle$, we have to know the power spectrum of the Bardeen potential $P_\Phi(k)$. Since at the time of decoupling the Universe is matter dominated, at first order in the perturbations,

$$\Phi = -\frac{3}{5}\zeta. \tag{3.11}$$

where we recall that ζ is the curvature perturbation introduced in Sec.2.6. Then from Eqs. (2.66) and (2.68) we get

$$\langle \Phi(\mathbf{k}) \Phi(\mathbf{k}') \rangle = (2\pi)^3 \delta^3(\mathbf{k} + \mathbf{k}') \frac{k^3}{2\pi^2} \mathcal{P}_\Phi(k) \tag{3.12}$$

with

$$\mathcal{P}_\Phi(k) = \frac{9}{25} \mathcal{P}_\zeta(k) = \left(\frac{3}{5} \frac{H^2}{2\pi\dot{\varphi}} \right)^2_k. \tag{3.13}$$

Finally we have all the tools to compute the angular 2-point function:

$$\begin{aligned} \langle a_{lm} a^*_{l'm'} \rangle &= (4\pi)^2 \int \frac{d^3k}{(2\pi)^3} \frac{d^3k'}{(2\pi)^3} \, (-i)^{l+l'} \langle \, \Phi(\mathbf{k}) \Phi(\mathbf{k}') \, \rangle \, \Delta_l(k) \Delta^*_{l'}(k') \\ &\qquad \times Y^*_{lm}(\hat{\mathbf{k}}) Y_{l'm'}(\hat{\mathbf{k}}') = \\ &= (4\pi)^2 \int \frac{d^3k}{(2\pi)^3} (-i)^{l+l'} \Delta_l(k) \Delta^*_{l'}(k) P_\Phi(k) Y^*_{lm}(\hat{\mathbf{k}}) Y_{l'm'}(\hat{\mathbf{k}}) = \\ &= \delta_{ll'} \, \delta_{mm'} \, C_l; \end{aligned} \tag{3.14}$$

where we used the orthonormality of the spherical harmonics to justify the last step. In Eq(3.14) we defined the temperature *angular power spectrum* [6] as

$$C_l = \frac{2}{\pi} \int dk \; k^2 P_\Phi(k) |\Delta_l(k)|^2. \tag{3.15}$$

Here, $|\Delta_l(k)|^2$ is called transfer function. It takes into account for both the projection of the plane expansion into the sphere and the physics occurred after recombination. If we consider only the Sachs-Wolfe effect, we have only the projection effects and hence, remembering Eq(3.9), the transfer function consists in the simple spherical Bessel function: $|\Delta_l(k)|^2 = (j_l(k\, x_{dec})/3)^2$.

Notice that in the angular expansion, homogeneity and isotropy states that two different coefficients a_{lm} and $a_{l'm'}$ are uncorrelated unless $l = l'$ and $m = m'$. Another interesting feature is that since the power spectrum of Φ

[6] Notice that in the next subsection we will add the superscript (TT) to refer to C_l

is expected to be almost scale invariant, the same is expected for the CMB power spectrum on the largest angular scales (those beyond the cosmological horizon at recombination). Hence without considering the effects of the acoustic oscillations, one finds that the quantity $l(l+1)C_l$ should be almost constant.

From the experimental point of view the angular power spectrum C_l is computed averaging on m the a_{lm} coefficients for a fixed l:

$$C_l = \frac{1}{2l+1} \sum_{m=-l}^{l} |a_{lm}|^2. \tag{3.16}$$

Such estimates leads to an intrinsic variance which affects the angular power spectrum C_l. This is the so called *cosmic variance* that is due to the fact that there is only one realization of the temperature fluctuations field. The cosmic variance decreases when l grows, unfortunately it is bigger just on the largest scales, the ones that are more interesting for us because they are directly related to inflation, since they are affected only by the Sachs-Wolfe effect.

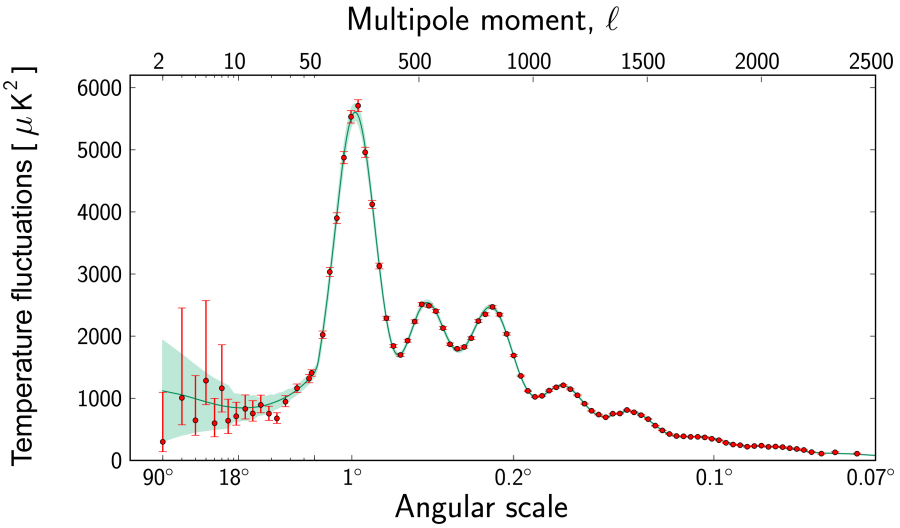

Figure 3.3: CMB angular power spectrum detected by Planck, [65]. The red dots correspond to measurements made with Planck, the error bars that account for cosmic variance. The green curve represents the best fit of the cosmological standard model.

The most recent measurement about the CMB anisotropies are shown in Fig.(3.3). In the figure the quantitiy $l(l+1)C_l$ is plotted, as a function either of the multipole (top) or of the subtended angle (bottom). All the data are

fitted by the ΛCDM theoretical model which has only six free parameters: the amplitude (A_s) of the scalar power spectrum and its spectral index (n_s), the optical depth to re-ionization (τ), the angular amplitude subtended by the sound horizon at recombination time ($\Delta\theta_*$) and the density ratio for baryons ($\Omega_b h^2$) and cold dark matter ($\Omega_c h^2$). In the plot we can distinguish three parts [75]: the Sachs-Wolfe plateaux ($l \leq 10$), the acoustic peaks ($10 \leq l \leq 1500$) and the damping tail ($l \geq 1500$). Let us analyze more in detail these three region.

THE SACHS-WOLFE PLATEAU ($l \leq 10$). The Sachs-Wolfe plateau corresponds to the region subtended by the lowest mulipoles. We expect an almost flat spectrum, because only the Sachs-Wolfe effect contributes to the temperature anisotropies on the largest angular scales. Such a region indeed, includes scales that are larger than the sound horizon, the maximum distance travelled by the acoustic oscillations before that matter and radiation decoupled. The sound horizon at recombination time subtended an angle $\Delta\theta_* \simeq 1^\circ$. For this reason anisotropies at largest scales have not evolved significantly, and hence directly reflect the "initial conditions" set by inflation.

This scales should be affected not only by scalar perturbations but also by the tensor ones. We have seen, indeed, that tensor perturbations are generated during inflation. During the super-horizon regime they are frozen, but when they re-enter the Hubble horizon they start to decay. Therefore they contribute only to angular scales corresponding to $l \lesssim 200$ or $\Delta\theta \gtrsim 1^\circ$, where 1° is the angular sound horizon at recombination time. To conclude: a fraction of the low multipoles signal is expected to be due to the contribution of primordial gravitational waves, although it is difficult to discriminate a small contribution of tensors from the scalar contribution. Anyway, as we will mention later, tensors can be distinguished using polarization information.

THE ACOUSTIC PEAKS ($10 \leq l \leq 1500$). At intermediate scales the effects of the primordial fluid of photons and baryons are relevant, indeed, the power spectrum at such angular scales is affected by the acoustic oscillations. Such oscillations were theoretically predicted long before they were discovered, and so they represent one of the triumphs of modern cosmology.

The underlying physics can be understood as follows. In the baryons-photons fluid photons provide most of the pressure while the baryons the inertia. The perturbations in the gravitational potential, dominated by the dark matter component, drive oscillations in the photon-baryon fluid, with photon pressure providing the restoring force. Such perturbations are quite small, and so evolve linearly. For this reason each Fourier mode evolves independently and is described by a harmonic oscillator, with frequency determined by the sound speed in the fluid, [75], [24]. Thus, there is an oscillation of the fluid density, with velocity $\pi/2$ out of phase and having amplitude re-

duced by the sound speed. After the Universe recombined the baryons and radiation decoupled, and the radiation could travel freely towards us. At that point the phases of the oscillations were frozen-in, and projected on the sky as a harmonic series of peaks. The main peak is the mode that went through 1/4 of a period, reaching maximal compression. The even peaks are maximal under-densities, which are generally of smaller amplitude because the rebound has to fight against the baryon inertia.

The scale associated with the peaks is the sound horizon at last scattering s_*. Its associated physical length is projected onto the sky, leading to an angular scale that depends on the background cosmology. Hence, the angular position of the peaks is a sensitive probe of the spatial curvature of the Universe (and so also of Ω_{tot}, the total density of the Universe). Again, the acoustic oscillations gives us a lot of information about other cosmological parameters, like the baryon and CDM density at recombination time [37]

THE DAMPING TAIL ($l \geq 1000$). The damping that occurs at small scales is essentially due to two processes. First of all, at these scales the typical photon free path is bigger than the typical scale of Compton scattering. This imperfect coupling lead to diffusion so the fluid hypothesis is no longer valid and so the oscillations have amplitude that decreases with time. Furthermore the recombination process is not instantaneous, giving a thickness to the last scattering surface. This leads to a further damping of the anisotropies at the highest ls, corresponding to scales smaller than that subtended by this thickness.

3.2.2 Polarization component

The linear CMB polarization is a spin 2 field on the sky. Usually, it is decomposed by splitting the polarization pattern into a curl-free plus a divergence-free part, called respectively *E-mode* and *B-mode*. The existence of linear polarization allows for 6 different cross correlation power spectra, however parity considerations suppress two of these, leaving with C_l^{TT}, C_l^{TE}, C_l^{EE} and C_l^{BB}. We have already seen that tensor perturbations contributes to angular power spectrum of the temperature fluctuations C_l^{TT}, in addition, also scalar perturbations can generate E-mode, so C_l^{TE} is non-vanishing. However, since scalar perturbations have no handedness, they cannot generate B-mode polarization. This latter is sourced only by tensor perturbation. For this reason a detection of such kind of polarization would be a confirm of the existence of primordial gravitational waves that were originated during inflation.

Nowadays, we have evidences of the presence of the E-mode, the WMAP experiment was also able to measure the TE cross-correlation power spectrum with high precision. This measurement was used in addition with the *Planck* data to give an upper bound on the tensor-to-scalar ratio r defined

in eq(2.100). What was found is

$$r \leq 0.11$$

at 95% of CL [66]. A remarkable fact to keep in mind is that this bound is an all-sky constraint.

More recently, a first ad of B-mode detection was made by the BICEP2 experiment, which analyzed a small patch in the sky near the south celestial pole. From its observation the experiment was able to measure a tensor-to-scalar ratio [4] :

$$r = 0.2^{+0.07}_{-0.05} \, .$$

This result need more insights to be definitively confirmed but if it were true it shows some tension with the *Planck* upper bound. In Chap.6 we will discuss more about this tension, showing a possible way to relax it.

3.3 CMB "Anomalies"

Statistical isotropy and homogeneity is a key prediction of the simplest inflation theories, so any evidence of a violation of rotational or translational invariance would be a significant challenge to the ΛCDM model. For this reason it is important to look for any possible anomaly in the temperature fluctuations map. With anomaly, here, we refer to a statistically unacceptable fit of the ΛCDM model to the C_l data, a statistically significant deviation of the a_{lm} coefficients from Gaussian random phases, or correlations between the a_{lm}. Notice that, here, with Gaussian deviation of the a_{lm} statistics we refer to an unexpected statistical deviation respect the prediction of the ΛCDM. Let us stress, indeed, that in the standard model of cosmology the a_{lm} coefficients are expected to be non-Gaussian distributed and with zero mean ($\langle a_{lm} \rangle = 0$), because they reflect the statistics of the curvature perturbations, which is expected to be non-Gaussian.

Since the release of the WMAP data [11], several anomalies have been analyzed. However an important issue we must emphasise is that we have few valuable principles to assess the statistical significance of such suspected anomalies. Further, the *a posteriori* search of the anomalies can amplify the apparent significance of some features. This happens mainly when one has to deal with a rich set of data as the temperature fluctuations map. In fact it is not difficult to find a 2σ anomalous feature for such data ensemble, however, to assess whether a particular 2σ feature is interesting, one is often tempted to narrow in on it to isolate its behavior. In this regard the Monte Carlo simulations are one of the most important tools to determine the significance of any possible deviation within the standard model. Claims of anomalies without Monte Carlo simulations are necessarily weak claims.

For instance, we consider the case of the so called *Four Fingers* and the related *Cold Spots* I & II. The first consists in warmer than average ridges

which lie between cooler valleys, while the latter are two regions colder than average. All these features are located in the southern celestial hemisphere, they may appear as anomalous, however Monte Carlo simulations showed they are reasonable statistical fluctuations. Indeed, it is the lack of these features in the Northern sky that may be the more unusual situation.

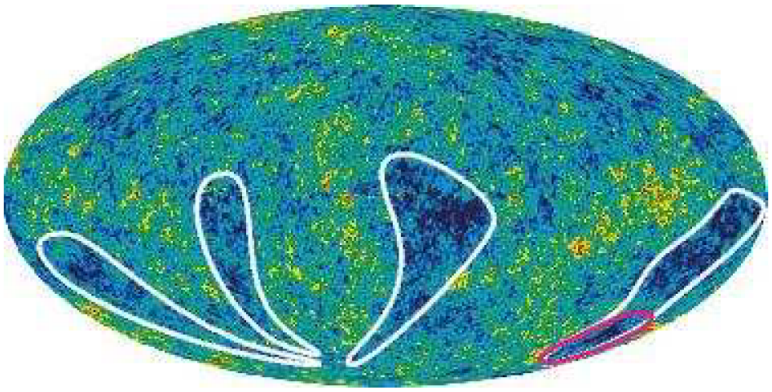

Figure 3.4: Visual inspection of the CMB map reveals four elongated valleys of cooler temperature that stretch from about the Galactic equator to nearly the south Galactic pole. Ridges of warmer-than-average temperature lie between the cooler fingers. These features are a consequence of large-scale power in the southern sky. It is more difficult to discern as much large-scale power in the northern sky. Cold Spot I is located near the northernmost part of one of the fingers, while Cold Spot II (within the red curve) is near the southernmost part of another finger, [11].

Another "anomaly", first seen by COBE consists in the *Low Quadrupole Amplitude* of the CMB spectrum. The CMB quadrupole is the largest observable structure in our universe. Its peculiar feature consists in the magnitude which is lower than the model prediction. However after a detailed analysis it was concluded that the quadrupole magnitude is not anomalously low, rather, part of its low amplitude may be due to the fact that the quadrupole is the large scale mode that is most prone to foreground contamination, owing to the disk-like structure of the Milky Way [11].

A more interesting feature found in the WMAP data consists in the *Alignement* between the quadrupole and the octupole moments. In general, each moment of a distribution identify a proper plane which we can label with the orthogonal axis. What it was found is that the axes of the quadrupole and octupole CMB temperature fluctuations are aligned to within 1°. The probability of such alignment is smaller than 10^{-3} in ΛCDM model. This anomaly was studied also by *Planck* that reassessed its significance. In particular *Planck collaboration* found that the two moments are misaligned of about 8°, a result well different than the previous estimate. This lowered

the statistical significance of such anomaly [67].

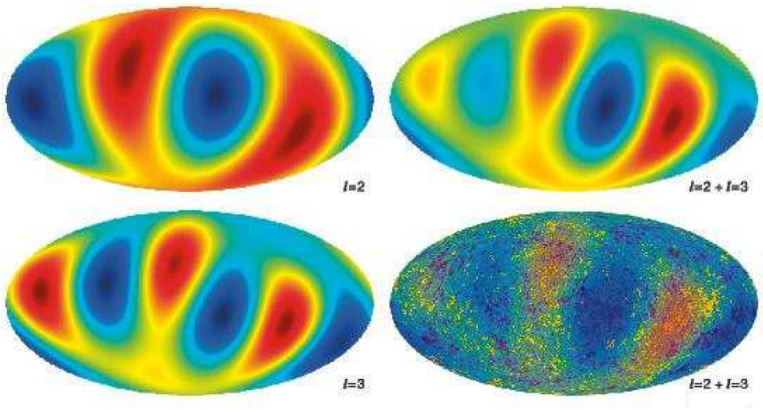

Figure 3.5: $l = 2$ quadrupole and $l = 3$ octupole maps are added. The combined map is then shown superposed on the CMB map from Figure 3.4. Note that the quadrupole and octupole components arrange themselves to match the cool fingers and the warm regions in between. The fingers and the alignment of the $l = 2$ and $l = 3$ multipoles are intimately connected. [11].

The *Hemispherical Power Asymmetry*, instead, thanks to the *Planck* data [67] has increased its significance. This anomaly consists in a different amplitude of the angular power spectrum between the southern and the northern celestial hemispheres, which breaks the statistical isotropy. Moreover, related to this anomaly, WMAP claimed also a quadrupolar modulation on the sky of the 2-point function, [11]. First seen only at the largest scales ($l \leq 64$), such asymmetry was reported to extend at least until $l = 600$. Several analyses were made also to determine a possible parametrization of the hemispherical asymmetry. Initially the power spectrum was assumed to change discontinuously across a great circle on the sky, afterwards a dipolar parametrization was proposed [30]. More in general, the *Planck collaboration* made a generalized search for power in the modulation field of such asymmetry. It was found that, while there is a statistically significant dipolar modulation of the CMB sky on large angular scales ($l \leq 64$) with an amplitude of about 7%, no quadrupolar modulation were observed, confirming the systematic origin of the corresponding anomaly seen in the WMAP data, [67]. Besides the 2-point function, were computed also high order N-point correlation functions separately in the two hemispheres. Also for these functions it was found a qualitative difference in behaviour between the two sides of the sky. Finally, it should be noted that the Doppler effect generated by the proper motion of the Earth creates a signature similar to that observed here. However, the present effect is clearly distinct from this, both because

the magnitudes of the two effects are very different[7] and because the two preferred directions are different.

For all these reasons the *Hemispherical Power Asymmetry* is considered one of the most important among the anomalies. In the next Chapter we will try to interpret such asymmetry in the context of standard cosmological model. In particular we will try to reconcile the hemispherical power asymmetry with the assumption of statistical isotropy that is one of the basics of modern cosmology. To do this we will assume that the Universe is much greater than what we observe, then statistical isotropy and homogeneity are still valid on the entire Universe, though, a small region (our observable Universe) may appear unisotropic and/or unhomogeneous.

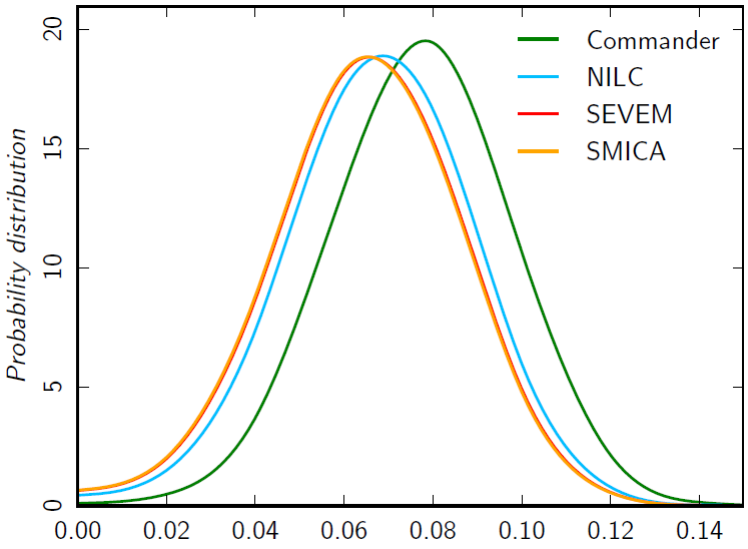

Figure 3.6: Modulation amplitude, A, obtained by the *Planck* analysis, [67].

[7] $A_{boost} \sim 0.002$ *versus* $A_{asym} \sim 0.07$.

Chapter 4

The Hemispherical Power Asymmetry

The *Hemispherical Power Asymmetry* (HPA) consists in a different amplitude of the CMB temperature fluctuations, between the Northern and the Southern celestial hemisphere. Such asymmetry, seen first in the WMAP data and then confirmed by *Planck*, is peaked at large angular scales ($l \leq 64$) but was seen also to extend to smaller scales (up to $l \approx 600$). This is one of the most important among the CMB anomalies, indeed Monte Carlo simulations revealed that less than 0.01% of the simulated maps showed a similar strong asymmetry, [27], [67].

On the largest scales ($l \leq 64$) HPA can be modelled as a dipolar modulation of an otherwise statistically isotropic distribution ($\theta(\hat{\mathbf{n}})^{iso}$) of the temperature fluctuations

$$\theta(\hat{\mathbf{n}}) = \theta(\hat{\mathbf{n}})^{iso}(1 + A\hat{\mathbf{p}} \cdot \hat{\mathbf{n}}). \tag{4.1}$$

Here, A and $\hat{\mathbf{p}}$ are respectively the amplitude and the orientation in the sky of the dipole. The best-fit dipole has direction, in galactic coordinates [1] $(l; b) = (227; -27)^\circ$ in galactic coordinates and amplitude $A = 0.072 \pm 0.022$. Let us stress that to agree with observations the dipole amplitude A must scale dependent, in particular A have to be smaller at smaller scales.

The presence of the modulation in the temperature anisotropies field $\theta(\hat{\mathbf{n}})$ changes the angular 2-point function or covariance matrix (3.14). The angular covariance matrix is explicitly calculated in Appendix B.1; here we report the final result:

$$\langle a_{lm} a^*_{l'm'} \rangle = \delta_{l\,l'} \delta_{mm'} C_l + \sum_{M=-1}^{1} A_{1M} \, [C_l + C_{l'}] \, \mathcal{G}^{l\,l'1}_{-mm'1}, \tag{4.2}$$

[1] The galactic coordinate system is a celestial coordinate system in spherical coordinates, with the Sun as its center, the primary direction aligned with the approximate center of the Milky Way galaxy, and the fundamental plane approximately in the galactic plane. The galactic longitude and latitude are respectively labelled with the symbols l and b.

where A_{1M} [2] is the multipole expansion of the dipole term $A(\hat{\mathbf{p}}\cdot\hat{\mathbf{n}})$ [3], and $\mathcal{G}^{l\,l'1}_{-mm'1}$ are Clebsch-Gordan coefficients. Notice that, because of the presence of the modulation, the matrix $\langle a_{lm}a^*_{l'm'}\rangle$ is no longer diagonal and hence different multipoles experience a non-vanish correlation. More in detail the symbol $\mathcal{G}^{l\,l'1}_{-mm'1}$ is non-zero in the case in which $l+l'+1$ is even, $m'-m+M=0$ and $|l-l'|\leq 1\leq l+l'$. Notice that the latter condition is particularly relevant because in general $l,\,l'\gg 1$.

The parametrization (4.1) can be interpreted as spatial variation experienced by the power spectrum $P_\theta(k)$ across the sky [23], [62]:

$$P_\theta(k,\mathbf{x})\approx P^{iso}_\theta(k)(1+2A\hat{\mathbf{p}}\cdot\mathbf{x}/x_{dec}), \tag{4.3}$$

where x_{dec} is the comoving distance to the surface of last scattering. Others parametrizations of the power spectrum were proposed in the literature (for instance in [32]) to explain some CMB anomalies, and more in general to test the CMB statistical anisotropy. Above them we mention the one which consists in a sort of expansion of the CMB power spectrum in Fourier Space:

$$P_\theta(\mathbf{k})=P^{iso}_\theta(k)\left[1+\sum_{n=1}^{\infty}A_n\left(\hat{\mathbf{p}}\cdot\hat{\mathbf{k}}\right)^n\right]. \tag{4.4}$$

Notice that this shape of the power spectrum breaks the statistical isotropy. In fact any non-vanishing coefficient A_n adds dependence on the direction $\hat{\mathbf{k}}$ to $P_\theta(\mathbf{k})$. In this power expansion the only term which could give rise to a dipole in the temperature fluctuations field, is the one with $n=1$. Therefore only a dipole in $P_\theta(\mathbf{k})$ generates a dipole in $\theta(\mathbf{x})$ through Eq(4.2). However, odd terms are forbidden in the power expansion (4.4). This is due to the reality condition that the Fourier modes $\theta(\mathbf{k})$ need to satisfy:

$$\theta(\mathbf{x})\in\mathbb{R}\Rightarrow\theta(\mathbf{k})^*=\theta(-\mathbf{k}). \tag{4.5}$$

This condition, in turn, implies

$$\begin{aligned}\langle\theta(\mathbf{k})\theta^*(\mathbf{k}')\rangle &= (2\pi)^3\delta^3(\mathbf{k}-\mathbf{k}')P(\mathbf{k})=\\ &= \langle\theta^*(-\mathbf{k})\theta(-\mathbf{k}')\rangle=(2\pi)^3\delta^3(\mathbf{k}-\mathbf{k}')P(-\mathbf{k})\end{aligned} \tag{4.6}$$

and hence $P(\mathbf{k})=P(-\mathbf{k})$ and therefore, we get that all the odd terms in (4.4) are suppressed. In conclusion, the HPA cannot rises from a preferred direction in Fourier Space (which would implies isotropy breaking) but we must consider a preferred direction in real space as in (4.3). This implies isotropy breaking.

[2] $A_{LM}=\int d\Omega_{\mathbf{n}}A(\hat{\mathbf{p}}\cdot\hat{\mathbf{n}})Y^*_{LM}(\hat{\mathbf{n}})$.

[3] Notice that, the spherical harmonics expansion of a dipole contains only terms with $L=1$.

A comment in the notation: thanks to the reality condition (4.5) we are allowed to construct the n-point functions in Fourier space of the type $\langle\theta\theta\rangle$ (notice that the second "θ" is not a complex conjugate). In this case homogeneity assures that $\langle\theta(\mathbf{k})\theta(\mathbf{k}')\rangle \propto \delta^3(\mathbf{k}+\mathbf{k}')$. This holds for every primordial perturbation. For this reason in this Chapter we will consider correlation functions with the form $\langle\theta\theta\rangle$, $\langle\zeta\zeta\rangle$, $\langle\phi\phi\rangle$ and so on.

The HPA is extremely difficult to reconcile with inflation. From what we pointed out, indeed, after its discovery the sky no longer appears isotropic as the inflationary paradigm predicts. The purpose of this Chapter consists in a discussion on possible interpretations of such an asymmetry in an inflationary context. More in details we will investigate the possible connection between the HPA and primordial non-Gaussianity. Such connection has already been studied in some papers, e.g. [25], [73], [53] and [63].

4.1 Non-Gaussainity and modes coupling

A possible way to reconcile inflation with HPA consists in assuming that all we can observe in the sky is contained in a volume much smaller than the entire Universe. In this way the CMB statistics would be isotropic and homogeneous in the entire volume, as inflation predicts, while in our box it might appear biased. According to this idea the HPA would be the signature of some large amplitude primordial density perturbation which occurred during inflation, with proper length greater than the size of the observable Universe. In this scenario, such super-horizon perturbation would have coupled with the observable (sub-horizon) ones thanks to the non-Gaussianity in the statistics of the primordial density fluctuations field.

As we have already discussed in Sec.1.2.3, primordial non-Gaussianity is inevitably generated also in the most simple models of inflation, [10] [15]. This feature of the statistical distribution of the quantum fluctuation field is expected to be present also in the CMB temperature fluctuations $\theta(\mathbf{x})$, leaving its signature in the cosmological observables. In the following we will investigate how this coupling between different wavelength perturbation modes can be caused from non-Gaussianity. Furthermore, we will focus on the modulation experienced by the 2-point function in this case.

In the following study we will work with the curvature field on uniform density hypersurfaces $\zeta(\mathbf{x})$. We stress that, during matter domination and on large scales, it is related to the Bardeen potential $\Phi(\mathbf{x})$ through $\zeta \approx -3/5\,\Phi$. In turn, $\Phi(\mathbf{x})$ generated the temperature anisotropies field $\theta(\mathbf{x})$ on the largest angular scales mainly through Sachs-Wolfe effect. Therefore any asymmetry in $\theta(\mathbf{x})$ comes from an asymmetry in $\zeta(\mathbf{x})$.

4.1.1 Mode coupling and Consistency Relation

A useful way to understand how mode coupling can occur, consists in revisit the calculation of the so called *consistency relation* for the bispectrum. Such relation holds between the power spectrum $P_\zeta(k)$ and the bispectrum $\mathcal{B}_\zeta(k_1, k_2, k_3)$ [4] of the curvature field $\zeta(\mathbf{x})$ in a particular configuration called the *squeezed limit*. The importance of such expression lies in the fact that it is a model-independent relation holding for any single-field models of inflation. This is discussed, for instance,[55], [16] and [21].

The consistency relation says that in the *squeezed limit*, when one side of the triangle, say $\mathbf{k_1}$, approaches to zero and hence the other two sides becomes equal and opposite $\mathbf{k_2} \approx -\mathbf{k_3}$, the bispectrum is fully determined by the power spectrum, computed in the long mode $P_\zeta(k_1)$, times the power spectrum of the short mode $P_\zeta(k_2)$, times the deviation from the scale invariance $n_s - 1$.

To get this relation we begin by assuming that, during inflation, the curvature field $\zeta(\mathbf{x})$ is originated by the quantum fluctuations of a single scalar field $\varphi(t, \mathbf{x})$. We stress once more the assumptions made on $\zeta(\mathbf{x})$: on the entire Universe the field is isotropic and homogeneous with a slightly component of non-Gaussianity. We set the uniform density gauge, which implies $\delta\varphi = 0$. On the uniform density hypersurfaces, the metric is affected only by the curvature and tensor perturbations, so neglecting tensor modes[5], it takes the form

$$ds^2 = -dt^2 + a(t)^2(1 + 2\zeta(\mathbf{x}))dx_i dx^i \approx -dt^2 + a^2(t)e^{2\zeta(\mathbf{x})}dx_i dx^i. \quad (4.7)$$

Notice that, shortly after inflation most of the Fourier modes $\zeta(\mathbf{k})$ are super-horizon ($k \ll H$), so they are constant in time, furthermore, we can treat them as classical, in the sense that the commutator $[\zeta(\mathbf{k}); \zeta(\mathbf{k}')] = 0$. During the super-horizon era the term $e^{2\zeta(\mathbf{x})}$ in the line element can be reabsorbed in a coordinate rescaling

$$\mathbf{x}' = e^{\zeta(\mathbf{x})}\mathbf{x}. \quad (4.8)$$

Therefore on large scales the metric takes the same form of the unperturbed FRW one (1.2). In conclusion we note that in each region separated by large distances the metric can be rewritten as the unperturbed FRW form, [71]. However, with this rescaling each patch has a different coordinate rescaling because of the different initial conditions [6].

Let us now focus on three Fourier modes $\zeta(\mathbf{k_1})$, $\zeta(\mathbf{k_2})$ and $\zeta(\mathbf{k_3})$ in the squeezed configuration. The mode with shortest wavenumber, $\zeta(\mathbf{k_1})$ has a wavelength much greater than the others two. In this configuration,

[4] Notice that as we have already shown in Sec.1.2.3 translational invariance requires that the 3 modes of the bispectrum $\mathbf{k_i}$, $i = 1, 2, 3$ must form a triangle.

[5] In this chapter we don't care about tensor perturbations because they are not relevant for the purpose of this section.

[6] The fluctuations of the inflation set different values of $\zeta(\mathbf{x})$ in different patches.

when k_2 and k_3 re-enter the horizon, $\mathbf{k_1}$ is still super-horizon. So, the only effect of $\zeta(\mathbf{k_1})$ consists in a rescaling of the coordinates. We can treat it as a background ζ_B. The presence of such background ζ_B modify the 2-point function on small scales. Neglecting the gradient of this super horizon perturbation, we expand the correlation function $\langle\zeta(\mathbf{x_2})\zeta(\mathbf{x_3})\rangle_B$, evaluated in real space, in power series of ζ_B:

$$\langle\zeta(\mathbf{x_2})\zeta(\mathbf{x_3})\rangle_B \simeq \langle\zeta(\mathbf{x_2})\zeta(\mathbf{x_3})\rangle + \zeta_B(\mathbf{x}_+)\frac{d}{d\zeta_B}\langle\zeta(\mathbf{x_2})\zeta(\mathbf{x_3})\rangle. \tag{4.9}$$

Notice that we approximated the value of the background perturbation as the value that ζ_B assumes in the middle point $\mathbf{x}_+ = (\mathbf{x_2}+\mathbf{x_3})/2$. Indeed, we are supposing that the scale of variation of ζ_B is much larger than the distance between the points $\mathbf{x_2}$ and $\mathbf{x_3}$. Here, $\langle\zeta(\mathbf{x_2})\zeta(\mathbf{x_3})\rangle$ is the 2-point function computed in the vacuum state. Recalling Eq(2.66) we find that it is equal to

$$\langle\zeta(\mathbf{x_2})\zeta(\mathbf{x_3})\rangle = \int \frac{d^3k}{(2\pi)^3} e^{-i\mathbf{k}(\mathbf{x_2}-\mathbf{x_3})} P_\zeta(k). \tag{4.10}$$

Notice that, at $zero^{th}$ order, when isotropy is still valid, the correlation function does not depend on the orientation of $(\mathbf{x_2}-\mathbf{x_3})$. Hereafter, for simplicity, we will write $\langle\zeta\zeta\rangle$ in place of $\langle\zeta(\mathbf{x_2})\zeta(\mathbf{x_3})\rangle$ and $\mathbf{x_s}$ in place of $\mathbf{x_2}-\mathbf{x_3}$. Exploiting the rescaling of coordinates $\mathbf{x}' = e^{\zeta_B}\mathbf{x}$, the derivative with respect to the background in Eq(4.9) can be replaced with a log derivative with respect to $x_s = |\mathbf{x_s}|$:

$$x_s' = e^{\zeta_B} x_s \;\Rightarrow\; \zeta_B = \log\left(x_s'/x_s\right) \;\Rightarrow\; d\zeta_B = d\log x_s' = d\log x_s + \mathcal{O}(\zeta_B^2). \tag{4.11}$$

Indeed, Eq(4.9) can be rewritten as:

$$\langle\zeta(\mathbf{x_2})\zeta(\mathbf{x_3})\rangle_B \simeq \langle\zeta\zeta\rangle + \zeta(\mathbf{x}_+)\frac{d\ \langle\zeta\zeta\rangle}{d\log x_s}. \tag{4.12}$$

Let us focus on the second term of the power series expansion (4.12). We write $\zeta_B(\mathbf{x}_+)$ in Fourier space

$$\zeta_B(\mathbf{x}_+) = \int \frac{d^3k_l}{(2\pi)^3} e^{-i\mathbf{k_l}\mathbf{x}_+}\zeta(\mathbf{k_l}), \tag{4.13}$$

we use the explicit expression of the correlation function (4.10), and the fact that $\frac{d}{d\log x_s} = (\mathbf{x_s})\cdot\frac{d}{d(\mathbf{x_s})}$, [7] to obtain, after some algebra,

$$\zeta(\mathbf{x}_+)\frac{d}{d\log x_s}\langle\zeta\zeta\rangle = \int \frac{d^3k_l}{(2\pi)^3}\frac{d^3k_s}{(2\pi)^3} e^{-i\mathbf{k_l}\mathbf{x}_+}\zeta(\mathbf{k_l})\ \mathbf{x_s}\cdot\frac{d}{d\mathbf{x_s}} e^{-i\mathbf{k_s}\mathbf{x_s}} P_\zeta(k_s). \tag{4.14}$$

[7] $\mathbf{y}\cdot\frac{d}{d\mathbf{y}} = y_i\frac{dy}{dy_i}\frac{d}{dy} = y\frac{d}{dy} = \frac{d}{d\ln y}$, with $y = |\mathbf{y}|$

Now, the derivative with respect $\mathbf{x_s}$ gives the factor $i\mathbf{k_s}$, while we write the $\mathbf{x_s}$ term as a derivative with respect to $\mathbf{k_s}$. Therefore the above expression rewrites as

$$\zeta(\mathbf{x}_+)\frac{d}{d\log x_s}\langle\zeta\zeta\rangle = \int\frac{d^3k_l}{(2\pi)^3}\frac{d^3k_s}{(2\pi)^3}e^{-i\mathbf{k_l}\mathbf{x}_+}\zeta(\mathbf{k_l})\ \mathbf{k_s}\cdot\frac{d}{d\mathbf{k_s}}\left(e^{-i\mathbf{k_s}\mathbf{x_s}}\right)P_\zeta(k_s) = \\ = -\int\frac{d^3k_l}{(2\pi)^3}\frac{d^3k_s}{(2\pi)^3}e^{-i(\mathbf{k_l}\mathbf{x}_+ + \mathbf{k_s}\mathbf{x_s})}\zeta(\mathbf{k_l})\ \frac{d}{d\mathbf{k_s}}(\mathbf{k_s}P_\zeta(k_s)) \quad (4.15)$$

where, in the last step we integrated by parts. Let us briefly comment the result obtained. We checked that in presence of super-horizon perturbations the 2-point correlation function in a small patch experiences a shift due to the super-horizon modulation. In this way, long wavelength modes affect the small scale power spectrum though they are not directly observables. The presence of these modes is clean also in the Fourier transform of $\langle\zeta\zeta\rangle_{\zeta_B}$. From the explicit calculation we get

$$\langle\zeta(\mathbf{k_2})\zeta(\mathbf{k_3})\rangle_B \simeq (2\pi)^3\delta^3(\mathbf{k_2}+\mathbf{k_3})P_\zeta(k_s) - (n_s-1)\,\zeta_B(\mathbf{k_2}-\mathbf{k_3})\,P_\zeta(k_s), \quad (4.16)$$

where we used the fact that $\frac{d}{d\mathbf{k}}(\mathbf{k}P(k)) = P(k)\frac{d\ln(k^3P(k))}{d\ln(k)} = P(k)(n_s-1)$. [8]. Notice that in the above expression we identified the short-wavelength modes $\mathbf{k_2}$ and $\mathbf{k_3}$ with $\mathbf{k_s} := (\mathbf{k_2}-\mathbf{k_3})/2$, where the subscript s denotes that we are dealing with sub-horizon (and hence observable) modes. Later we will use also the subscript l which refers to super-horizon modes. Notice also that the modulus of $\mathbf{k_s}$ is the mean of the moduli of $\mathbf{k_2}$ and $\mathbf{k_3}$. The 2-point function (4.16) tells us that the presence of the super-horizon background breaks the translational invariance and indeed the statistical homogeneity of the perturbation field $\zeta(\mathbf{x})$ in the small patch. In fact, since the second term in Eq(4.16) is not proportional to $\delta^3(\mathbf{k_2}+\mathbf{k_3})$, two different modes have now non-vanishing correlation. On the other hand, isotropy, that here manifests as the independence of the 2-point function from the direction of $\mathbf{k_s}$, at least at first order, is still valid.

Now that we computed the 2-point function in presence of a background $\langle\zeta\zeta\rangle_B$ it is straightforward to calculate the consistency relation. We average, in the entire Universe, the background mode $\zeta_B(\mathbf{k_1})$ with the modulated 2-point function (4.16). Notice that the piece which is independent of the

[8] We can see it computing explicitly $\frac{d}{d\mathbf{k}}(\mathbf{k}P(k))$ and $P(k)\frac{\ln(k^3P(k))}{d\ln(k)}$:

- $\frac{d}{d\mathbf{k}}(\mathbf{k}P(k)) = 3P(k) + k_i\frac{d}{dk_i}P(k) = 3P(k) + \frac{dP(k)}{d\ln k}$
- $P(k)\frac{d\ln(k^3P(k))}{d\ln(k)} = P(k)\frac{1}{kP(k)}\left(3k^3P(k) + k^2\frac{dP(k)}{dk}\right) = 3P(k) + \frac{dP(k)}{d\ln k}$

background gives no contribution:

$$\begin{aligned}\langle\zeta(\mathbf{k_1})\zeta(\mathbf{k_2})\zeta(\mathbf{k_3})\rangle &= \langle\,\zeta_B(\mathbf{k_1})\,\langle\,\zeta(\mathbf{k_2})\zeta(\mathbf{k_3})\,\rangle_B\,\rangle = \\ &= -(2\pi)^3\delta^3(\mathbf{k_1}+\mathbf{k_2}+\mathbf{k_3})(n_s-1)P_\zeta(k_l)P_\zeta(k_s).\end{aligned} \tag{4.17}$$

Under the hypotheses of statistical homogeneity and isotropy, the three-point function can be written as

$$\langle\zeta(\mathbf{k_1})\zeta(\mathbf{k_2})\zeta(\mathbf{k_3})\rangle = (2\pi)^3\delta^3(\mathbf{k_1}+\mathbf{k_2}+\mathbf{k_3})\;f_{NL}\,\mathcal{B}_\zeta(k_1,k_2,k_3); \tag{4.18}$$

then, comparing Eqs (4.17) and (4.18) we get:

$$f_{NL}\,\mathcal{B}_\zeta(k_1,k_2,k_3) = -(n_s-1)\,P_\zeta(k_l)\,P_\zeta(k_s). \tag{4.19}$$

Now, for a single scalar field, it has been found that the f_{NL} parameter is, in the squeezed limit, equal to $f_{NL} \simeq -(n_s-1)/4$, [10]. This means that, from Eq(4.19) we can read the expression for the bispectrum:

$$\mathcal{B}_\zeta(k_1,k_2,k_3) = 4\;P_\zeta(k_l)\;P_\zeta(k_s). \tag{4.20}$$

Notice that in the above expressions both f_{NL} and $\mathcal{B}_\zeta(k_1,k_2,k_3)$ refers to the statistics defined in the entire Universe. This in general is different from the one that we measured in the observable sky. This implies that the values of f_{NL} and f_{NL}^{obs}, where f_{NL}^{obs} is the measured parameter, are, in general, different. We will show this fact explicitly in Sec.4.2.2.

Having calculated the consistency relation, we can plug Eq(4.19) into the biased correlation function (4.16). In this way we highlight an explicit dependence on the bispectrum (of the biased 2-point function):

$$\begin{aligned}\langle\zeta(\mathbf{k_2})\zeta(\mathbf{k_3})\rangle_B \;\simeq\; & (2\pi)^3\delta^3(\mathbf{k_2}+\mathbf{k_3})P_\zeta(k_s) \\ & + f_{NL}\,\frac{\mathcal{B}_\zeta(k_l,|\mathbf{k_s}+\frac{\mathbf{k_l}}{2}|,|-\mathbf{k_s}+\frac{\mathbf{k_l}}{2}|)}{P_\zeta(k_l)}\zeta(\mathbf{k_l}),\end{aligned} \tag{4.21}$$

where, again, we have used $\mathbf{k_s} = (\mathbf{k_2}-\mathbf{k_3})/2$ and $\mathbf{k_l} = \mathbf{k_2}+\mathbf{k_3}$.

Although the sky appears anisotropic, we can still define a power spectrum. However, the definition (2.66) that we gave is no longer valid, and we must use another expression to define $P_\zeta(k)$. To do this we start considering the variance of the curvature field $\langle\zeta^2(\mathbf{x})\rangle$ or, more in general, the 2-point correlation function on the observable scales: $\langle\zeta(\mathbf{x})\zeta(\mathbf{x}')\rangle$, Eq(4.10). That expression is valid for a homogeneous and isotropic field. Anyway, anti-Fourier transforming Eq(4.21) we see that, in a more general context, when both isotropy and homogeneity are broken, we can write a sort of generalization of Eq(4.10):

$$\langle\zeta(\mathbf{x_2})\zeta(\mathbf{x_3})\rangle = \int\frac{d^3k_s}{(2\pi)^3}e^{-i\mathbf{k_s}\mathbf{x_s}}P_\zeta(\mathbf{k_s},\mathbf{x}_+). \tag{4.22}$$

Here, $P_\zeta(\mathbf{k_s}, \mathbf{x}_+)$ is the generalized power spectrum on the observable scales; it explicit expression contains the integration over the super-horizon and hence unobservable modes. Notice that according to Eq(4.22) the generalized power spectrum $P_\zeta(\mathbf{k_s}, \mathbf{x}_+)$ turns out to be equal to the anti-Fourier transforming of Eq(4.21) respect to the variable $\mathbf{k_l}$ [9]:

$$P_\zeta^{mod}(\mathbf{k_s}, \mathbf{x}_+) \simeq P_\zeta(k_s) + f_{NL} \int \frac{d^3k_l}{(2\pi)^3}\, e^{-i\mathbf{k_l}\mathbf{x}_+}\, \frac{\mathcal{B}_\zeta(k_l, |\mathbf{k_s}+\frac{\mathbf{k_l}}{2}|, |-\mathbf{k_s}+\frac{\mathbf{k_l}}{2}|)}{P_\zeta(k_l)}\, \zeta(\mathbf{k_l}). \tag{4.23}$$

Let us briefly comment on this formula. First of all we stress that it is valid in a small sub-volume of the entire Universe (like the observable sky). The statistics of the primordial perturbation is isotropic and homogeneous in the entire volume. However in the small region it appears as biased because of the presence of fluctuations with characteristic length $\lambda \approx {k_l}^{-1}$ grater than the size of the region H_0^{-1}. The super-horizon realization which form the background is coupled with small scale field. Non-gaussianity allowed this coupling between super- and sub-horizon perturbations.

Notice that, in Eq(4.23), the power spectrum is, in general, a function of the direction of $\mathbf{k_s}$ thus, in principle, breaking statistical isotropy. In fact, in a wide class of models (like the one studied here), while homogeneity is broken at leading order, it can be shown [21] that isotropy is still valid up to the second order in k_l/k_s. However, what the modulated power spectrum get, since the first order, is a dependence on $\mathbf{x}_+$. This dependence can be linked to the real space dependence of $P_\theta(k, \mathbf{x}_+)$ given in the parametrization (4.3). Therefore, we remark that the way we are following seems to be a proper way to reconcile with observation.

The next step will consist in specifying the super-horizon realization, i.e. to specify the form of $\zeta(\mathbf{k_l})$. However before doing that we will introduce an other formalism to explain the mode coupling just seen in this section, that turns out to be useful to understand some relevant details.

4.1.2 Splitting into long and short wavelength perturbation modes

The result of the previous section can be recovered also with a slightly different formalism which highlights the coupling between different modes.

Since observations tell us that the curvature perturbation $\zeta(\mathbf{x})$ is an almost gaussian field, it was proposed a phenomenological model to parametrize this field based on a power expansion from a gaussian distribution. Explicitly:

$$\zeta(\mathbf{x}) = \zeta_G(\mathbf{x}) + f_{NL}\, \zeta_G^2(\mathbf{x}) + \cdots . \tag{4.24}$$

Here $\zeta_G(\mathbf{x})$ is a gaussian field. This power expansion is called *local model*[10]. In the local model of non-Gaussianty, the leading term is precisely $\zeta_G(\mathbf{x})$

[9] The explicit calculation can be found in Appendix B.2

[10] Non-Gaussian models containing quadratic non-linearities, as in Eq.(4.24), were in-

while the deviation from the gaussian statistics is contained in the additional terms. The first term of the expansion follows a χ^2 distribution. The field $\zeta(\mathbf{x})$ is defined on the entire Universe, however, as before, we are interested in the fluctuations inside a small region of it. Therefore we can split any field $A(\mathbf{x})$ into a short- and long-wavelength piece: $A_s(\mathbf{x})$ and $A_l(\mathbf{x})$. Here, with "long" wavelengths we mean those comparable or larger than the cosmological horizon. Therefore, if L is the size of the entire Universe and H_0^{-1} is the scale of our observable region, we have

$$A(\mathbf{x}) = A_s(\mathbf{x}) + A_l(\mathbf{x}) \tag{4.25}$$

where $A_s(\mathbf{x})$ and $A_l(\mathbf{x})$ are respectively

$$A_s(\mathbf{x}) = \int_{H_0^{-1}}^{k_{max}} \frac{d^3k}{(2\pi)^3} e^{-i\mathbf{kx}} A(\mathbf{x}), \tag{4.26}$$

$$A_l(\mathbf{x}) = \int_{L^{-1}}^{H_0^{-1}} \frac{d^3k}{(2\pi)^3} e^{-i\mathbf{kx}} A(\mathbf{x}). \tag{4.27}$$

Notice that we have defined also a maximum wavenumber k_{max} from the smallest scale we smoothed over. Splitting the field $\zeta_G(\mathbf{x})$, Eq(4.24) as in Eq(4.25) bring us to

$$\zeta(\mathbf{x}) \quad = \quad \zeta_{G,s}(\mathbf{x}) + \zeta_{G,l}(\mathbf{x}) + f_{NL}\left(\zeta_{G,s}(\mathbf{x}) + \zeta_{G,l}(\mathbf{x})\right)^2 + \mathcal{O}(f_{NL}^2). \tag{4.28}$$

Therefore, the curvature field we observe in our region is the short wavelength part of $\zeta(\mathbf{x})$:

$$\zeta_s(\mathbf{x}) = \zeta_{G,s}(\mathbf{x}) + f_{NL}[\zeta_{G,l}(\mathbf{x})\zeta_{G,s}(\mathbf{x}) + \zeta_{G,s}^2(\mathbf{x})]. \tag{4.29}$$

From this expression, the coupling between super- and sub-horizon perturbations is evident. Since it is proportional to the f_{NL} parameter we see immediately that it is due to a possible primordial non-Gaussianity. Notice that, inside the sub-sample of size H_0^{-1}, the super-horizon part of the curvature field, $\zeta_{G,l}(\mathbf{x})$, assumes a deterministic value that modulates the statistics inside the volume. To calculate the biased power spectrum in the sub-sample, we write Eq(4.29) in Fourier space. Remembering that the Fourier transform of a product of two fields is a convolution of the two we get

$$\zeta_s(\mathbf{k}) = \zeta_{G,s}(\mathbf{k}) + f_{NL}\int \frac{d^3k'}{(2\pi)^3}\left[\zeta_{G,l}(\mathbf{k}-\mathbf{k}')\,\zeta_{G,s}(\mathbf{k}') + \zeta_{G,s}(\mathbf{k}-\mathbf{k}')\,\zeta_{G,s}(\mathbf{k}')\right], \tag{4.30}$$

troduced in the study of inflationary perturbations in [35], [41] and [70], and have become a sort of "standard lore" for the comparison of theoretical predictions on primordial non-Gaussianity to CMB and LSS observational data.

and hence

$$\begin{aligned}\langle\zeta_s(\mathbf{k_2})\zeta_s(\mathbf{k_3})\rangle &= (2\pi)^3\delta^3(\mathbf{k_2}+\mathbf{k_3})P_\zeta(k_2) + f_{_{NL}}[P(k_2)\ \zeta_{G,l}(\mathbf{k_2}+\mathbf{k_3}) \\ &\quad + P(k_3)\ \zeta_{G,l}(\mathbf{k_3}+\mathbf{k_2})] = \\ &\simeq (2\pi)^3\delta^3(\mathbf{k_2}+\mathbf{k_3})P_\zeta(k_s) + 2f_{_{NL}}P(k_s)\zeta_{G,l}(\mathbf{k_l}),\end{aligned} \tag{4.31}$$

where in the last step we have defined the long and short wavelength modes, respectively $\mathbf{k_l} := \mathbf{k_2} + \mathbf{k_3}$ and $\mathbf{k_s} := (\mathbf{k_2} - \mathbf{k_3})/2$. As we had already anticipated we recovered the same results we obtained with the previous formalism and summarized in Eq(4.16). Again, we can find the explicit dependence respect to the bispectrum, computed in the entire Universe, in Eq(4.31). The formula for the bispectrum in the local model (4.24) is [11]

$$\mathcal{B}_\zeta(k_1,k_2,k_3) = 2\left[P(k_1)P(k_2) + \text{"}cyclic\text{"}\right], \tag{4.32}$$

that reduces to

$$\mathcal{B}_\zeta(k_1,k_2,k_3) \simeq 4P(k_1)P(k_s), \tag{4.33}$$

in the squeezed limit: $k_1 \ll k_2 \approx k_3 \approx k_s$. Plugging Eq(4.33) into Eq(4.31) it is straightforward to obtain, also with this formalism, the biased two-point function (4.21) and indeed, anti-Fourier transforming this expression, the modulated power spectrum (4.23).

Let us stress that the formalism used in this section on more general than the one used in Sec. 4.1.1. Indeed, while this latter is valid in the context of the single-field inflationary models, the formalism developed in this section can be generalized to deal also with multi-field models.

The results obtained need some important comments (see Secs 4.2.1 and 4.2.2). However before to coming to them we now show how the HPA can be obtained. To do this we will specify the form of the super-horizon realization $\zeta(\mathbf{k_l})$.

4.2 Dipolar modulation across the sky

In the literature, many authors proposed an explanation of the power asymmetry assuming only a single super-horizon mode with an anomalous large amplitude $\zeta(\mathbf{p})$. This kind of modulation can lead to an asymmetry as studied in [63] and [62], [52], and finally to [27] and [28]. In the last two references a super-horizon perturbation generated from an additional single scalar field present during inflation is considered (we will discuss this case in details in Chap.5). This is not the only way to obtain a modulation of the temperature fluctuations across the sky, indeed, there have been works to obtain scale-dependent asymmetry either by using more than two fields or non-Bunch-Davies initial state or again assuming some sort of non-Gaussianity that increases the bispectrum in the squeezed limit, [22], [22], [29] and [73].

[11] See Appendix B.3 for the details on how to derive Eq(4.32).

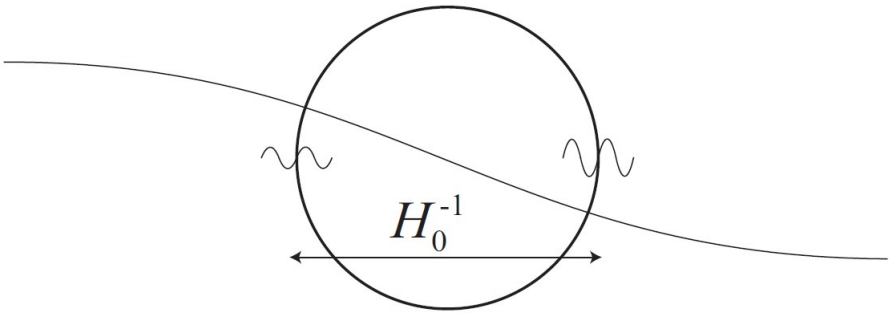

Figure 4.1: Measurement of temperature fluctuations in the CMB show that the mean square temperature fluctuations is larger in one side of the sky than in the other. The asymmetry may be generate by a large amplitude fluctuation in the curvature perturbation field $\zeta(\mathbf{x})$, [27].

Let us show how a single super-horizon mode can give rise to a dipolar modulation across the sky, using the developed formalism. We assume this large mode to be $\zeta(\mathbf{x}) = \zeta_L \sin(\mathbf{p}\cdot\mathbf{x})$, with $p \ll H_0$. In Fourier space it reads

$$\zeta(\mathbf{k_l}) = (2\pi)^3 \frac{\zeta_L}{2i}\left[\delta^3(\mathbf{k_l}-\mathbf{p})-\delta^3(\mathbf{k_l}+\mathbf{p})\right]. \tag{4.34}$$

Then we can plug this expression into Eq(4.23) getting (we report here only the second term of the modulated power spectrum)

$$\begin{aligned} & f_{NL}\int d^3k_l\; e^{-i\mathbf{k_l}\mathbf{x}_+}\frac{\mathcal{B}_\zeta(k_l,|\mathbf{k}+\frac{\mathbf{k_l}}{2}|,|-\mathbf{k}+\frac{\mathbf{k_l}}{2}|)}{P_\zeta(k_l)}\frac{\zeta_L}{2i}\left[\delta^3(\mathbf{k_l}-\mathbf{p})-\delta^3(\mathbf{k_l}+\mathbf{p})\right] = \\ & = -f_{NL}\frac{\mathcal{B}_\zeta(p,|\mathbf{k}+\frac{\mathbf{p}}{2}|,|\mathbf{k}+\frac{\mathbf{p}}{2}|)}{P_\zeta(p)}\frac{\zeta_L}{2i}\left[e^{i\mathbf{p}\mathbf{x}_+}-e^{-i\mathbf{p}\mathbf{x}_+}\right] = \\ & = -f_{NL}\frac{\mathcal{B}_\zeta(p,|\mathbf{k}+\frac{\mathbf{p}}{2}|,|-\mathbf{k}+\frac{\mathbf{p}}{2}|)}{P_\zeta(p)}\zeta_L\,\sin(\mathbf{p}\mathbf{x}_+). \end{aligned} \tag{4.35}$$

We recall that $|\mathbf{p}| \gg H_0$, while $\mathbf{x}_+$, points inside our observable Universe and hence it holds $x_+ \leq H_0^{-1}$. Therefore the sine argument in the above expression is much smaller than unity and so we can expand the sine in power series. In conclusion the modulated power spectrum results

$$P_\zeta^{mod}(k,\mathbf{x}) = P_\zeta^{iso}(k)\left[1 - \; f_{NL}\; p\; x_{dec}\;\zeta_L\;\frac{\mathcal{B}_\zeta(p,|\mathbf{k}+\frac{\mathbf{p}}{2}|,|-\mathbf{k}+\frac{\mathbf{p}}{2}|)}{P_\zeta(p)\;P_\zeta(k)}\;\hat{\mathbf{p}}\cdot\mathbf{x}\right], \tag{4.36}$$

where x_{dec} is the comoving distance to the surface of last scattering and where we have identified $\mathbf{x}$ with $\mathbf{x}_+$. Thanks to the above result we recovered the dipole parametrization given in Eq(4.3). Obviously the dipole term present in Eq(4.36), is only the first order of the sine wave expansion, in general in the modulated part of the power spectrum there are also other types

of modulation due to the higher terms in the power expansion. Comparing Eq(4.36) with the phenomenological parametrization given in eq(4.3) we find the following parametrization for the dipolar amplitude:

$$A = f_{NL}\ p\ x_{dec}\ \zeta_L\ \frac{\mathcal{B}_\zeta(p, |\mathbf{k}+\frac{\mathbf{p}}{2}|, |-\mathbf{k}+\frac{\mathbf{p}}{2}|)}{P_\zeta(p)\ P_\zeta(k)}. \tag{4.37}$$

Notice that this amplitude depends explicitly on the non-Gaussian parameter f_{NL} which, we stress is the parameter quantifying the level of primordial non-Gaussianity.

If we assume the local model (4.24), where the bispectrum in the squeezed limit is given by Eq(4.33), we find an amplitude of the dipolar modulation

$$A = 4\ f_{NL}\ p\ x_{dec}\ \zeta_L. \tag{4.38}$$

This result is in agreement with the dipolar amplitude computed in [62], [63] and [52]. However, we want to point out that the local model predicts a scale invariant dipole modulation. Therefore this model cannot give rise to the observed HPA which is parametrized as dipole modulation with a scale dependent amplitude. For this reason, some authors tried to go beyond this simple model assuming the so-called *quasi* local model, in which the parameter f_{NL} is allowed to vary with the scale. In this regard we present some comments to clarify some confusion that has been made in the literature. More in details, in the following we will briefly discuss:

i. the shape of primordial non-Gaussianity we must consider when we are dealing with long and short mode coupling in the context of HPA;

ii. the possibility to argue informations about the value of the non-Gaussian parameter f_{NL}.

4.2.1 The shape of primordial non-Gaussianity

In the literature many processes that might led to a non-gaussian statistics of the CMB temperature fluctuations have been studied in details [12]. Different processes lead to different types of non-Gaussianity that peaks in different mode configurations or "shapes". We have already introduced the squeezed configuration, consisting in dealing with three Fourier modes such that one of them is much smaller than the other two. Now we shall introduce also the equilateral shape, another type of configuration which occurs when one considers three modes with the same modulus; so they form an equilateral triangle in Fourier space. We shall come back on the issue of the shape of the primordial bispectrum in Sec. 4.3.

Returning to the HPA, recently, some papers, [52] and [53], appear discussing a scale dependent dipolar modulation, based on a quasi local model,

[12] Some of them are listed here [10], [15] and [68].

in which the scale dependence of $A = A(k)$ is due to the scale dependence of f_{NL}. The starting point to calculate the expression of $A(k)$ consists in the splitting of the field $\zeta(\mathbf{x})$ between short and long modes, as we have done in Eq(4.28). The difference is that, now, f_{NL} was considered as function of the cosmological scale: $f_{NL} = f_{NL}(k)$. Summarizing in Refs [52] and [53] the splitting of $\zeta(\mathbf{x})$ has been done in real space, but the f_{NL} parameter were written as in Fourier space. In this way, the parameter f_{NL} result computed in the equilateral configuration. This result is in contrast with the statement that mode coupling occurs in the squeezed configuration.

We want to stress that the coupling between super- and sub-horizon mode is due only to non-Gaussianity computed in the squeezed configuration. This makes sense both physically and mathematically. First of all, let us give an intuitive explanation. We are dealing with Fourier modes that have very different wavelengths. Therefore, it is intuitive to think that their coupling can occur only in the squeezed configuration. In this regard we recall that, our starting point to obtain a modulated statistics on sub-horizon modes, was the *consistency relation*. This relation holds between the bispectrum and the power spectrum in the *squeezed limit*. Also, mathematically, the formalism used in [53] is not correct. In fact, the author considered a scale dependent f_{NL} (in Fourier space) while he was splitting the curvature field $\zeta(\mathbf{x})$ in real space.

A more appropriate formalism to work with a non-local form of non-Gaussianity, consists in the use of kernels, following Refs [72] and [74]. In this formalism, the most general expression of the curvature perturbation $\zeta(\mathbf{x})$, that preserve statistical homogeneity and isotropy is a 2-dimensional convolution

$$\zeta(\mathbf{x}) = \zeta_G(\mathbf{x}) + f'_{NL} \int d^3y\, d^3z\; W(\mathbf{y},\mathbf{z})\; \zeta_G(\mathbf{x}+\mathbf{y})\, \zeta_G(\mathbf{x}+\mathbf{z}), \tag{4.39}$$

where $\zeta_G(\mathbf{x})$ is a homogeneous, isotropic and gaussian distributed field. Notice that, in the above expression, the kernel $W(\mathbf{y},\mathbf{z})$ takes into account the scale dependence of non-Gaussianity. Here, with f_{NL} parameter we mean

$$f_{NL}(\mathbf{y},\mathbf{z}) = f'_{NL} W(\mathbf{y},\mathbf{z}), \tag{4.40}$$

which is a function of position in real space. In Fourier space Eq(4.39) reads

$$\zeta(\mathbf{k}) = \zeta_G(\mathbf{k}) + f'_{NL} \int \frac{d^3k'}{(2\pi)^3}\; \widetilde{W}(\mathbf{k},\mathbf{k}')\; \zeta_G(\mathbf{k}')\, \zeta_G(\mathbf{k}-\mathbf{k}'). \tag{4.41}$$

The statistical isotropy requires that the kernel, $\widetilde{W}(\mathbf{k},\mathbf{k}')$ does not depend on the direction of $\mathbf{k}$ and $\mathbf{k}'$. This means that it can be function only of k, k' and $\mathbf{k}\cdot\mathbf{k}'$, or equivalently k, k' and $|\mathbf{k}-\mathbf{k}'|$. Notice that we can recover the local model with this formalism by setting $W(\mathbf{y},\mathbf{z}) \equiv \delta^3(\mathbf{y})\delta^3(\mathbf{z})$ which, in Fourier space, correspond to $\widetilde{W}(k_1,k_2,k_3) \equiv 1$. Using Eqs (4.39) and (4.41)

and following the same steps made in Sec. 4.1.2 for the local model, we can compute a generalization of the modulated power spectrum. A detailed computation is made in Appendix B.4, here we present just the final results. The modulated power spectrum has the same form of Eq(4.36) with the difference that here f_{NL} is scale dependent:

$$f_{NL}(k_1, k_2, k_3) := f'_{NL}\ \widetilde{W}(k_1, k_2, k_3). \tag{4.42}$$

From the explicit calculation [13] we get that f_{NL} is computed precisely in the squeezed configuration: $f_{NL}(k_l, k_s, k_s)$ thus proving the validity of our statement.

In conclusion a scale dependent power asymmetry can be obtained assuming a quasi-local model, in which the non-Gaussian parameter f_{NL} is allowed to vary with the scale. A suitable formalism to describe a non-gaussian statistics, more general than the local model, consists in the kernel formalism. In this case, the expression of the asymmetry generated by a large super-horizon mode of amplitude ζ_L and wavenumber $\mathbf{p}$ is

$$A = f_{NL}(k_l, k_s, k_s)\ p\ x_{dec}\ \zeta_L\ \frac{\mathcal{B}_\zeta(p, |\mathbf{k}+\frac{\mathbf{p}}{2}|, |-\mathbf{k}+\frac{\mathbf{p}}{2}|)}{P_\zeta(p)\ P_\zeta(k)}. \tag{4.43}$$

4.2.2 The estimate of the f_{NL} parameter

Another important comment we would highlight is about the correct value that have to be assigned to the f_{NL} parameter. We know that the dipolar amplitude A generated from a non-gaussian coupling is proportional to f_{NL}. In this regard, many authors, assigned to f_{NL} affecting in Eq(4.38) the value provided by the observations on primordial non-Gaussianity, when they gave a theoretical estimate of the the HPA amplitude. This is the case, for instance, of [27], [28] and [39] in which f_{NL} is required to be lower than the experimental upper bound.

In our opinion, this requirement is not correct. The reason lies in the fact that, the modulation couples short-wavelength modes with super-horizon modes. Hence the f_{NL} parameter affecting, e.g., in Eq(4.38), refers to the f_{NL} parameter of the theory related to a "box" much bigger than our observable Universe. Conversely, all the measurements on the cosmological parameters, refers to perturbations modes inside our Universe by definition. A theoretical argument in support of this thesis arises from the mode splitting we made in Eq(4.28). In that expression with f_{NL} we meant the parameter defined on the entire Universe. However, in a small sub-sample the statistics may appear biased from the one in the entire volume, as a result, the parameter f_{NL} might be different.

[13] For details see Appendix B.4.

The key point to keep in mind is that although a model of HPA predicts a level of f_{NL} greater than the current bounds [14], this model is not automatically ruled out, because its prediction refers to the statistics of the entire Universe, not to the one defined on the small sub-sample of size corresponding to H_0^{-1} (our observable Universe), the one to which measurements refer to.

In this regard the references [13] and [64] address the problem of the understanding the "true" statistics in the entire Universe, showing explicitly that in a given small sub-sample the statistics may appear biased respect to the total one. Inspired from their results, we decided to make a simple calculation to show what we stated, namely that the observed parameter f_{NL} in a small region, is in general different to the one defined in the entire volume.

Let be L the size of the entire Universe, such that $L \gg H_0^{-1} \equiv M$, where H_0^{-1} is the size of our observable region.

Inside the big box L the curvature perturbation field $\zeta(\mathbf{x})$ is defined. $\zeta^{obs}(\mathbf{x})$ represents, instead, the field in the small sub-sample M. In the uniform density gauge, the curvature field affects the scale factor in such a way that $a(t,\mathbf{x}) = a(t)(1+\zeta(\mathbf{x}))$, where $a(t)$ is the background average made in the sky. The background value $a(t)$ depends on the volume of integration. As a result, $a(t)$ is different if computed in the big and in the small box:

$$a(t,\mathbf{x}) = a_L(t)(1+\zeta(\mathbf{x})) = a_M(1+\zeta^{obs}(\mathbf{x})), \tag{4.44}$$

where $\mathbf{x} \in Vol_M$. To relate the two average values we have to smooth $\zeta(\mathbf{x})$ on scales with wavelength $k^{-1} > H_0^{-1}$. In this way we obtain

$$a_M = a_L(1+\langle\zeta\rangle_M), \tag{4.45}$$

where $\langle\zeta\rangle_M$ is the average of $\zeta(\mathbf{x})$ in the sub-sample M. We want to relate also $\zeta(\mathbf{x})$ with $\zeta^{obs}(\mathbf{x})$. To do this we split $\zeta(\mathbf{x})$ into two parts, in the same way we made for $\zeta_G(\mathbf{x})$ (Eqs(4.26) and (4.27)):

$$\zeta(\mathbf{x}) = \zeta_s(\mathbf{x}) + \zeta_l(\mathbf{x}) \tag{4.46}$$

Plugging this splitting into Eq(4.44) and taking into account also Eq(4.45) we find:

$$a_L[1+\zeta_l(\mathbf{x})+\zeta_s(\mathbf{x})] = a_L(1+\langle\zeta\rangle_M)[1+\zeta^{obs}(\mathbf{x})]. \tag{4.47}$$

Now, $\zeta_l(\mathbf{x})$ represents a sort of average of $\zeta(\mathbf{x})$ on the super-horizon scale, therefore it assumes the same value of $\langle\zeta\rangle_M$. Furthermore, we did not split

[14] At present, the smallest bound of non-gaussianity were provided by the *Planck* satellite. It measured, for the Bardeen potential Φ: $(f_{NL}^{local})_\Phi = 2.7 \pm 5.8$, which means $(f_{NL}^{local})_\zeta \lesssim 14$ (68% *C.L.*). This result is valid in the case a single scalar field during inflation, [68].

$\zeta^{obs}(\mathbf{x})$ because it is defined only in the observable scales. Then with these requirements we get

$$\zeta_s(\mathbf{x}) = (1 + \langle\zeta\rangle_M)\zeta^{obs}(\mathbf{x}). \tag{4.48}$$

Now let us assume that we can parametrize the field $\zeta(\mathbf{x})$ following the local expansion (4.24). So, as usually, we split $\zeta_G(\mathbf{x})$ into a sub- and super-horizon part, obtaining

$$\zeta(\mathbf{x}) = \zeta_{G,s}(\mathbf{x}) + \zeta_{G,l}(\mathbf{x}) + f_{NL}\,(\zeta_{G,s}(\mathbf{x}) + \zeta_{G,l}(\mathbf{x}))^2 + \mathcal{O}(f_{NL}^2). \tag{4.49}$$

Therefore, in the small region M the field is

$$\zeta_s(\mathbf{x}) = \zeta_{G,s}(\mathbf{x}) + f_{NL}\,\zeta_{G,l}(\mathbf{x})\,\zeta_{G,s}(\mathbf{x}) + f_{NL}\,\zeta_{G,s}^2(\mathbf{x}). \tag{4.50}$$

What we find from the splitting is that also the statistics inside M follows the local expansion, however the coefficients that multiply the gaussian field $\zeta_{G,s}(\mathbf{x})$ now depend on a local background or bias B. An estimate of B consists in the quantity $\zeta_{G,l}(\mathbf{x})$ which is almost constant in M. Hereafter we will use B in place of $\zeta_{G,l}(\mathbf{x})$. In terms of the bias $\zeta_s(\mathbf{x})$ rewrites as

$$\zeta_{G,s}(\mathbf{x}) = (1 + f_{NL}\,B)\;\zeta_{G,s}(\mathbf{x}) + \;f_{NL}\,\zeta_{G,s}^2(\mathbf{x}). \tag{4.51}$$

We parametrize the observed curvature field $\zeta^{obs}(\mathbf{x})$, inside the sub-sample M, as

$$\zeta^{obs}(\mathbf{x}) = \zeta_G^{obs}(\mathbf{x}) + \;f_{NL}^{obs}\,(\zeta_G^{obs}(\mathbf{x}))^2, \tag{4.52}$$

where f_{NL}^{obs} is the observed non-gaussian parameter. Finally, plugging Eqs(4.51) and (4.48) into Eq(4.52), after some algebra, we get the final result

$$\zeta_G^{obs}(\mathbf{x}) = \frac{1 + f_{NL}\,B}{1 + \langle\zeta\rangle_M(B)}\zeta_{G,s}(\mathbf{x}), \tag{4.53}$$

$$f_{NL}^{obs} = \frac{1 + \langle\zeta\rangle_M(B)}{[1 + f_{NL}\,B]^2}\;f_{NL}. \tag{4.54}$$

In conclusion, with this simple calculation we showed that the statistics of the observable non-Gaussian field in a small sub-sample is, in general, biased from the statistics of the entire sample. Indeed the observed field $\zeta^{obs}(\mathbf{x})$ is different from $\zeta_s(\mathbf{x})$, as one may naively expect. Moreover the measured f_{NL}^{obs} parameter is not the same that refers to the entire Universe. A measurement of the bias B is obtained by averaging the field in the sub-sample, $B = \zeta_{G,l}(\mathbf{x}),\ \mathbf{x} \in M$. The bias, usually, is greater as the sub-volume is smaller. For this reason all the parameters (like f_{NL}) which characterize the statistics suffer a shift that depends on the bias B.

As a next step, we could specialize the study making a choice of the statistics in the entire Universe and calculating the bias in the sub-sample. However we did not made this full calculation which is left for the future. Anyway, an interesting result of [64] is that, for sufficiently biased sub-samples,

a strongly non-Gaussian model in the large volume generates weakly non-Gaussian sub-samples. Therefore even if the detected f_{NL}^{obs} is small, in the entire Universe the statistics of the curvature perturbation may be highly non-Gaussian.

4.3 Another mechanism to produce a power asymmetry

In the previous section we studied how a single super-horizon curvature perturbation $\zeta(\mathbf{p})$, with an anomalous large amplitude, could give rise to a dipolar asymmetry, by varying the background value of ζ across the observable sky. Anyway, this is not the only mechanism which could generate a modulation in the sky. Ref.[73], for instance, investigates an other possible mechanism to generate a power asymmetry. In [73] it is assumed that a particular realization of the super-horizon fluctuation field $\zeta(\mathbf{k_l})$ [15] statistically picks out a certain direction $\hat{\mathbf{p}}$ in the sky. The key point is that in [73], the asymmetry is not due to the very large amplitude of the realization $\zeta(\mathbf{k_l})$ in the preferred direction $\hat{\mathbf{p}}$ [16], which, instead, is assumed to be small. To recover a modulation across the sky the authors demand that the bispectrum of the primordial perturbations has some specific features. The fact that the amplitude of the super-horizon realization is not much large implies that we can neglect the dependence on $\mathbf{x}_+$ in the modulated power spectrum $P_\zeta^{mod}(k)$ given in Eq(4.23):

$$P_\zeta^{mod}(\mathbf{k_s},\mathbf{x}_+) \simeq P_\zeta(k_s)+f_{NL}\int\frac{d^3k_l}{(2\pi)^3}\,e^{-i\mathbf{k_l}\mathbf{x}_+}\,\frac{\mathcal{B}_\zeta(k_l,|\mathbf{k_s}+\frac{\mathbf{k_l}}{2}|,|-\mathbf{k_s}+\frac{\mathbf{k_l}}{2}|)}{P_\zeta(k_l)}\,\zeta(\mathbf{k_l}). \tag{4.55}$$

In fact, since the argument of the exponential $e^{-i\mathbf{k_l}\mathbf{x}_+}$ is, in modulus, much smaller than one, we expand it in power series, keeping only the $zero^{th}$ order term: $e^{-i\mathbf{k_l}\mathbf{x}_+} = 1+\mathcal{O}(k_l\,x_+)$. Thus we obtain

$$P_\zeta^{mod}(\mathbf{k_s},\mathbf{x}_+) \simeq P_\zeta(k_s)+f_{NL}\int\frac{d^3k_l}{(2\pi)^3}\,\frac{\mathcal{B}_\zeta(k_l,|\mathbf{k_s}+\frac{\mathbf{k_l}}{2}|,|-\mathbf{k_s}+\frac{\mathbf{k_l}}{2}|)}{P_\zeta(k_l)}\,\zeta(\mathbf{k_l}). \tag{4.56}$$

Plugging this result into Eq.(4.22) we get the following the 2-point correlation function in real space

$$\langle\zeta(\mathbf{x_2})\zeta(\mathbf{x_3})\rangle = \int\frac{d^3k_s}{(2\pi)^3}e^{-i\mathbf{k_s}(\mathbf{x_2}-\mathbf{x_3})}P_\zeta^{mod}(\mathbf{k_s}). \tag{4.57}$$

Then, anti-Fourier transforming the above expression we easily get the formula for the 2-point function in Fourier space on observable scales:

$$\langle\zeta(\mathbf{k_2})\zeta(\mathbf{k_3})\rangle = (2\pi)^3\delta^3(\mathbf{k_2}+\mathbf{k_3})P_\zeta^{mod}(\mathbf{k_s}), \tag{4.58}$$

[15] Notice that with particular realization, we are not necessarily meaning a single perturbation mode, but more perturbation ones which conspired to pick out a certain direction.

[16] This is the hypothesis we made in Sec. 4.2

where, we recall that $P_\zeta^{mod}(\mathbf{k_s})$ is given by Eq(4.56). Notice that this result implies statistical homogeneity. This is because the super-horizon field $\zeta(\mathbf{k_l})$ is assumed to be not much ample in the preferred direction, and so it gives a negligible non isotropic contribution.

In [73] the same calculation that we made for the curvature perturbation is carried out for the Bardeen potential Φ. The power spectrum obtained by the authors of [73] is:

$$P_\Phi^{mod}(\mathbf{k}) = P_\Phi(k)\left[1+\int \frac{d^3k_l}{(2\pi)^3} P_\Phi(k)\, G(\mathbf{k},\mathbf{k_l})\,\Phi(\mathbf{k_l})\right] \tag{4.59}$$

$$G(\mathbf{k},\mathbf{k_l}) \equiv \frac{\mathcal{B}_\Phi(k_l, |\mathbf{k_s}+\frac{\mathbf{k_l}}{2}|, |-\mathbf{k_s}+\frac{\mathbf{k_l}}{2}|)}{P_\Phi(k_l)\,P_\Phi(k)}.$$

Notice that, here the bispectrum $\mathcal{B}_\Phi$ includes the dimensionless non-linearity parameter $f_{_{NL}}$. Let us stress that the kernel $G(\mathbf{k},\mathbf{k_l})$ has a dependence on the super-horizon modes $\mathbf{k_l}$ and hence is not observable (see the previous section). The corresponding 2-point function in Fourier space of the Bardeen potential is

$$\langle\Phi(\mathbf{k})\Phi^*(\mathbf{k}')\rangle = (2\pi)^3\delta^3(\mathbf{k}-\mathbf{k}')P_\Phi(k)\left[1+\int\frac{d^3k_l}{(2\pi)^3}P_\Phi(k)G(\mathbf{k},\mathbf{k_l})\Phi(\mathbf{k_l})\right] \tag{4.60}$$

Thanks to the above equation, in the angular space, they found a covariance matrix for the coefficients a_{lm}, which are the spherical expansion of the field of the CMB temperature anisotropies $\theta(\hat{\mathbf{n}})$ [17]:

$$\langle a_{lm}a^*_{l'm'}\rangle = \delta_{l\,l'}\delta_{mm'} + \int\frac{k_l^2dk_l}{(2\pi)^3}\sum_{L\,M}\mathcal{G}^{l\,l'\,L}_{-mm'M}\,\mathcal{C}_{l\,l'}(k_l)\,\Phi_{LM}(k_l), \tag{4.61}$$

where $\mathcal{G}^{l\,l'\,L}_{-mm'M}$ are Clebsch-Gordan coefficients and they have set

$$C_{l\,l'}(k_l) = \frac{1}{\pi}\int k^2dk[\Delta_l(k)\Delta^*_{l'}(k)+\Delta^*_l(k)\Delta_{l'}(k)]P_\Phi(k)G_L(k,k_l). \tag{4.62}$$

Here $\Delta_l(k)$ are the transfer functions defined in Sec. 3.2.1. Notice also that the kernel $G(\mathbf{k},\mathbf{k_l})$ and the long modes realization were expanded in spherical harmonics

$$G(\mathbf{k},\mathbf{k_l}) = \sum_{L\,M} G_L(k,k_l)\,Y^*_{LM}(\hat{\mathbf{k}_l})\,Y_{LM}(\hat{\mathbf{k}}), \tag{4.63}$$

$$\Phi_{LM} = \int d\Omega_{k_l}\Phi(\mathbf{k_l})Y^*_{LM}(\hat{\mathbf{k}_l}). \tag{4.64}$$

[17] The explicit calculation can be found in Appendix B.5.

To get a modulation in the power spectrum the authors did not demand a large amplitude anisotropy. Conversely they consider a bispectrum $\mathcal{B}_\Phi(k_l, |\mathbf{k_s} + \frac{\mathbf{k_l}}{2}|, |-\mathbf{k_s} + \frac{\mathbf{k_l}}{2}|)$ with some specific features, that often arises from inflaionary models with an initial non Bunch-Davies vacuum. In details the bispectrum need to have the following properties:

i. a bispectrum that consists in a non-trivial function of $\mathbf{k} \cdot \mathbf{k_l}$;

ii. a bispectrum that peaks in the squeezed limit.

In fact, the coefficients $C_{ll'}(k_l)$ are equal to the temperature power spectrum C_l when replacing $P_\Phi(k) \to G_L(k, k_l)P_\Phi(k)$. Thus, apart from the fact that the covariance matrix involves $C_{l\,l'}$, instead of $C_l + C_{l'}$ (see Eq(4.2)), it is identical in structure to the covariance obtained for the anisotropic field (B.2). In conclusion, if we focus only ion the dipole term, with $L = 1$, we see that Eq(4.61) becomes similar to Eq(4.2), and so the temperature anisotropies field experiences a dipole modulation in the sky.

Let us stress that this idea is very interesting, because of its originality: the dipole asymmetry is, indeed, due not to the presence of a very large super-horizon perturbation, but to the bispectrum with particular properties that is assumed to have the primordial curvature field. Moreover, this process is very general and can be used also for different type of perturbations. In Sec.6.3.2, for instance, we will show that such a mechanism can generate a modulation also in the power spectrum of tensor perturbations.

Chapter 5

Application to inflationary models

In the previous Chapter we developed a sort of phenomenological model to describe a possible way to generate the HPA, which exploits the coupling between perturbations of different wavelengths. In this model we gave a parametrization of the primordial curvature field ζ, or equivalently of the Bardeen potential Φ. We did not care about details on the origin of these fields which occurred during inflation. Therefore, such a phenomenological model must be put in the context of in a well determined inflationaty theory. With the necessary precautions it can be specialized for different inflationary models. With this goal in mind in this Chapter we will describe several simple toy models that try to implement the phenomenological models of HPAwe introduced. To do this we will follow some results available in the literature.

First of all we will focus on the simplest models of single-fields slow-roll inflation, showing explicitly that, because of the experimental bounds on the CMB temperature anisotropy multipoles, it cannot generate a large enough dipolar asymmetry, [27] [62]. Then we will turn our attention on the *curvaton model*. It is a two fields inflationary theory. We will describe its main features and then we will show that, in such model, a scale invariant power asymmetry can be generated without violating the experimental bounds on the CMB temperature anisotropy multipoles. Finally we will discuss some toy models which try to explain the particular scale dependence of the observed HPA, [28], [22] and [39].

5.1 Standard models of infaltion

In the simplest model of inflation a real scalar field $\varphi(t, \mathbf{x})$, with the usual kinetic term and minimally coupled to gravity, causes both the accelerated expansion of the Universe and the generation of the primordial curvature perturbations ζ. We discussed the inflationary dynamics of this model in Chap.1 and the generation of the primordial curvature perturbations in Sec.2.6.1.

The inflaton was the first field which was assumed to have a super-horizon fluctuations that generated the power asymmetry in the literature. Now we

show that the inflaton field cannot support a dipole modulation large enough to explain the HPA. Let be $\Delta\zeta$ a super-horizon curvature perturbation. This were generated by the change of the inflaton field acroos the observable Universe $\Delta\varphi$. Thus,

$$|\Delta\zeta| = \frac{H_I}{\dot{\varphi}}\Delta\varphi = 4\pi\sqrt{\frac{2}{\epsilon}}\,\frac{\Delta\varphi}{M_{Pl}}, \tag{5.1}$$

where we recall that H_I is the Hubble rate during inflation, $\epsilon = 3\dot{\varphi}^2/(2V(\varphi))$ is a slow-roll parameter and $M_{Pl} = \sqrt{8\pi/G}$ is the reduced Planck mass.

Thanks to non-gaussianity the super-horizon perturbation $\Delta\zeta$ couples with sub-horizon fluctuations. Inside the observable Universe we experience its presence as a dipolar modulation across the sky of the field $\zeta(\mathbf{x})$. The amplitude A of the modulation is given by Eq(4.38). Remembering that for the inflaton model, in the squeezed limit, $f_{_{NL}} \simeq (n_s - 1)/4$, in terms of $\Delta\varphi$ we get the following expression:

$$A = 4\ f_{_{NL}}\ \Delta\zeta = 8\pi\sqrt{\frac{2}{\epsilon}}(n_s - 1)\frac{\Delta\varphi}{M_{Pl}}. \tag{5.2}$$

The above expression differs from Eq(4.38), because, here we have not yet explained the shape $\Delta\zeta$ (or equivalently $\Delta\varphi$) and then we wrote $\Delta\varphi$ in place of $\zeta_L \sin(\mathbf{p}\cdot\mathbf{x_{rec}}) \approx \zeta_L \mathbf{p}\cdot\mathbf{x_{rec}}$.

The curvature field $\Delta\zeta$ affects the Bardeen gravitational potential Φ, which, in turn, generates the CMB temperature fluctuations field, $\theta(t,\mathbf{x})$ (see Eq(4.3)). Therefore, $\Delta\zeta$ creates a super-horizon fluctuation $\Delta\Phi$ which in turn produces a modulation of $\theta(t,\mathbf{x})$ on $\theta(t,\mathbf{x})$. During matter domination, when decoupling and hence CMB anisotropies formation occurred, Φ is related to ζ by $\Phi = -3/5\,\zeta$. Thus

$$|\Delta\Phi| = \frac{12\pi}{5}\sqrt{\frac{2}{\epsilon}}\,\frac{\Delta\varphi}{M_{Pl}}. \tag{5.3}$$

Plugging the above expression into Eq(5.2) we find the relation between the modulation of the Bardeen potential and the generated dipole amplitude:

$$\Delta\Phi = \frac{3}{10}\frac{A}{n_s - 1}. \tag{5.4}$$

The fluctuation $\Delta\Phi$ leaves its footprint in the CMB multipoles a_{lm}. To quantify such a footprint we give an explicit shape to the long wavelength perturbation. We assume it has a sinusoidal shape $\Delta\Phi = \Phi_L \sin(\mathbf{p}\cdot\mathbf{x})$. Since $p\,x_{rec} \ll 1$, where x_{rec} is the distance from recombination surface, we expand $\Delta\Phi$ in power series. Let us now focus on the second term of the expansion

$$\Phi(\mathbf{x}) = \Phi_L\frac{(\mathbf{p}\cdot\mathbf{x})^3}{6}. \tag{5.5}$$

Mainly through the Sachs-Wolfe effect, this latter term affects the octupole coefficient C_3 of the CMB anisotropies field. Then we have

$$\theta(\hat{\mathbf{n}}) \simeq \frac{\Phi_L}{3}\frac{(p\,x_{rec})^3}{6}\,\hat{\mathbf{p}}\cdot\hat{\mathbf{x}}_{rec}, \tag{5.6}$$

where $\hat{\mathbf{x}}_{rec} = \hat{\mathbf{n}}$. To get a consistent power asymmetry ($A \simeq 0.07$) the induced octupole have to be smaller than C_3, the measured one. More precisely, we require

$$\Phi_L(p\,x_{rec})^3 \lesssim 32\,\mathcal{O}, \tag{5.7}$$

where $\mathcal{O}$ is the upper bound on the coefficient a_{30}, in a coordinate system aligned with the power asymmetry [27]. The coefficient $\mathcal{O}$ is taken to be $\mathcal{O} = 3\sqrt{C_3} \lesssim 2.7\cdot 10^{-5}$, three times the measured value of the octupole as a 3σ upper limit (this accounts for cosmic variance), [26].

For fixed $\Delta\Phi$, the induced temperature octupole (5.6) can be made arbitrarily small by choosing a sufficiently small p. However the Bardeen potential is a perturbation of the metric and we demand $\Phi_L \lesssim 1$, namely that the amplitude of the super-horizon mode is less than unity everywhere. With this requirement approximatively $\Delta\Phi \sim (k\,x_{rec})$, and hence we get

$$\Delta\Phi \lesssim (32\mathcal{O})^{1/3}. \tag{5.8}$$

Combining the above expression with Eq(5.4) we finally obtain

$$A \lesssim \frac{10}{3}(n_s - 1)(32\,\mathcal{O})^{1/3} \approx 0.0127. \tag{5.9}$$

We obtained the last result setting $|n_s - 1| \approx 0.04$, [66], [69]. We see that the upper amplitude consistent with observations is far too small to be consistent with the detected power asymmetry. Notice that to estimate the maximum amplitude we used the central value *Planck* results of the spectral index. Let us stress that $n_s - 1$ in Eq(5.9) should refer to the spectrum scale-dependence spanning over scales larger than the our observable Universe. However, since the inflaton model predicts $(n_s - 1) \sim \mathcal{O}(\epsilon, \eta)$, due to a smooth slow-roll dynamics over many e-folds, we expect that the "correct" value does not differ much from the measured one. In conclusion, it seems that the HPA cannot be reconciled with the simplest models of inflation.

5.2 The Curvaton model

Since with the standard inflaton model we have not reached a positive result, we decided to turn our attention to a slightly more complicated model of inflation named the *Curvaton model*. This multi-field model was studied in detail over the last 15 years. We refer to some papers like [8], [47], [48] (even though its original idea can be traced back to [46] and [60]). Such model

could generate higher level of primordial non-Gaussianity, with respect to the case of the standard single-field scenario, which also peaks in the squeezed limit. A greater f_{NL} encourages the generation of a stronger asymmetry. This is the reason that led us to turn our attention to multi-fields models.

This scenario introduces a second scalar field, the *curvaton*, $\sigma(t, \mathbf{x})$, during the inflationary era. This field is not responsible for the inflationary dynamics, indeed during inflation it acts as a spectator. Conversely the curvaton could be responsible for the primordial curvature perturbation (hence the name "curvaton"). It is assumed that the curvaton too has a standard kinetic term and minimally couples with gravity, thus giving the Lagrangian

$$\mathcal{L} = g^{\mu\nu} \left[\partial_\mu \varphi \partial_\nu \varphi + \partial_\mu \sigma \partial_\nu \sigma\right] - V(\varphi, \sigma). \tag{5.10}$$

The potential $V(\varphi, \sigma)$ is assumed to be separable,

$$V(\varphi, \sigma) = V(\varphi) + V(\sigma). \tag{5.11}$$

As a result, the inflaton and the curvaton does not interact.

We can distinguish two different phases of the early Universe in which the curvaton has a different behaviour: the inflationary epoch and the reheating phase.

5.2.1 Dynamics during infation

During inflation, the curvaton is effectively massless, $V_{\sigma\sigma} = m_\sigma \ll H_I$, thus, we stress that it does not interact with any other field, especially with the inflaton. Furthermore, it is assumed that it has a negligible energy density.

To study the dynamic of the curvaton field, we split the field $\sigma(t, \mathbf{x})$ into a background plus fluctuations

$$\sigma(t, \mathbf{x}) = \sigma_0(t) + \delta\sigma(t, \mathbf{x}), \tag{5.12}$$

and we look separately at the evolution of the two quantities. From the explicit calculation we find that the equation of motion for the background value has the same form of Eq(1.23), which governs the motion of φ_0. Neglecting the subscript 0,

$$\ddot{\sigma} + 3H\dot{\sigma} = V_\sigma, \tag{5.13}$$

where $V_\sigma = \partial V / \partial \sigma$. Since the curvaton is assumed to be sufficiently decoupled, also the equation of motion for the quantum fluctuations is formally equal to the one of $\delta\varphi$, (1.28):

$$\ddot{\delta\sigma} + 3H\dot{\delta\sigma} + \frac{\nabla^2 \delta\varphi}{a^2} = -V_{\sigma\sigma}\delta\sigma, \tag{5.14}$$

where $V_{\sigma\sigma} = m_\sigma^2 \ll H_I^2$. We can thus neglect the latter term in the above equation. It is assumed that, on cosmological scales, each Fourier component

stays in the vacuum state well before horizon exit. The vacuum fluctuation, then causes a classical perturbation, (in general) gaussian distributed, well after horizon exit, which in conformal time $\tau := \int dt/a(t)$, satisfies Eq(1.37):

$$\delta\sigma_{\mathbf{k}}'' - \frac{a''}{a}\delta\sigma_{\mathbf{k}} = 0. \tag{5.15}$$

This means that, when the perturbation modes are super-horizon, $\delta\sigma_{\mathbf{k}}$ is frozen. In this limit, when the above expression is well satisfied, its dimensionless power spcetrum is given by

$$\mathcal{P}_{\delta\sigma}(k) = \left(\frac{H_k}{2\pi}\right)^2, \tag{5.16}$$

where H_k is the value of the Hubble rate at the time in which the comoving scale $\mathbf{k}$ left the horizon ($k = a_k(t)H_k(t)$). Notice that both the inflaton and the curvaton quantum fluctuations have the same power spectrum. Then both the two fields have a nearly scale invariant spectrum. As we have done for the inflaton, we quantify the departure of scale invariance of $\mathcal{P}_{\delta\sigma}(k)$ introducing the coefficient n, similar to the one defined in eq(2.70). It can be easily checked that

$$(n-1) := \frac{d\ln\mathcal{P}_\sigma(k)}{d\ln k} = 2\eta_\sigma - 2\epsilon, \tag{5.17}$$

a result which also accounts properly in Eq(5.14) for the mass term $\eta_\sigma := V_{\sigma\sigma}/3H^2$, [48]. As we expected, the deviation from scale invariance, is of order of the slow-roll parameters.

5.2.2 The reheating phase

Shortly after inflation, the inflaton decays into radiation and the Universe becomes radiation dominated (see discussion in Sec. 3.1). This marks the beginning of the usual FRW Universe and the Hubble rate starts to decrease in time as $H \sim 1/t$. When $H \simeq m_\sigma$ the curvaton starts to oscillate around the minimum of its potential, so it acquires a non-negligible mass. During the oscillating phase $\sigma(t, \mathbf{x})$ behaves like matter, [42]. Therefore, its energy density scales like $\rho_\sigma \propto a^{-3}$. Since the radiation energy density scales as $\rho_\gamma \propto a^{-4}$,

$$\frac{\rho_\sigma}{\rho_\gamma} \propto a(t), \tag{5.18}$$

the curvaton energy density becomes relevant, and it can happen that it starts to dominate the total density of the Universe.

Notice that, if we expand the curvaton potential $V(\sigma)$ in power series, when $\sigma(t, \mathbf{x})$ begins to oscillate around its minimum, only the quadratic term is relevant. Therefore, at least during the oscillating phase,

$$V(\sigma) \simeq \frac{1}{2}m_\sigma^2\sigma^2. \tag{5.19}$$

We will use this expression for the potential to compute the curvaton contribution to the final curvature perturbations.

Few Hubble times after the beginning of the curvaton oscillations, it is expected that also the curvaton decays into radiation and relativistic particles. Just before the decay, the primordial energy density perturbations, thanks to Eq(5.19), are, up to first order,

$$\delta\rho_\sigma \simeq V_\sigma \delta\sigma = m_\sigma^2 \delta\sigma. \tag{5.20}$$

We define the density contrast, $\delta = \delta\rho_\sigma/\rho_\sigma$, which will be useful later. It turns out to be

$$\delta = 2\left(\frac{\delta\sigma}{\sigma_*}\right), \tag{5.21}$$

where σ_* is the classical background value σ_0, evaluated just before the decay.

5.2.3 Generation of the curvature perturbation

Now we move to the calculation of the primordial curvature perturbations. Notice that in this case, we have a mixture of two different fluid, so we shall use the multi-fields formalism developed in Sec.2.6.2.

Shortly after inflation the Universe is radiation dominated because the inflaton decays into relativistic particles, so there are curvature perturbations in the radiation fluid ζ_γ that arose from the inflaton quantum fluctuations. Together with these there are also isocurvature perturbations $S_{\gamma\,\sigma}$ that are due to presence of the curvaton field. According to the definition (2.75) their explicit form is

$$S_{\gamma\,\sigma} = -3(\zeta_\gamma - \zeta_\sigma). \tag{5.22}$$

In the above expression we considered separately the curvature perturbations ζ_γ and ζ_σ defined respectively on slices of uniform radiation and matter density (see Eq(2.62)). Since the radiation and the curvaton are non-interacting fluids, these are separately conserved. The curvature perturbations ζ_γ and ζ_σ are given by (in the spatially flat gauge)

$$\zeta_\gamma = -H\frac{\delta\rho_\gamma}{\dot\rho_\gamma}, \tag{5.23}$$

$$\zeta_\sigma = -H\frac{\delta\rho_\sigma}{\dot\rho_\sigma}. \tag{5.24}$$

Notice that, using the continuity equation (1.6) with $P = 0$, in terms of the density contrast (5.21) ζ_σ reads

$$\zeta_\sigma = \frac{\delta}{3} \tag{5.25}$$

Once the curvaton begins to oscillate the energy density becomes a mixture of matter (the curvaton) and radiation. Because of the presence of

matter and radiation, the total fluid which permeates the Universe has no longer an equation of state of the form $P = w\rho$. This implies the existence of non-adiabatic pressure perturbations δP_{nad}, that, according to Eq(2.63), generates curvature perturbations.

We can compute precisely the total amount of curvature perturbation ζ, on large scales, using

$$\dot{\zeta} = -\frac{H}{P+\rho}\delta P_{nad}. \tag{5.26}$$

In a two-field model, we can use a transfer matrix to describe the evolution of the perturbations after Hubble exit, [57]:

$$\begin{pmatrix} \zeta^{(f)} \\ S^{(f)} \end{pmatrix} = \begin{pmatrix} 1 & \tau_{\zeta S} \\ 0 & \tau_{SS} \end{pmatrix} \begin{pmatrix} \zeta^{(i)} \\ S^{(i)} \end{pmatrix}. \tag{5.27}$$

The initial curvature perturbations $\zeta^{(i)}$ comes from the inflaton (ζ_γ), while the final one $\zeta^{(f)}$ are a mixture of the initial curvature and isocurvature ($S^{(i)} = S_{\gamma\sigma}$) perturbations; the coefficients $\tau_{\zeta S}$ and τ_{SS} are model dependent. In the case in which the curvaton decays when all particle species are still in thermal equilibrium with radiation we have $\tau_{SS} = 0$. This means that $S^{(i)}$ generates only curvature perturbations on super-horizon scales (i.e. only adiabatic perturbations are left over the curvaton decay). The coefficient $\tau_{\zeta S}$ is, in general, more involved to calculate, because it requires the knowledge of the curvaton decay rate Γ_σ, [9]. Fortunately, to give an estimate of $\tau_{\zeta S}$, it is enough to assume that the σ decay occurs instantaneously at the epoch $H = \Gamma_\sigma$ (the so called instantaneous decay), namely when σ is no longer decoupled from radiation. In that case one can avoid to use $\tau_{\zeta S}$ altogether [47] by considering Eq(2.74) which gives the total curvature perturbation:

$$\zeta = \frac{\dot{\rho}_\gamma\zeta_\gamma + \dot{\rho}_\sigma\zeta_\sigma}{\dot{\rho}_\gamma + \dot{\rho}_\sigma} = \frac{-4\rho_\gamma \frac{H}{\dot{\varphi}}\delta\varphi + \rho_\sigma\delta}{4\rho_\gamma + 3\rho_\sigma}. \tag{5.28}$$

In conclusion, we found that, in general in the curvaton model the quantum fluctuation of both the inflaton and the curvaton contributes to generation of the total curvature perturbation field $\zeta(\mathbf{x})$.

Notice that Eq(5.28) can be rewritten using the δN formalism (see Sec. 2.6.3), at first order, as

$$\zeta = N_\varphi\delta\varphi + N_\sigma\delta\sigma, \tag{5.29}$$

while we recall that $N_\varphi = \partial V/\partial\varphi$, $N_\sigma = \partial V/\partial\sigma$ and $N_{\sigma\sigma} = \partial^2 V/\partial\sigma^2$ and $\delta\varphi$ and $\delta\sigma$ are the quantum fluctuations of the fields evaluated at horizon crossing. Then, in general, since $\langle\delta\varphi(\mathbf{k})\delta\sigma(\mathbf{k})\rangle = 0$, the dimensionless power spectrum reads

$$\mathcal{P}_\zeta(k) = (N_\varphi^2 + N_\sigma^2)\mathcal{P}_{\delta\varphi}, \tag{5.30}$$

where we have used the fact that at horizon crossing $P_{\delta\varphi} \simeq P_{\delta\sigma}$. Once we have the curvature power spectrum, before proceeding, we define two useful quantities: the energy density ratio R and the fraction between the curvaton contribution to the total power spectrum ξ, which are respectively

$$R = \frac{\rho_\sigma}{\rho_{tot}} = \frac{\rho_\sigma}{\rho_\gamma + \rho_\sigma}, \tag{5.31}$$

$$\xi = \frac{\mathcal{P}_{\zeta,\sigma}(k)}{\mathcal{P}_\zeta(k)} = \frac{N_\sigma^2}{N_\varphi^2 + N_\sigma^2}. \tag{5.32}$$

The last parameter is obtained using Eqs (5.29) and (5.30).

5.2.4 Non-Gaussianity

In the curvaton model primordial non-Gaussianity is assumed to be generated mainly from the quantum fluctuations $\delta\sigma(t, \mathbf{x})$, [50]. A full calculation of the level of non-Gaussianity requires the use of perturbation theory up to second order, [9], [10], that we did not develop in this thesis. Fortunately, as we see in the next subsections, for our purpose we need to know the level of non-gaussianity only when $R, \xi \ll 1$. In that case the following naive calculation agrees with the correct calculation.

Let us write the density contrast δ, considering also the second order perturbation in $\delta\sigma$:

$$\delta = \left[2\left(\frac{\delta\sigma}{\sigma_*}\right) + \left(\frac{\delta\sigma}{\sigma_*}\right)^2 \right], \tag{5.33}$$

which follows from perturbing Eq(5.19). The density contrast affects the total curvature perturbation (5.28), that can be rewritten as (in the limit $R \ll 1$):

$$\begin{aligned} \zeta &\simeq -\frac{H}{\dot\varphi}\delta\varphi + \frac{R}{4}\left[2\left(\frac{\delta\sigma}{\sigma_*}\right) + \left(\frac{\delta\sigma}{\sigma_*}\right)^2 \right] \\ &\equiv N_\varphi \delta\varphi + N_\sigma \delta\sigma + N_{\sigma\sigma}\delta\sigma^2. \end{aligned} \tag{5.34}$$

Notice that we reintroduced the δN formalism in the last line and we neglected primordial non-Gaussianity in the inflaton field $\delta\varphi$ since, at least for the standard models of slow-roll considered here, it is very small, [3], [55]. Recalling the results of Sec.2.6.3 we get a non-Gaussian parameter

$$f_{NL} = \frac{N_\sigma^2 N_{\sigma\sigma}}{(N_\varphi^2 + N_\sigma^2)^2}. \tag{5.35}$$

Therefore, since

$$N_{\sigma\sigma} = \frac{N_\sigma^2}{R} \tag{5.36}$$

substituting it and Eq(5.32) in the expression for f_{NL} we find

$$f_{NL} = \frac{\xi^2}{R} \tag{5.37}$$

This result is in agreement with the correct one computed taking into account the full second order calculation [9] and [27, 28] [1]. Notice that a considerable level of non-Gaussianity, can be generated if $\xi > R$ and $R \ll 1$ especially in the limit $R \ll 1$.

Before concluding this section we give some comments about the isocurvature perturbations. We stated that if the curvaton decays into particles in thermal equilibrium the final isocurvature perturbations vanish. However may happen that one or more particle species decoupling from radiation before the curvaton decay. In this case τ_{SS} is non-vanish and therefore some final isocurvature perturbations do survive. One can show that [28]

$$S^{(f)} = \tau_{SS} S_{\gamma\sigma} = \tau_{SS} \left[2\left(\frac{\delta\sigma}{\sigma_*}\right) + \left(\frac{\delta\sigma}{\sigma_*}\right)^2 \right]. \tag{5.38}$$

We see that $S^{(f)}$ contains a non-gaussian component which gives an f_{NL} parameter equal to

$$f_{NL}^{(iso)} = \frac{1}{4\tau_{SS}}. \tag{5.39}$$

That has been computed using the δN formalism. Once weighted with the isocurvature-to-curvature ratio, f_{NL}^{iso} contributes to the total non-Gaussianity of the CMB temperature fluctutuations field $\theta(\hat{\mathbf{n}})$. Interestingly, even if f_{NL}^{iso} is scale independent, it gives a scale dependent non-Gaussian contribution to $\theta(\hat{\mathbf{n}})$, because once the isocurvature modes re-enter the horizon, their amplitude decays.

5.3 Dipolar modulation in the curvaton model

Now we ask whether if the curvaton model can support a dipolar asymmetry consistent with the current observational limits. To answer this question, following [27], we assume the presence of a super-horizon fluctuation $\Delta\sigma$, where $\Delta\sigma$ is the variation of the mean curvaton value across the observable Universe. This affects the curvature perturbation ζ_σ, and in turn the final total curvature perturbation ζ. The generated super-horizon perturbation is

$$\Delta\zeta = \frac{r}{4}\left[2\left(\frac{\Delta\sigma}{\sigma_*}\right) + \left(\frac{\Delta\sigma}{\sigma_*}\right)^2 \right]. \tag{5.40}$$

[1] These references compute the f_{NL} for the Bardeen potential, thus $f_{NL}^{\zeta} \approx -\frac{3}{5} f_{NL}^{\Phi} = -\frac{\xi^2}{R}$.

This leads to a dipolar asymmetry across the sky with amplitude A. To calculate A the formula we used for the inflaton, eq(5.2), is no longer valid. In fact in Chap.4, to compute it considering a model in which the curvature perturbation is generated by only one field (the inflaton model). Therefore, in a two-field model eqs (4.38) and (5.2) are still valid only in the limit $\xi = 1$. In general, to get the correct amplitude we must multiply eq(5.2) for a factor $1/\xi$: [2]

$$A = \frac{4\, f_{NL}\, \Delta\zeta}{\xi}. \tag{5.41}$$

Plugging the explicit formulae of the super-horizon perturbation $\Delta\zeta$ and the non-gaussianity parameter, given respectively by eqs (5.40) and (5.35), we get the final expression

$$A \simeq 2\xi\, \frac{\Delta\sigma}{\sigma_*}, \tag{5.42}$$

which is in perfect agreement with the dipole amplitude computed in [27]. Following the computation made in Sec.5.1 we assume the sinusoidal shape for the quantum fluctuation $\Delta\sigma$:

$$\Delta\sigma = \sigma_L \sin(\mathbf{p}\cdot\mathbf{x}), \tag{5.43}$$

where we will, at the end, are interested in evaluating this expression on the last scattering surface at the time of decoupling. As usually, we take $\mathbf{p}$ such that $p \ll x_{rec}$, where x_{rec} is the distance from the last scattering surface. Since the super-horizon perturbation $\Delta\Phi$ (or $\Delta\zeta$ contains a term quadratic in $\Delta\sigma$, the power expansion reveals a non-vanishing quadrupole term, which add a contribution to the CMB temperature anisotropies multipole a_{20}, computed in a coordinate system aligned with the asymmetry. The contribution is

$$\theta(\hat{\mathbf{n}}) \simeq \frac{R}{20}\left(\frac{\Delta\sigma}{\sigma_*}\right)^2 (p\, x_{rec})^2\, (\hat{\mathbf{p}}\cdot\hat{\mathbf{x}}_{rec})^2. \tag{5.44}$$

To compute the above result we calculated the explicit expression of $\Delta\Phi = -3/5\,\Delta\zeta$, where $\Delta\zeta$ is given in Eq(5.40) and then we compute the quadrupole contribution to $\Delta\Phi$. This result places an observational constraint on the dipolar amplitude [26], [27]:

$$R\left(\frac{\Delta\sigma}{\sigma_*}\right)^2 \lesssim 14.5\mathcal{Q}, \tag{5.45}$$

where $\mathcal{Q}$ is taken to be three times the measured rsm value of the quadrupole, $\mathcal{Q} = 3\sqrt{C_2} \lesssim 1.8\cdot 10^{-5}$. Plugging Eq(5.42) into the observational constraint equation (5.45) we get

$$\frac{r}{\xi^2} \lesssim 4A^2(14.8\mathcal{Q}) \simeq 0.002, \tag{5.46}$$

[2] The full calculation about the correct formula (5.41) can be found in Appendix C.

for $A \simeq 0.7$. If this bound is satisfied a dipolar asymmetry is not in contrast with the observational limit on the amplitude of the CMB quadrupole. This limit imposes also a lower bound on non-gaussianity:

$$f_{NL}^{\Phi} \gtrsim 0.1 \frac{A^2}{\mathcal{Q}} \simeq 28. \tag{5.47}$$

The authors of [27] take the view of considering f_{NL}^{Φ} affecting in Eq(5.47), the same as the one which is observed in our local patch of the Universe. Therefore, since the present limit on f_{NL} obtained by *Planck* in the squeezed configuration is $f_{NL}^{\Phi} = 8.5$ (68% C.L.), [68], the authors conclude that the the model is not consistent with data. However we have a different opinion: let us stress, indeed, that although f_{NL}^{Φ} is greater than the *Planck* bound, this does not means that the model is inconsistent. Indeed, $f_{NL}^{\Phi} \approx 28$ refers to the statistics of the entire Universe which could be greater than the measured parameter (see discussion in Sec.4.2.2). However, we recall that such an asymmetry has the same amplitude at all scales and so it is not consistent with the detected HPA(which has a non-trivial scale dependence). In the next section we describe a simple toy model that add a scale dependence on such asymmetry, making it consistent with the data.

5.4 Scale dependent power asymmetry

Several models were proposed to explain the scale dependence of the HPA, all of them consider a multi field inflationary scenario. More in detail, ref[28] discusses some possible methods that may generate a scale dependent asymmetry in the context of the curvaton model. For instance, to dilute the power asymmetry, the authors tried to introduce several types of discontinuities in the inflaton potential and its derivative, in order to change the relative contributions of the curvaton and the inflaton fields to the primordial perturbation. However, the only way that they found to get a power asymmetry consistent with data consists in assuming the presence of isocurvature modes which survived after the curvaton decay.

5.4.1 Scale dependence from isocurvature perturbations

Assuming that some final isocurvature modes are generated after the curvaton decay one finds that they remain constant when they are on super-horizon scales then, as soon as they re-enter the Hubble horizon, they start to decay. Since the first scales that re-entered the horizon are the smallest ones, the contribution of the isocurvature perturbations to the CMB anisotropies will be damped at small scales, and as a result, they will contribute mainly on the largest-scales ($l \lesssim 100$).

Let be $\Delta\sigma$ a super-horizon fluctuation of the curvaton field. In the observable Universe, such fluctuation generates a scale invariant dipolar asymmetry

both in curvature and isocurvature perturbations. However, as one considers smaller and smaller scales, the decreasing of the isocurvature contribution to the total power spectrum, makes the asymmetry scale dependent. Consequently, the desired scale-dependence of the asymmetry is a natural feature of isocurvature perturbations.

Notice that, as we said in the previous section, to generate a non-vanishing isocurvature mode, there must be at least a particle specie which decouples before the curvaton decay. In [28], the authors assumed that dark matter is the species decoupling before the curvaton decay. In this case an isocurvature perturbation between radiation and dark matter $S_{\gamma m}$ is created.

To compute the amplitude of the final curvature and isocurvature fluctuations, respectively $\zeta^{(f)}$ and $S_{\gamma m}$ they use the transfer matrix (5.27). The authors assumed that the curvaton never dominated the energy density, they set $R \ll 1$. In that case, with the additional hypothesis of the instantaneous curvaton decay, one finds [28]

$$\tau_{\zeta S} \simeq \frac{R^{(bd)}}{4}, \tag{5.48}$$

where the superscript (bd) means that the density ratio r is evaluated just before the curvaton decay. To compute τ_{SS} the authors considered the two limiting cases depending on whether the curvaton created or not most of the dark matter. They find

$$\tau_{SS} = 1 - R, \tag{5.49}$$

if the curvaton creates nearly all the dark matter, while if its contribution is negligible, one finds

$$\tau_{SS} = \kappa R, \tag{5.50}$$

where κ is found to be a constant which can assume values between $[-1; 1/R]$.

Once $\tau_{\zeta S}$ and τ_{SS} have been computed the early time perturbations in the matter-radiation fluid can be easily calculated from the initial ones that arise from the inflaton and the curvaton fluctuations. They are:

$$\zeta^{(f)} = \zeta_\gamma + \frac{R^{(bd)}}{4} S_{\gamma\sigma} \tag{5.51}$$

$$S_{\gamma m} = \tau_{SS} S_{\gamma\sigma} \tag{5.52}$$

We uses these as initial conditions to calculate the CMB power spectrum. Notice that both $\zeta^{(f)}$ and $S_{\gamma m}$ depend on $S_{\gamma\sigma}$ and hence they have a non-vanishing correlation which will affect also the CMB anisotropies field $\theta(\hat{\mathbf{n}})$. To compute the spectrum of the initial perturbations the authors quantize the primordial perturbations of the inflaton and the curvaton field related respectively to ζ_γ and $S_{\gamma\sigma}$. Then they define the dimensionless power spectra

of the perturbations of the initial matter-radiation fluid as

$$\mathcal{P}_\zeta(k) \equiv \frac{k^3}{2\pi^2}\langle\zeta^{(f)}(\mathbf{k})\zeta^{(f)*}(\mathbf{k})\rangle, \tag{5.53}$$

$$\mathcal{P}_S(k) \equiv \frac{k^3}{2\pi^2}\langle S_{\gamma m}(\mathbf{k})S^*_{\gamma m}(\mathbf{k})\rangle, \tag{5.54}$$

$$\mathcal{C}_{\zeta S}(k) \equiv \frac{k^3}{2\pi^2}\langle\zeta^{(f)}(\mathbf{k})S^*_{\gamma m}(\mathbf{k})\rangle. \tag{5.55}$$

They use a similar convention for the perturbations from inflation: remembering Eqs (2.65) and (5.15) the power spectra reads

$$\mathcal{P}_\zeta(k) \equiv \mathcal{A}^2 \simeq \left(\frac{H_I^2}{2\pi\dot{\varphi}}\right)^2, \tag{5.56}$$

$$\mathcal{P}_{S_{\gamma\sigma}}(k) \equiv \mathcal{B}^2 \simeq \left(\frac{H_I}{\pi\sigma_k}\right)^2, \tag{5.57}$$

With these definitions the power spectra of the initial matter-radiation fluid are straightforward to calculate. They results

$$\mathcal{P}_\zeta(k) \equiv \mathcal{A}^2 + \tau^2_{\zeta S}\mathcal{B}^2, \tag{5.58}$$

$$\mathcal{P}_S(k) \equiv \tau^2_{SS}\mathcal{B}^2, \tag{5.59}$$

$$\mathcal{C}_{\zeta S}(k) \equiv \tau_{\zeta S}\ \tau_{SS}\mathcal{B}^2. \tag{5.60}$$

Finally the CMB power spectrum may be divided into contributions to adiabatic and isocurvature perturbations [28]:

$$C_l = (\mathcal{A}^2 + \tau^2_{\zeta S}\mathcal{B}^2)\,\hat{C}_l^{ad} + \tau^2_{SS}\,\mathcal{B}^2\,\hat{C}_l^{iso} + \tau_{\zeta S}\ \tau_{SS}\,\mathcal{B}^2\,\hat{C}_l^{corr}. \tag{5.61}$$

In this decomposition, $\hat{C}_l^{ad}$ and $\hat{C}_l^{iso}$ are the CMB power spectra derived respectively from a flat spectrum of adiabatic and isocurvature fluctuations with $\mathcal{P}_\zeta(k) = \mathcal{P}_S(k) = 1$, while $\hat{C}_l^{corr}$ represent the correlation function between the two. Figure 5.1 shows the relative contributions to the CMB power spectrum, calculated in [28]. Notice the distinctive imprint of the isocurvature perturbations on the CMB power spectrum which decay on small angular scales. The different components in the CMB spectra are constrained using the CMB data. For this purpose, together with the already defined fraction of the curvaton contribution to the adiabatic power spectrum ξ, the authors used also the fraction of the isocurvature perturbations α, and the correlation contributions γ, to the CMB spectrum. From their definition,

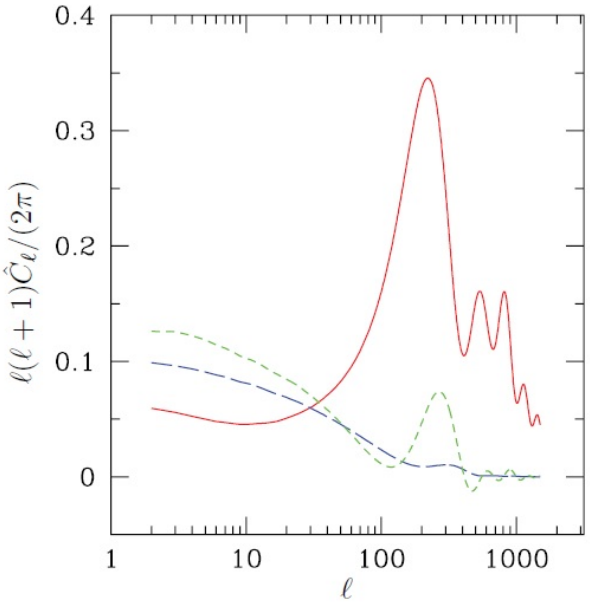

Figure 5.1: CMB power spectra for unit-amplitude initial perturbations, computed in [28]. The solid red curve is $\hat{C}_l^{ad}$, the long-dashed blue curve is $\hat{C}_l^{iso}$ and the shortdashed green curve is $\hat{C}_l^{cor}$.

these three quantities turns out to be

$$\xi = \frac{\tau_{\zeta S}^2 \mathcal{B}^2}{\mathcal{A}^2 + \tau_{\zeta S}^2 \mathcal{B}^2}, \tag{5.62}$$

$$\alpha = \frac{\tau_{\zeta S}^2 \, \mathcal{B}^2}{\mathcal{A}^2 + \tau_{\zeta S}^2 \, \mathcal{B}^2 + \tau_{SS}^2 \, \mathcal{B}^2}, \tag{5.63}$$

$$\gamma = \mathrm{sign}(\tau_{\zeta S} \, \tau_{SS}) \, \frac{\tau_{\zeta S}^2 \, \mathcal{B}^2}{\mathcal{A}^2 + \tau_{\zeta S}^2 \, \mathcal{B}^2}. \tag{5.64}$$

Now that we have discussed how the CMB power spectrum changes in presence of isocurvature modes let us show how the authors calculated the amplitude of the power asymmetry due to them.

We have already shown in the previous section that a super-horizon fluctuation $\Delta\sigma$ produces a dipole amplitude

$$A \simeq 2\xi \, \frac{\Delta\sigma}{\sigma_*}, \tag{5.65}$$

where σ_* is the value of $\sigma_0(t)$ just before the curvaton decay. However, in this scenario the asymmetry is scale invariant. Here, the case is different,

because the isocurvature modes start to decay when they re-enter the Universe, making the asymmetry scale dependent. Therefore, the authors of [28] consider a power asymmetry into each coefficient C_l, l by l, that according to Eq(5.65), have the form

$$\left|\frac{\Delta C_l}{C_l}\right| \equiv 2\frac{\Delta\sigma}{\sigma_k} K_l, \tag{5.66}$$

where, it has been added the coefficient K_l that is different for different l and hence takes into account the scale dependence of the asymmetry. To relate the scale dependent power asymmetry described by K_l to A, it is assumed that all modes l between 2 and $l_{max} \simeq 64$ are weighted equally in determining the measured amplitude A: since there are $(l_{max}-1)(l_{max}+3)$ modes in total, the estimate of the dipolar asymmetry is

$$A = \frac{\Delta\sigma_*}{\sigma_*} \sum_{l=2}^{l_{max}} \frac{2l+1}{(l_{max}-1)(l_{max}+3)} K_l \equiv \frac{\Delta\sigma_*}{\sigma_*}\tilde{A}, \tag{5.67}$$

where $\tilde{A}$ does not depend on the amplitude of the super-horizon fluctuation; it is determined by τ_{SS}, the density ratio R and the fraction of the adiabatic perturbations from the curvaton ξ. Also, the authors of [28] treated the curvaton super-horizon fluctuation as a sine wave, $\Delta\sigma = \sigma_p \sin(\mathbf{p}\cdot\mathbf{x})$, whit $p \ll H_0$. This places an upper bound on $\Delta\sigma_*/\sigma_*$ from the CMB quadrupole, that results [26] [28]

$$(0.26\ R + 1.67\ \tau_{SS})\left(\frac{\Delta\sigma_*}{\sigma_*}\right)^2 \lesssim 4.7\mathcal{Q}. \tag{5.68}$$

Together with this, another bound can be placed. Indeed, since the curvaton field affects also the curvature perturbations ζ, also a scale independent power asymmetry is generated, the one contained in the field ζ. Therefore, such scale independent asymmetry has to respect some experimental bounds. In particular, an analysis of quasar number counts reveals that any asymmetry in the direction of HPA $(l;b) = (225;-27)^\circ$ in the rms amplitude of primordial density fluctuations on scales that form quasars, must correspond to $A \lesssim 0.012$ (95% C.L.). Then the scale independent part of the asymmetry must be at most equal to the quasar bound, this means that most of asymmetry must be due to isocurvature perturbations.

Finally, the authors studied separately the two different scenarios, in which the curvaton decay create or do not create the most of the dark matter. In those cases τ_{SS} is respectively given by Eq(5.49) and by Eq(5.50).

After their study they concluded that a power asymmetry can arise only in the scenario in which the curvaton contribution to Dark Matter is negligible.

In fact, in the first scenario, the isocurvature fluctuations from the curvaton are much larger than the adiabatic perturbations from the curvaton, and

all of the adiabatic power comes from the inflaton fluctuations. Since in this case, we can state that only the isocurvature fluctuations are asymmetric, it is very difficult to generate the observed asymmetry without violating the current bound on power from isocurvature modes. It is necessary to introduce an order-unity variation in the curvaton density across the observable Universe, and since the curvaton creates the dark matter in this model, this would have profound observational consequences.

Instead in the second scenario, when the curvaton contribution to Dark Matter is negligible, the curvaton produces a roughly equal amplitude of adiabatic and isocurvature fluctuations. This makes more easier to generate the observed asymmetry. Anyway, in this scenario too, the variation in the curvaton field across the observable Universe have to be quite large: more than 50% to generate the observed asymmetry. To get a result consistent with both the observed HPA and the experimental bounds on α and on the quadrupole CMB moment, the authors of [28], found that must be $\xi \lesssim 0.016$, and $0.7 \lesssim \kappa \lesssim 1.4$. Then, to satisfies the CMB constraints (5.68), we find $r \lesssim 0.00013$ and consequently, from Eq(5.50) must be $\tau_{SS} \lesssim 1.82 \cdot 10^{-4}$. This implies, trough equations Eqs (5.37) and (5.39), a level of non-Gaussianity of the order $f_{NL} \gtrsim \mathcal{O}(1)$.

5.4.2 Other mechanisms proposed to obatin the scale dependence

Although the toy model that we have just described is considered the most realistic, other mechanisms were proposed to obtain a scale dependent power asymmetry.

As an example we report the case of [22]. In that scenario, the inflationary perturbations arise from two sources: the fluctuations of the inflaton φ and the fluctuations due to particle production during inflation. The authors assumed the following Lagrangian:

$$\begin{aligned}\mathcal{L} &= \frac{1}{2}(\partial\varphi)^2 + \frac{1}{2}m_\varphi^2\varphi^2 + \frac{1}{2}(\partial\mu)^2 + \frac{1}{2}m_\mu^2\mu^2 \\ &\quad + \sum_i \left[\frac{1}{2}(\partial\chi_i)^2 + \frac{g^2}{2}\left(\mu^2 + (\varphi - \varphi_i)^2\right)\chi^2\right], \quad (5.69)\end{aligned}$$

where $(\partial\varphi)^2 = g^{\mu\nu}\partial_\mu\varphi\partial_\nu\varphi$ and so on, and $\varphi_i = i\Delta\varphi$ (with i integer) are evenly spaced points. We see that in this Lagrangian there are several fields: an inflaton, $\varphi(t, \mathbf{x})$ that is slow-rolling down its potential, another field $\mu(t, \mathbf{x})$ that acts as spectator during inflation and N different fields $\chi_i(t, \mathbf{x})$, that are coupled with both $\varphi(t, \mathbf{x})$ and $\mu(t, \mathbf{x})$. For slow roll, the background value of the inflaton is $\varphi_0(t) \sim \dot{\varphi}t$ so the intervals φ_i are equally spaced in physical time. Since the mass of $\chi_i(t, \mathbf{x})$ is time dependent, χ_i particles may be produced spontaneously at the times t_i when $\varphi_0 = \varphi_i$. Because of the $\mu^2\chi_i^2$ coupling in Eq(5.69), also the background value $\mu_0(t)$ of $\mu(t, \mathbf{x})$ contributes to the mass of χ_i and controls the amount of particle production. If μ_0 is

large, χ_i is heavy even when $\varphi_0 = \varphi_i$ and few χ_i particles are produced. On the other hand if $\mu_0 \approx 0$ the χ_i particles are massless when $\varphi_0 = \varphi_i$, leading to significant particle production. In this way the $\mu(t, \mathbf{x})$ controls the production of the χ_i quanta. Notice that, in this scenario, the curvature perturbations ζ depends on all these primordial fields. In particular, we expect that if are produced few χ_i particles (therefore μ_0 is large), ζ is due almost exclusively by the quantum fluctuations of the inflaton field while, if there is a massive production of χ_i particles (and hence $\mu \approx 0$) their contribution to ζ is relevant. Having this in mind the authors of [22] assumes that the background value μ_0 experience a gradient across the sky due to a super-horizon perturbation,

$$\mu_0(t_i, \mathbf{x}) \approx \alpha(\hat{\mathbf{p}} \cdot \mathbf{x} + x_{dec}), \tag{5.70}$$

where α is some parameter, $\hat{\mathbf{p}}$ the preferred direction and x_{dec} the distance from last scattering surface. In presence of such a modulation particle production will be more suppressed in one part of the Universe than another. This will create a dipole modulation on the CMB temperature fluctuations field equal to the phenomenological parametrization given in Eq(4.1). The amplitude of the generated asymmetry can be made scale dependent exploiting the dynamics of μ_0. In fact in [22] is shown that if $m_\mu \neq 0$, the gradient of μ_0 will change during inflation, specifically, it might relax to zero everywhere and the asymmetry will disappear at high l, giving rise to the observed scale dependence. In this way the authors of [22] are able to build a toy model which explains a HPA of amplitude $A \sim 10\%$ on large scale, and a suppression in average on low-l power across the entire sky.

Finally, we report an other paper, [39], that proposed a model based on three scalar fields: the inflaton $\varphi(t, \mathbf{x})$, responsible for the inflationary dynamics, another field $\chi(t, \mathbf{x})$ that carries a super-horizon curvature perturbation $\Delta\chi$ and a curvaton type field $\sigma(t, \mathbf{x})$. Their idea consists in modulating the dynamics of the curvaton σ by using the field χ, without affecting the inflationary dynamics. This is realized by assuming that the kinetic term of σ depends on χ. For the Lagrangian they assumed

$$\mathcal{L} = \frac{1}{2}(\partial_\varphi)^2 + \frac{1}{2}m_\varphi^2\varphi^2 + \frac{1}{2}(\partial\chi)^2 + \frac{1}{2}m_\chi^2\chi^2 + \frac{1}{2}f(\chi)\,(\partial\sigma)^2 + \frac{1}{2}m_\sigma^2\sigma^2. \tag{5.71}$$

Owing to the function $f(\chi)$, the amplitude of the fluctuations of σ is modulated as $\langle\delta\sigma^2\rangle \approx H^2/(2\pi\, f(\chi))^2$. Therefore, an appropriate choice of $f(\chi)$ can easily explain the dipolar statistical anisotropy and its scale dependence. Notice that this toy model model is similar to the one discussed in Sec. 5.4. Indeed, although the super-horizon perturbation is contained in χ, this one is used to modulate the curvaton-type field σ, like in the model discussed in Sec. 5.4. The difference is that now the asymmetry is is due by a suitable choice of the function $f(\chi)$; while in in Sec. 5.4 the scale dependence is

achieved through isocurvature perturbations.

In conclusion, in this chapter we saw that there are different ways to generate a dipolar power asymmetry, also with a non trivial scale dependence. In those models the asymmetry is consistent with data and, at the same time, respects the assumptions of the phenomenological model developed in Chap. 4. This shows that the study made in Chap. 4 could be a viable explanation of the *Hemispherical Power Asymmetry*. However, let us stress, that the models we have proposed are going to be more and more complicated. Indeed, we started discussing the case of a single-field model and we arrived to discuss more than three-fields models, in which the fields have a non-trivial kinetic term.

Chapter 6

Beyond the scalar perturbations

In the previous chapters we tried to interpret the HPA as the imprint of a scalar perturbation with proper length $\lambda \gg H_0^{-1}$, where H_0^{-1} is the present Hubble radius, an estimate of the size of the observable Universe. We developed a sort of phenomenological model to parametrize the scalar curvature perturbations ζ, and we discussed how perturbations of different wavelengths can couple giving rise to observational consequences like a dipolar modulation of the temperature fluctuations across the sky.

However the formalism we developed is very general and can be applied not only to the scalar perturbations but also to any kind of observable of the early Universe, like tensor perturbations (gravitational waves). Therefore, in this chapter we will generalize the developed formalism, going beyond the HPA. More in details we will show that a possible primordial non-Gaussianity in the perturbation fields could give rise to a generalized coupling between different kinds of perturbations. For instance, a super-horizon curvature mode modifies the correlation function, on small scales, of any observable $\mathcal{O}$ introducing a bias in the 2-point function of the quantity $\mathcal{O}$. This means that, also $\mathcal{O}$ can experience a dipolar modulation across the sky as we found for the curvature perturbations. Moreover, we will show that, the super-horizon tensor perturbations act in a similar way, biasing the n-point functions of any generic observable $\mathcal{O}$.

The calculation we will perform can be exploited in different ways. First of all we will use it to compute some *generalized consistency relations* that hold between scalar and tensor perturbations. Such consistency relations are valid in the squeezed limit and hence, they are similar to the one computed in Eq(4.19). Since they are model-independent relations that holds for any single-field model of inflation, they are useful tools which could be used in the next future to test such class of models. In our treatment we will calculate them assuming that only one field generated the primordial curvtaure perturbations.

Moreover these generalized mode coupling, we are going to discuss, could be a viable explanation to alleviate the tension that seems to exist between

the measurements of the tensor-to-scalar ratio r made by *Planck* and by BICEP2, [4]. In fact, a tensor modulation across the sky may be a possible argument to alleviate this tension in the case that it will be confirmed by the Planck data of polarization that will be released soon.

6.1 General biased two-point function

In this section we show how the presence of a long-wavelength perturbation background changes the statistics of a generic observable $\mathcal{O}(\mathbf{x})$, which could be a scalar perturbation or a tensor one. Let be $\mathcal{O}(\mathbf{x})$ a random field, which is assumed to be homogeneous and isotropic in the entire Universe [1]. In Fourier space $\mathcal{O}$ reads

$$\mathcal{O}(\mathbf{x}) = \int_{L^{-1}}^{k_{max}} \frac{d^3k}{(2\pi)^3} e^{-i\mathbf{kx}} \mathcal{O}(\mathbf{k}), \tag{6.1}$$

where L and k_{max}^{-1} are respectively the size of the entire Universe and the minimum scale we smooth over. Evaluated on the vacuum state of the homogeneous and isotropic background the 2-point function of $\mathcal{O}$ is

$$\langle \mathcal{O}(\mathbf{k})\mathcal{O}(\mathbf{k}')\rangle = (2\pi)^3\delta^3(\mathbf{k}+\mathbf{k}')P_{\mathcal{O}}(k), \tag{6.2}$$

where $P_{\mathcal{O}}(k)$ is its power spectrum. We define also the dimensionless power spectrum as

$$\mathcal{P}_{\mathcal{O}}(k) = \frac{k^3}{2\pi^2} P_{\mathcal{O}}(k), \tag{6.3}$$

We recall that $\mathcal{P}_{\mathcal{O}}(k)$ represents also the the logarithmic scale contribution to the variance: $\sigma^2_{\mathcal{O}} = \int dk/k\ \mathcal{P}_{\mathcal{O}}(k)$. As we have already done for $\mathcal{P}_\zeta(k)$, we introduce the coefficient $n_{\mathcal{O}}$, which gives us information about the scale dependence of $\mathcal{P}_{\mathcal{O}}(k)$:[2]

$$n_{\mathcal{O}} = \frac{d\ln \mathcal{P}_{\mathcal{O}}(k)}{d\ln k}. \tag{6.4}$$

We stress that, thanks to the definition of $n_{\mathcal{O}}$, we can state that, if $n_{\mathcal{O}}$ is scale independent, $\mathcal{P}_{\mathcal{O}}(k) \propto k^{n_{\mathcal{O}}}$, while $P_{\mathcal{O}}(k) \propto k^{n_{\mathcal{O}}-3}$.

Let us now specialize the gauge choice. During our treatment we will work in the uniform density gauge. Then curvature and tensor perturbations affect the line element in the following way:

$$ds^2 = -dt^2 + a^2(t)(1 + 2\zeta(\mathbf{x})\ \delta_{ij} + 2h_{ij}(\mathbf{x}))\ dx^i\, dx^j. \tag{6.5}$$

[1] We stress that we are supposing the entire Universe much greater than the observable volume.

[2] Notice that the definition of $n_{\mathcal{O}}$ is different to the one used for the scalar index defined in Eq(2.70): here we used $n_{\mathcal{O}}$ in place of $n_s - 1$.

Shortly after inflation most of the Fourier modes $\zeta(\mathbf{k})$ and $h_{ij}(\mathbf{k})$ are still super-horizon ($k \ll H$), so they are constant in time [3]. Notice that this is the same situation we met in Sec.4.1.1. In that case we reabsorbed in a coordinate rescaling the curvature modes $\zeta(\mathbf{k_l})$ that was still super-horizon. Here we can made the same thing taking into account also the tensor perturbations. Now the difference is that, because of the tensor perturbations, the coordinates rescaling is no longer a simple diagonal matrix. This means that while the scalar mode ζ defines a coordinate rescaling which consists in a dilation, h_{ij} must satisfy the constraints

$$h_{ii}(\mathbf{x}) = \partial_i h_{ij}(\mathbf{x}) = 0, \tag{6.6}$$

by definition and hence defines an other type of scaling which mixes together the coordinate components. Treating the super-horizon component of $\zeta(\mathbf{x})$ and $h_{ij}(\mathbf{x})$ as an almost flat background [4], the coordinate rescaling is thus given by

$$x_i \to x_i' = \Lambda_{ij} x^j, \qquad \text{with} \qquad \Lambda_{ij} = (1+\zeta_B)\delta_{ij} + h_{B\,ij}. \tag{6.7}$$

Notice that, with this coordinate rescaling, on super-horizon scales, the metric takes the same form of an unperturbed FRW one (1.2), though different patches experience a different scaling because of the different initial conditions. Such a redefinition of the coordinats is crucial in order to obtain a biased n-point function of the observable $\mathcal{O}$.

In fact, in presence of a background the correlation function of $\mathcal{O}(\mathbf{x})$ can no longer be evaluated in the vacuum state. To compute it we exploit the coordinate rescaling (6.7). In this way the correlation function in presence of a background can be rewritten as the correlation function expressed in the new coordinates and evaluated on the vacuum (i.e. without the background wave):

$$\langle \mathcal{O}(\mathbf{x_2})\mathcal{O}(\mathbf{x_3})\rangle_B = \langle \mathcal{O}(\mathbf{x_2'})\mathcal{O}(\mathbf{x_3'})\rangle \tag{6.8}$$

Thanks to Eq(6.7), and recalling that isotropy requires that $\langle \mathcal{O}(\mathbf{x_2})\mathcal{O}(\mathbf{x_3})\rangle$ is a function only of the modulus of the vector $\mathbf{x_s} = \mathbf{x_2} - \mathbf{x_3}$, the above expression can be expanded in power series of the old coordinates:

$$\langle \mathcal{O}(\mathbf{x_2'})\mathcal{O}(\mathbf{x_3'})\rangle \simeq \langle \mathcal{O}(\mathbf{x_2})\mathcal{O}(\mathbf{x_3})\rangle + (\zeta_B\,\delta_{ij} + h_{B\,ij})\, x_s^j \frac{d}{dx_s^i}\langle \mathcal{O}(\mathbf{x_2})\mathcal{O}(\mathbf{x_3})\rangle. \tag{6.9}$$

We stress that in the vacuum state the correlation function is

$$\langle \mathcal{O}(\mathbf{x_2})\mathcal{O}(\mathbf{x_3})\rangle = \int \frac{d^3k_s}{(2\pi)^3} e^{-i\mathbf{k_s}\mathbf{x_s}} P_{\mathcal{O}}(k_s). \tag{6.10}$$

[3] Notice that ζ is constant on super-horizon scales because we are assuming that there is only one scalar field during inflation.

[4] Flat in the sense tha we can neglect the gradient.

Plugging the above expression into Eq.(6.9) we get

$$\langle \mathcal{O}(\mathbf{x_2'})\mathcal{O}(\mathbf{x_3'})\rangle \simeq \langle \mathcal{O}(\mathbf{x_2})\mathcal{O}(\mathbf{x_3})\rangle + (\zeta_B\,\delta_{ij} + h_{B\,ij}) \times \int \frac{d^3k_s}{(2\pi)^3} x_s^j \frac{d}{dx_s^i}\left(e^{-i\mathbf{k_s}\mathbf{x_s}}\right) P_{\mathcal{O}}(k_s). \tag{6.11}$$

Notice that the above formula tells us that the 2-point function experiences a bias due to both scalar and tensor perturbations. It is better to study the two sources of bias separately, therefore we split it into the sum of two different components:

$$\langle \mathcal{O}\mathcal{O}\rangle_B \equiv \langle \mathcal{O}\mathcal{O}\rangle + \Delta\langle \mathcal{O}\mathcal{O}\rangle, \tag{6.12}$$

with the bias splitted as

$$\Delta\langle \mathcal{O}\mathcal{O}\rangle \equiv \Delta\langle \mathcal{O}\mathcal{O}\rangle|_{\zeta_B} + \Delta\langle \mathcal{O}\mathcal{O}\rangle|_{h_{B\,ij}}. \tag{6.13}$$

Let us compute the explicitly the form of $\Delta\langle \mathcal{O}\mathcal{O}\rangle|_{\zeta_B}$ and $\Delta\langle \mathcal{O}\mathcal{O}\rangle|_{h_{B\,ij}}$ the biases due respectively to the super-horizon scalar and tensor perturbations.

6.1.1 Computation of $\Delta\langle \mathcal{O}\mathcal{O}\rangle|_{\zeta_B}$

From Eqs.(6.11) and (6.13) we see that

$$\Delta\langle \mathcal{O}\mathcal{O}\rangle|_{\zeta_B} = \zeta_B(\mathbf{x}_+)\;\delta_{ij}\int \frac{d^3k_s}{(2\pi)^3} x_s^j \frac{d}{dx_s^i}\left(e^{-i\mathbf{k_s}\mathbf{x_s}}\right) P_{\mathcal{O}}(k_s), \tag{6.14}$$

where, we approximated the bias ζ_B with its value in the middle point $\mathbf{x}_+ = (\mathbf{x_2}+\mathbf{x_3})/2$, because we are assuming that ζ_B has a wavelength $\lambda \gg |\mathbf{x_2}-\mathbf{x_3}|$. We immediately sum the term $x_s^j \frac{d}{dx_s^i}$ with the Kronecker delta δ_{ij}, thus obtaining

$$\Delta\langle \mathcal{O}(\mathbf{x_2})\mathcal{O}(\mathbf{x_3})\rangle|_{\zeta_B} = \zeta_B\;\mathbf{x_s}\cdot\frac{d}{d\mathbf{x_s}}\int \frac{d^3k_s}{(2\pi)^3}\, e^{-i\mathbf{k_s}(\mathbf{x_2}-\mathbf{x_3})} P_{\mathcal{O}}(k_s). \tag{6.15}$$

The expression is now much more simple to handle: the derivative with respect to $-\mathbf{x_s}$ gives the factor $i\mathbf{k_s}$, while we write the $\mathbf{x_s}$ term as a derivative with respect to $\mathbf{k_s}$. Therefore the above expression rewrites as

$$\begin{aligned}\Delta\langle \mathcal{O}(\mathbf{x_2})\mathcal{O}(\mathbf{x_3})\rangle|_{\zeta_B} &= \zeta_B \int \frac{d^3k_s}{(2\pi)^3}\;\mathbf{k_s}\cdot\frac{d}{d\mathbf{k_s}}\left(e^{-i\mathbf{k_s}(\mathbf{x_2}-\mathbf{x_3})}\right) P_{\mathcal{O}}(k_s) = \\ &= -\zeta_B \int \frac{d^3k_s}{(2\pi)^3}\, e^{-i\mathbf{k_s}(\mathbf{x_2}-\mathbf{x_3})}\frac{d}{d\mathbf{k_s}}\cdot\left(\mathbf{k_s}P_{\mathcal{O}}(k_s)\right),\end{aligned} \tag{6.16}$$

where, in the last line we integrated by parts. Finally we exploit the fact that $\frac{d}{d\mathbf{k_s}} \cdot (\mathbf{k_s} P_{\mathcal{O}}(k_s)) = n_{\mathcal{O}} P_{\mathcal{O}}(k)$ [5]. In conclusion, the additional term in the correlation function of $\mathcal{O}$ due to the coupling with the super-horizon curvature perturbation is:

$$\Delta\langle \mathcal{O}(\mathbf{x_2})\mathcal{O}(\mathbf{x_3})\rangle|_{\zeta_B} = -n_{\mathcal{O}}\ \zeta_B \int \frac{d^3k_s}{(2\pi)^3}\ e^{-i\mathbf{k_s}(\mathbf{x_2}-\mathbf{x_3})} P_{\mathcal{O}}(k_s). \tag{6.17}$$

6.1.2 Computation of $\Delta\langle\mathcal{O}\mathcal{O}\rangle|_{h_{B\,ij}}$

The part of the bias which is due to the super-horizon tensor perturbation is

$$\Delta\langle \mathcal{O}\mathcal{O}\rangle|_{h_{B\,ij}} = h_{B\,ij}(x_+) \int \frac{d^3k_s}{(2\pi)^3} x_s^j \frac{d}{dx_s^i} \left(e^{-i\mathbf{k_s}\mathbf{x_s}}\right) P_{\mathcal{O}}(k_s), \tag{6.18}$$

where, also here, the background is evaluated in the middle point $\mathbf{x}_+$. Notice that the computation of the bias due to a super-horizon tensor perturbation is slightly more complicated, because we cannot explicitly make the sum $h_{B\,ij}\, x_s^j \frac{d}{dx_s^i}$.

The first steps are similar to the ones we have already done in the previous calculation: we compute the derivative with respect to x_s^i obtaining $i\mathbf{k_s} e^{-i\mathbf{k_s}\mathbf{x_s}}$ to realize that x_s^j can be replaced by $i\frac{d}{dk_s^j}$, finally, we integrate by part. In conclusion we get

$$\Delta\langle \mathcal{O}\mathcal{O}\rangle|_{h_{B\,ij}} = -h_{B\,ij} \int \frac{d^3k_s}{(2\pi)^3}\ e^{-i\mathbf{k_s}\mathbf{x_s}} \frac{d}{dk_s^j} \left(k_s^i P_{\mathcal{O}}(k_s)\right). \tag{6.19}$$

To make explicit the derivative, we use the fact that $h_{B\,ij}$ is a traceless and divergence free tensor, as stated in Eq(6.6). This implies that the terms in which $i = j$ do not contribute to the final result. We therefore set $i \neq j$. With this requirement we are allowed to take k_s^j out off the parentheses in Eq(6.19) thus obtaining:

$$\begin{aligned} \frac{d}{dk_s^i}\left(k_s^j P_{\mathcal{O}}(k_s)\right) &= k_s^j \frac{d}{dk_s^i}\left(P_{\mathcal{O}}(k_s)\right) = \\ &= k_s^j \frac{dP_{\mathcal{O}}(k_s)}{dk_s} \cdot \frac{dk_s}{dk_s^i} = \\ &= \frac{k_s^i k_s^j}{k_s} \frac{dP_{\mathcal{O}}(k_s)}{dk_s} = (n_{\mathcal{O}} - 3)\, \frac{k_s^i k_s^j}{k_s^2} P_{\mathcal{O}}(k_s), \end{aligned} \tag{6.20}$$

where in the last line we use the fact that $P_{\mathcal{O}}(k) \propto k^{(n_{\mathcal{O}}-3)}$. As a result the final expression for $\Delta\langle\mathcal{O}\mathcal{O}\rangle|_{h_{B\,ij}}$ is

$$\Delta\langle \mathcal{O}\mathcal{O}\rangle|_{h_{B\,ij}} = -(n_{\mathcal{O}} - 3)\ h_{B\,ij} \int \frac{d^3k_s}{(2\pi)^3}\ e^{-i\mathbf{k_s}\mathbf{x_s}} \frac{k_s^i k_s^j}{k_s^2} P_{\mathcal{O}}(k_s). \tag{6.21}$$

[5] We stress that we have proved it in Sec.4.1.1 in the special case in which $\mathcal{O} = \zeta$,

***

Once we obtained $\Delta\langle\mathcal{O}\mathcal{O}\rangle|_{\zeta_B}$ and $\Delta\langle\mathcal{O}\mathcal{O}\rangle|_{h_{B\,ij}}$ we can compute the total 2-point function of $\mathcal{O}$ in Fourier space. Before doing that we write the super-horizon background $\zeta_B(\mathbf{x}_+)$ and $h_{B\,ij}(\mathbf{x}_+)$ in Fourier space:

$$\zeta_B(\mathbf{x}_+) = \int_{L^{-1}}^{H_0^{-1}} \frac{d^3k_l}{(2\pi)^3}\, e^{-i\mathbf{k_l}\mathbf{x}_+}\, \zeta(\mathbf{k_l})\ , \tag{6.22}$$

$$h_{B\,ij}(\mathbf{x}_+) = \int_{L^{-1}}^{H_0^{-1}} \frac{d^3k_l}{(2\pi)^3}\, e^{-i\mathbf{k_l}\mathbf{x}_+} \sum_{s=+,\times} h^s(\mathbf{k_l})\epsilon^s_{ij}(\mathbf{k_l}) \tag{6.23}$$

Taking into account these expressions, and anti Fourier transforming the total correlation function we get the correlation function expressed in momentum space [6]:

$$\begin{aligned}\langle\mathcal{O}(\mathbf{k_2})\mathcal{O}(\mathbf{k_3})\rangle \simeq\ & (2\pi)^3\delta^3(\mathbf{k_2}+\mathbf{k_3})P_{\mathcal{O}}(k_s) - n_{\mathcal{O}}\ \zeta_B(\mathbf{k_l})\ P_{\mathcal{O}}(k_s) \\ & -(n_{\mathcal{O}}-3)\sum_{s=+,\times} h^s_B(\mathbf{k_l})\ \epsilon^s_{ij}(\mathbf{k_l})\frac{k^i_s k^j_s}{k^2_s}\ P_{\mathcal{O}}(k_s).\end{aligned} \tag{6.24}$$

Let us comment on the results that we have found: the presence of super-horizon curvature and tensor fluctuations modulates the statistics of the most generic observable $\mathcal{O}(\mathbf{x})$ in a sub-volume smaller than the entire Universe (of typical size H_0^{-1} corresponding to the size of observable Universe). More in detail, in the above formula we explicitly computed the changes which the 2-point function $\langle\mathcal{O}(\mathbf{k_2})\mathcal{O}(\mathbf{k_3})\rangle$ experiences due to the long-wavelength perturbations. Both curvature and tensor perturbations contribute to these changes but in different ways.

In fact, the bias in the 2-point function due to curvature perturbations ζ is proportional to the scale dependence $n_{\mathcal{O}}$ of $\mathcal{P}_{\mathcal{O}}(k)$, thus, if the dimensionless power spectrum $\mathcal{P}_{\mathcal{O}}(k)$ is scale invariant ($n_{\mathcal{O}}=0$), curvature perturbations cannot shift the two point function. Conversely, tensor perturbations affect the n-point functions of $\mathcal{O}(\mathbf{x})$ even in the case in which $\mathcal{P}_{\mathcal{O}}(k)$ is scale independent, because of the proportionality coefficient of the bias that is $(n_{\mathcal{O}}-3)$. This is due to the different type of rescaling which is generated by the tensor perturbations with respect to the curvature ones. The latter, indeed, define a simple dilation, while tensor perturbations generate a scaling

[6] Notice that in the following expression the superscript s does not label the "short" modes but the polarization of the gravitational wave state of tensor perturbation.

of the coordinates which mixes the components of the coordinates together. This breaks explicitly the isotropy of the field $\mathcal{O}(\mathbf{x})$, as we can see from the second term of eq(6.24).

In conclusion we found that, while scalar super-horizon perturbations induce a breaking of homogeneity, tensor ones because of the presence of the $\epsilon^s_{ij}(\mathbf{k_l})k_{s\,i}k_{s\,j}$ term breaks both homogeneity and isotropy.

6.2 Generalized consistency relations

The results obtained in the previous section have several consequences. Here, we will exploit them to find some consistency relations that generalize the one found in Eq(4.19). In this study we will specialize $\mathcal{O}$ assuming it to be first the curvature perturbations ζ and then the tensor perturbations h_{ij}.

6.2.1 Case 1: $\mathcal{O} = \zeta$

The curvature perturbation field satisfies the hypothesis made on $\mathcal{O}(\mathbf{x})$, indeed, it is assumed to be a random, homogeneous and isotropic field. The effect of a super-horizon curvature background perturbation consists in the usual consistency relation (4.19). On the other hand the effect of the super-horizon tensor perturbation lead to the first generalized consistency relation that we are going to compute.

We start showing the bias experienced by the 2-point function in presence of a super-horizon tensor realization. Thanks to Eq.(6.24) we find:

$$\Delta\langle\zeta(\mathbf{k_2})\zeta(\mathbf{k_3})\rangle|_{h_B\,ij} = -(n_s-4)\sum_s h^s_B(\mathbf{k_l})\epsilon^s_{ij}(\mathbf{k_l})\frac{k^i_s k^j_s}{k^2_s}P_\zeta(k_s). \tag{6.25}$$

Then we use this formula to compute the "mixed" bispectrum $\mathcal{B}_{h^s\zeta\zeta}(\mathbf{k_1},\mathbf{k_2},\mathbf{k_3})$, defined through the relation

$$\langle h(\mathbf{k_1})\zeta(\mathbf{k_2})\zeta(\mathbf{k_3})\rangle \equiv (2\pi)^3\ \delta^3(\mathbf{k_1}+\mathbf{k_2}+\mathbf{k_3})\ f^{h\zeta}_{NL}\ \mathcal{B}_{h^s\zeta\zeta}(\mathbf{k_1},\mathbf{k_2},\mathbf{k_3}), \tag{6.26}$$

where we have used $\mathbf{k_l} = \mathbf{k_2}+\mathbf{k_3}$. To compute it we multiply Eq.(6.2.1) for $h^{s'}(\mathbf{k_1})$ and we make the operation of ensemble average. Then we obtain:

$$\begin{aligned}\langle h^{s'}(\mathbf{k_1})\zeta(\mathbf{k_2})\zeta(\mathbf{k_3})\rangle &= \langle h^{s'}(\mathbf{k_1})\ \Delta\langle\zeta(\mathbf{k_2})\zeta(\mathbf{k_3})\rangle|_{h_B\,ij}\ \rangle = \\ &= -(n_s-4)\sum_s\langle h^{s'}(\mathbf{k_1})h^s(\mathbf{k_l})\rangle\epsilon^s_{ij}(\mathbf{k_l})\frac{k_{s\,i}k_{s\,j}}{k^2_s}P_\zeta(k_s) = \\ &= -(2\pi)^3\,\delta^3\left(\sum_{i=1}^3\mathbf{k_i}\right)(n_s-4)P_h(k_l)P_\zeta(k_s)\epsilon^{s'}_{ij}(\mathbf{k_l})\frac{k^i_s k^j_s}{k^2_s}.\end{aligned} \tag{6.27}$$

Comparing among them Eqs.(6.26) and (6.27), we get the *first generalized consistency relation*:

$$f_{NL}^{h\zeta}\mathcal{B}_{h^{s'}\zeta\zeta}(\mathbf{k_1},\mathbf{k_2},\mathbf{k_3}) = -(n_s-4)\ P_h(k_l)\ P_\zeta(k_s)\ \epsilon_{ij}^{s'}(\mathbf{k_l})\frac{k_s^i k_s^j}{k_s^2}, \tag{6.28}$$

where we recall that $\mathbf{k_s} = (\mathbf{k_2}-\mathbf{k_3})/2$ and $\mathbf{k_l} = \mathbf{k_2}+\mathbf{k_3}$. Notice that it holds only in the squeezed limit, when $k_1 \ll k_2 \sim k_3$. s well as $f_{NL}^{\zeta} \simeq -(n_s-1)/4$, we set $f_{NL}^{h\zeta} = -(n_s-4)/4$. That is the non-gaussian parameter that allows the coupling between the curvature and tensor modes. [7].

6.2.2 Case 2: $\mathcal{O} = h_{ij}$

Tensor perturbations $h_{ij}(\mathbf{x})$ too satisfies the hypothesis made on $\mathcal{O}(\mathbf{x})$. Therefore non-gaussianity couples sub-horizon modes with super-horizon ones. This means that we can extract other two consistency relations computing the bispectra $\mathcal{B}_{\zeta hh}(k_1,k_2,k_3)$ and $\mathcal{B}_{h^shh}(\mathbf{k_1},\mathbf{k_2},\mathbf{k_3})$ in the squeezed limit. They are respectively defined through

$$\langle\zeta(\mathbf{k_1})h^{s'}(\mathbf{k_2})h^{s''}(\mathbf{k_3})\rangle \equiv (2\pi)^3\delta^{s's''}\delta^3(\mathbf{k_1}+\mathbf{k_2}+\mathbf{k_3})f_{NL}^{\zeta h}\ \mathcal{B}_{\zeta hh}(k_1,k_2,k_3), \tag{6.29}$$

$$\langle h^s(\mathbf{k_1})h^{s'}(\mathbf{k_2})h^{s''}(\mathbf{k_3})\rangle \equiv (2\pi)^3\delta^{s's''}\delta^3(\mathbf{k_1}+\mathbf{k_2}+\mathbf{k_3})f_{NL}^{h}\ \mathcal{B}_{h^shh}(\mathbf{k_1},\mathbf{k_2},\mathbf{k_3}). \tag{6.30}$$

We compare these expressions with their respective ones, calculated in the squeezed limit in the same way we have done for Eq.(6.27): first we give the explicit form of the bias in the 2-point function $\Delta\langle h^{s'}(\mathbf{k_2})h^{s''}(\mathbf{k_3})\rangle$ and then we correlate it with, respectively $\zeta_B(\mathbf{k_1})$ and $h_B^s(\mathbf{k_1})$. Their final expression are then

$$\langle\zeta(\mathbf{k_1})h^{s'}(\mathbf{k_2})h^{s''}(\mathbf{k_3})\rangle = -(2\pi)^3\ \delta^{s's''}\ \delta^3\left(\sum_{i=1}^{3}\mathbf{k_i}\right)\ n_t P_\zeta(k_l)\ P_h(k_s), \tag{6.31}$$

and

$$\begin{aligned}\langle h^s(\mathbf{k_1})h^{s'}(\mathbf{k_2})h^{s''}(\mathbf{k_3})\rangle \quad &= \quad -(2\pi)^3\ \delta^3\left(\sum_{i=1}^{3}\mathbf{k_i}\right)\ \delta^{s's''}\ (n_t-3) \\ &\times\ P_h(k_l)\ P_h(k_s)\ \epsilon_{ij}^{s'}(\mathbf{k_l})\frac{k_s^i k_s^j}{k_s^2}.\end{aligned} \tag{6.32}$$

[7] Notice that the definition of $f_{NL}^{h\zeta}$ is different for the "experimental" one given in Eq(1.47) that is used to quantify the level of primordial non-Gaussianity of tensor modes. In particular with our normalization we find $f_{NL}^{h\zeta} \sim \mathcal{O}(1)$ while with the "correct" one we expect $f_{NL}^{h\zeta} \sim \mathcal{O}(\epsilon)$, where ϵ is the slow-roll parameter 1.26.

In conclusion the *second consistency relation* is

$$f_{NL}^{\zeta h}\ \mathcal{B}_{\zeta hh}(k_1,k_2,k_3) = -n_t\ P_\zeta(k_l)\ P_h(k_s), \tag{6.33}$$

and the *third* one

$$f_{NL}^{h}\ \mathcal{B}_{h^s hh}(\mathbf{k_1},\mathbf{k_2},\mathbf{k_3}) = -(n_t-3)\ P_h(k_l)\ P_h(k_s)\ \epsilon_{ij}^{s}(\mathbf{k_l})\frac{k_s^i k_s^j}{k_s^2}. \tag{6.34}$$

Also now, in analogy with f_{NL}^{ζ}, we define $f_{NL}^{\zeta h}$ and f_{NL}^{h} respectively as $f_{NL}^{\zeta h} = -n_t/4$ and $f_{NL}^{h} = -(n_t-3)/4$.

***

Summarizing, in this section we found other three-important consistency relations which holds under very general assumptions:

i. there is only one field which contributes to the density perturbations;

ii. there is a non-Gaussian component both in the curvature and tensor perturbations which couples the two fields between them;

iii. the Universe is much bigger than what we observe, this allows the existence of super-horizon perturbations.

Notice that the obtained generalized consistency relations perfectly agrees with the ones computed in [43] [8].

Recently, there has been a great deal of progress in measuring the 3-point function of curvature perturbations from the CMB and LSS, [44]. Moreover the *Planck* collaboration will release soon the first map of the polarized component of the CMB. Perhaps it will allow us to measure the tensor power spectrum, and hopefully also other kinds of n-point functions (including those involving tensor perturbations) will be measured. In this view the obtained consistency relations might be tested.

6.3 Long modes modulation and the tensor–to–scalar ratio r

To conclude the chapter, we briefly discuss about the possibility of a tensor modulation across the sky.

The results of Sec.6.1 implies that curvature and tensor super-horizon modes affect both scalar and tensor perturbations. This means that, if, for instance, the HPA was generated by a curvature perturbation with wavelength greater than the size of observable Universe, such a perturbation would left its signature also in the tensor realization $h_{ij}(\mathbf{x})$ inside our observable patch. This idea was explored for the first time in [2].

[8] Also in [55] have been made a similar computation for the three point functions between scalar and tensor perturbations.

Recently, there has been some investigation about a super-horizon modulation in the context of the tensor-to-scalar ratio r, which consists in the ratio between the power spectra of tensor and scalar perturbations

$$r = \frac{2P_h(k)}{P_\zeta(k)}. \tag{6.35}$$

This is one of the most relevant parameters in the study of the early Universe, since its knowledge would tell us how much tensor perturbations were created during inflation [9]. Moreover the knowledge of r implies also the knowledge of the tensor power spectrum from which we can argue the energy of inflation (see discussion in Sec. 2.7).

There are various planned and ongoing experimental probes aiming to detect primordial gravitational waves. The the *Planck* satellite, combining data with the E-mode polarization measured by WMAP, constrained r to be less than 0.11 (at 95% of c.l.), [66], [69]. BICEP2, focused on the detection of the B-mode of polarizazion of the CMB, made recently a measurement in a small portion of the sky, which is placed approximately near the south celestial pole. The BICEP2 team found $r = 0.20^{+0.07}_{-0.05}$, [4]. This measurement is not definitive and needs additional checks. As one can see there is some tension between the two values (however see discussion in Ref.[6]) . Many arguments were proposed to reconcile these two results, (e.g. [18] , [38]); here we focused on the idea discussed in [17].

In [17] the authors state that an eventual tension between BICEP2 and *Planck* may be reconciled, linking the two measurements of r with the HPA. The idea is motivated by the fact that the BICEP2 footprint is about 60° away from the dipole axis of the HPA. Therefore, if this anomaly is due to a super-horizon curvature mode, $\zeta(\mathbf{p})$, with $p \ll H_0^{-1}$, such mode would couple also with tensor perturbations giving rises also to a modulated tensor spectrum.

6.3.1 Curvature super-horizon perturbation

If $P_h(k)$ experience a dipolar modulation across the sky, also r varies. We can therefore parametrize r as

$$r(\theta) \approx r_0 + \Delta r \cos\theta, \tag{6.36}$$

with θ defining the angle relative to the maximum of the HPA, this suggest $r_{BICEP} \approx r_0 + \Delta r/2$. *Planck*, instead, obtained its measurement from a full sky calculation, thus averaging the modulation. This means $r_{Planck} = r_0$. Assuming

$$r_0 \simeq \Delta r \simeq 0.11 \tag{6.37}$$

[9] We stress that a certain amount of gravitational waves is inevitably generated during inflation.

one thus finds $r_{BICEP} \approx 0.17$, consistent with the BICEP2 result. This model, by construction, is also consistent with the *Planck* all-sky constraint. It furthermore suggests that in the direction $(l, b) = (227, -27)^\circ$ the contribution of tensor modes is close to $r_{max} \approx 0.22$, while in the opposite direction $r_{min} \approx 0$, a hypothesis that can be checked by future B-mode experiments.

Unfortunately a curvature super-horizon perturbation gives rise to a tensor dipolar amplitude that is too small to generate $\Delta r \simeq 0.11$. Let us check it. Let be $P_h^{mod}(k)$ the modulated power spectrum of tensor perturbations, in presence of a super-horizon curvature mode. We define it through the definition made in Eq.(4.22) which generalizes to the case of a power spectrum with a spatial modulation. The explicit formula can be obtained by Fourier transforming, with respect to the variable $\mathbf{k_l}$ Eq(6.24) where $\mathcal{O}(\mathbf{x}) = h_{ij}(\mathbf{x})$, and taking into account the formula of the bispectrum $\mathcal{B}_{\zeta hh}(k_1, k_2, k_3)$ given in eq(6.31):

$$P_h^{mod}(k) = P_h(k)\left[1 + \int \frac{d^3k_l}{(2\pi)^3} e^{-i\mathbf{k_l}\mathbf{x}_+} \; f_{NL}^{\zeta h} \; \frac{\mathcal{B}_{\zeta hh}(k_l, |k - \frac{\mathbf{k_l}}{2}|, |-k + \frac{\mathbf{k_l}}{2}|)}{P_\zeta(k_l) P_h(k)} \zeta(\mathbf{k_l})\right]. \tag{6.38}$$

Let be $\zeta(\mathbf{x}) = \zeta_L \sin(\mathbf{p} \cdot \mathbf{x})$ the super-horizon perturbation, such that $p \ll H_0^{-1}$. Following the same steps made in Sec.4.2 to compute the amplitude of the dipolar modulation in the curvature power spectrum, we find that also the tensor perturbations power spectrum experiences a dipolar modulation, whose amplitude is

$$A^h = 4 \; f_{NL}^{\zeta h} \; p \; x_{dec} \; \zeta_L. \tag{6.39}$$

The modulations in the scalar and tensor power spectrum are related among them. Thanks to Eqs.(4.38) and (6.39) we find that its ratio is

$$\frac{A^h}{A^\zeta} = \frac{f_{NL}^{\zeta h}}{f_{NL}^{\zeta}} = \frac{n_t}{n_s - 1}. \tag{6.40}$$

Notice that the ratio between the two amplitudes is equal to the ratio between the scale dependence of $\mathcal{P}_h(k)$ and $\mathcal{P}_\zeta(k)$. We can exploit the useful relation between r and n_t,

$$r = -8 \; n_t \tag{6.41}$$

which holds under the assumption of a single-field inflation, to give an estimate of the ratio:

$$\left|\frac{A^h}{A^\zeta}\right| = \left|\frac{r}{8(n_s - 1)}\right| \simeq 0.34, \tag{6.42}$$

where, $n_s - 1 \simeq 0.04$ and $r \simeq 0.11$, [66]. This means that a power asymmetry in the curvature field, with amplitude $A^\zeta \simeq 0.07$ generates an asymmetry in the tensor power of amplitude $A \approx 0.02$. So, this amplitude is much smaller than the one required in Eq(6.37).

In conclusion it seems that the super-horizon mode responsible for the HPA cannot generate a dipole amplitude in the tensor power spectrum large enough to explain the difference between r_{Planck} and r_{BICEP}.

6.3.2 Tensor super-horizon perturbation

Since with a super-horizon modulating curvature perturbation we did not obtain any result, we decided to investigate the effects of an eventual super-horizon tensor perturbation which affects the tensor 2-point function of short modes. This situation is more complicated than the case of a scalar modulation, because the presence of tensor modes breaks not only statistical homogeneity, but also statistical isotropy.

In fact, thanks to Eqs. (6.24) and (6.32) we find that the correlation function on short modes is

$$\begin{aligned}\langle h^{s'}(\mathbf{k_2}) h^{s''}(\mathbf{k_3})\rangle &= (2\pi)^3\,\delta^{s's''}\,\delta^3(\mathbf{k_2}+\mathbf{k_3})\;P_h(k_s) \\ &\quad + f^h_{NL}\sum_s \frac{\mathcal{B}_{h^s hh}(\mathbf{k_l}, \mathbf{k_s}+\frac{\mathbf{k_l}}{2}, -\mathbf{k_s}+\frac{\mathbf{k_l}}{2})}{P_h(k_l)}\;h^s(\mathbf{k_l}).\end{aligned} \tag{6.43}$$

Notice the explicit dependence on the direction of $\mathbf{k_s}$ in the term $\epsilon^{s'}_{ij}(\mathbf{k_l})k^i_s\,k^j_s$. The presence of such term generates a modulated tensor power spectrum $P^{mod}_h(\mathbf{k_s}, \mathbf{x}_+)$ which is function of the direction of $\mathbf{k_s}$. The explicit dependence of the modulated power spectrum on $\mathbf{k_s}$ makes $P^{mod}_h(\mathbf{k_s}, \mathbf{x}_+)$ more complicate to handle. In particular, from the explicit computation, we find that if we take a single super-horizon tensor perturbation $h^s(\mathbf{k_l})$ with an anomalous large amplitude, we are no longer able to reproduce the dipolar modulation of the tensor power spectrum across the sky (as we have done in Sec. 4.2 for scalar perturbations). This happens because, now, the super-horizon mode acts in different way for $\mathbf{k_s}$ that have different directions. Therefore, we conclude that, the procedure followed in Sec.4.2 applied in this case does not produces the requested dipolar asymmetry.

Fortunately, we discussed other mechanism which can generate a modulation of the perturbations across the sky. In fact, the idea of Ref. [73], studied in detail in Sec. 4.3 could generate a modulation also in the tensor perturbations power spectrum. Indeed, the power spectrum (6.43) satisfies the hypotheses required in [73], namely a bispectrum that peaks in the squeezed limit and that consists in a non trivial function of $\mathbf{k_l}\cdot\mathbf{k_s}$. [10]. Therefore, such a procedure could explain the modulation invoked in [17] to reconcile the BICEP2 and *Planck* results.

[10] We stress that with non-trivial function of $\mathbf{k_l}\cdot\mathbf{k_s}$ we mean a bispectrum of the type $\mathcal{B} \approx \sum_{i=0}^{\infty} b_n(\mathbf{k_l}\cdot\mathbf{k_s})^n$, with at least one $b_n \neq 0$, with $n \neq 0$.. In this case the non-trivial function is contained in the term $\epsilon^s_{ij}(\mathbf{k_L})\,\frac{k^i_s k^j_s}{k^2_s}$.

Chapter 7

Summary and Conclusions

The ΛCDM model explains with very impressive success the state and the evolution of our Universe, from early times (after the first seconds) until today. Several predictions of this models, about the abundances of the light elements, the expansion of the Universe, the CMB radiation are in very good agreement with observations. However to reproduce the observable Universe one has to set the initial conditions (i.e. initial primordial density perturbations) and the model by itself does not explain their origin. Even if the ΛCDM model is the fundamental building block upon modern cosmology is based on, it presents some open problems that cannot be explained in the context of the Hot-Big-Bang model (such as the horizon, the flatness and the magnetic monopoles problems).

An inflationary phase occurring at very early times (much before primordial nucleosynthesis) namely an epoch of quasi exponential accelerated expansion of the Universe, provides a wonderful solution to open problems of the Hot-Big-Bang model, moreover inflation gives a fine justification of the cosmological principle. After inflation, indeed, the Universe is naturally smoothed and flat. But the successes of inflation does not stop here: it explains also in a compelling way the production of the first density perturbations in the early Universe which are the seeds for the LSS in the distribution of galaxies and the underlying dark matter and for the CMB temperature anisotropies that we observe today. For these reasons inflation has become the dominant paradigm to understand the initial conditions of the early Universe and it is nowadays a crucial ingredient of the standard cosmological model, the so called Inflation+ΛCDM model.

Despite of its successes, recently, some features that show an anomalous behaviour in the CMB temperature fluctuations were found by the WMAP satellite [11], [12] (some of them were also confirmed by *Planck*, [67]). These features seem in conflict with the standard cosmological model. We focused our attention on one of the most important anomalies, the so called *Hemispherical Power Asymmetry* (HPA). Such asymmetry consists in a different amplitude of the CMB temperature fluctuations between two opposite hemi-

spheres. As a result, HPA seems in conflict with the assumptions of statistical isotropy and homogeneity implied by the cosmological principle, and in turn, HPA shows some tension with the most simple models of inflation. For this reason, in this thesis we investigated some of the theoretical problems implied by this asymmetry, searching some possible ways which could reconcile such anomaly with the inflationary paradigm.

Starting from some results already presented in the literature, [25], [73], we developed a sort of phenomenological model in which the asymmetry is due to a super-horizon curvature perturbations field $\zeta(\mathbf{x})$ during inflation. Thanks to primordial non-Gaussianity, the super-horizon fluctuation couples with the perturbations modes inside the observable sky causing a sort of modulation of the latter. Therefore this model assumes that the Universe consists in a "box" much bigger than our observable region, in this way, isotropy and homogeneity are recovered in the entire box, while inside our observable region, we experience a biased statistics. In this context there are two possibilities to obtain an asymmetry in the sky through a super-horizon fluctuation mode:

i. a single super-horizon curvature perturbation mode associated to an anomalous large amplitude fluctuation can generate mainly a dipolar asymmetry in the CMB temperature fluctuations [25]. The presence of the super-horizon mode breaks explicitly statistical homogeneity, while isotropy is still valid;

ii. super-horizon fluctuations that do not need to have very large amplitude might generate a modulation across the sky if the bispectrum of the primordial fluctuations peaks in the squeezed limit and if it is a non trivial function of $\mathbf{k_s} \cdot \mathbf{k_l}$, the scalar product between, respectively the sub- and the super-horizon wavelength perturbation modes [73]. Notice that a bispectrum with these properties breaks statistical isotropy, while homogeneity at leading order is still valid.

After this phenomenological description, we applied the developed ideas and formalism to some simple models of inflation. First of all we focused on the simplest model of inflation (a single scalar field slow-rolling along its potential), checking that a super-horizon perturbation cannot generate a dipolar asymmetry consistent with the upper bounds on the octupole CMB moment [27]. Then, we turned our attention to the *curvaton* model, a 2-fields inflationary theory. We checked that a scale invariant power asymmetry can be generated and therefore this theory might be a candidate to explain the origin of HPA. In the context of the curvaton model we described also a toy model studied in [28] that explains in a successful way the peculiar scale dependence of the observed HPA. In [28], the scale dependence is due to the fact that together with the adiabatic curvature perturbations are generated also isocurvature ones that survived until today. In this toy model part of the

asymmetry is contained in the isocurvature perturbations, whose peculiarity is that once they re-enter the horizon, during radiation and matter dominated epochs, they start to decay. In this way the asymmetry is naturally dropped at small scales, in agreement with observations.

Finally, in the last Chapter, we tried to extend our formalism also to tensor perturbations (gravitational waves) that are inevitably generated during inflation. We showed that, in all generality, both super-horizon scalar and tensor perturbation modes can affect the sub-horizon, and hence observable, statistics of both scalar and tensor perturbations. We used this fact to obtain some consistency relations between scalar and tensor modes that hold for any model of inflation driven by a single scalar field, and hence that could be used in the next future to confirm or rule out different inflationary theories. Then, inspired from [17], we tried to alleviate the tension between the two measurement of the tensor-to-scalar-ratio r made by *Planck* and BICEP2 that seem in conflict among themselves. To alleviate such tension we assumed a modulation of the tensor power spectrum across the sky, so also the value of r experiences the same modulation. This could be realized in two ways: a scalar or a tensor super-horizon modulating field. In the first case in [2] has been shown that a scalar super-horizon perturbation cannot generate a dipole modulation in the tensor power spectrum large enough to resolve the tension that respects also the observational bounds. Fortunately, we found that also a super-horizon tensor perturbation mode could gives rise to a modulation in the tensor power spectrum (that is more general of a dipole modulation). At present, there are no experimental constraints on such type of modulation. The *Planck* satellite will soon provide some constraints on the level of non-Gaussianity in the tensor perturbations. Therefore we think that these latter models (and also the various consistency relations discussed in this thesis) are worth to be investigate further.

Appendix A

Spectral indexes in the Inflaton Model

In this Apendix we explicitly compute the expression for the spectral scalar and tensor indexes in the context of the Inflaton model.

Scalar Spectral index $(n_s - 1)$ The scalar spectral index is defined as

$$n_s - 1 = \frac{d \ln \mathcal{P}_\zeta(k)}{d \ln k}. \tag{A.1}$$

To compute it we rewrite $d \ln k$ in a different way, exploiting the definition of the number of e-folding N_k (1.9):

$$N_k = \int_{t_I}^{t_k} H dt = \ln \left(\frac{a(t_I)}{a(t_k)} \right), \tag{A.2}$$

Where t_I is the time in which inflation begone while t_k is the time at which the scale k left the horizon. Remembering that at this time holds the relation $a(t_k)k = H_k$ we rewrite the above expression as

$$N_k = \ln \left(\frac{a(t_I H_k)}{k} \right), \tag{A.3}$$

and hence, since the Hubble rate, during inflation, is almost constant we can fix H_k at the value H_I approximation $H_k = H_I = const.$. Then differentiating Eqs (A.2) and (A.3) we get

$$d \ln k = H dt, \tag{A.4}$$

which implies

$$n_s - 1 \frac{d \ln \mathcal{P}_\zeta(k)}{H dt}. \tag{A.5}$$

The explicit expression of $\mathcal{P}_\zeta(k)$ is given in Eq(2.68); differentiating it with respect the time we get

$$\begin{aligned} n_s - 1 &= 2\frac{H^2}{\dot\varphi}\ \frac{2H\dot H\dot\varphi - h^2\ddot\varphi}{\dot\varphi^2}\ \frac{1}{H}\ \frac{\dot\varphi^2}{H^4} = \\ &= 4\frac{\dot H}{H^2} - \frac{\ddot\varphi}{H\dot\varphi} = \\ &= -4\epsilon + 2\eta - 2\epsilon = \\ &= -6\epsilon + 2\eta. \end{aligned} \tag{A.6}$$

Tensor Spectral index $(n_s - 1)$ The tensor spectral index can be calculated following the same steps of the previous calculation. Thanks to Eqs(A.4) and (2.96) we find,

$$\begin{aligned} n_t &= \frac{d\ln\mathcal{P}_h(k)}{Hdt} = \\ &= \frac{2\ H\ \dot H}{H^2}\ \frac{1}{H} = \\ &= 2\frac{\dot H}{H^2} = \\ &= -2\epsilon. \end{aligned} \tag{A.7}$$

Appendix B

Explicit calculations

In this appendix we show explicitly some calculation made in Chap.4.

B.1 Dipolar modulation in the spherical harmonics expansion

We start expanding in spherical harmonics the modulated temperature anisotropies field (4.1). For an isotropic field we have

$$\theta_{lm} = \int d\Omega_{\mathbf{n}}\ \theta(\hat{\mathbf{n}})\ Y^*_{lm}(\hat{\mathbf{n}}). \tag{B.1}$$

Then, for a generic field in the form

$$\theta(\hat{\mathbf{n}}) = \theta^{iso}(\hat{\mathbf{n}})[1 + f(\hat{\mathbf{n}})], \tag{B.2}$$

where $\langle \theta_{lm}\theta^*_{l'm'}\rangle = \delta_{l\,l'}\delta_{mm'}C_l$ we get

$$\theta(\hat{\mathbf{n}}) = \theta^{iso}_{lm} + \sum_{LM\ l'm'} \theta^{iso}_{l'm'}\ f_{LM} \int d\Omega_{\mathbf{n}}\ Y^*_{lm}(\hat{\mathbf{n}})\ Y_{l'm'}(\hat{\mathbf{n}})\ Y_{LM}(\hat{\mathbf{n}}). \tag{B.3}$$

Then, at first order in f_{lm} the covariance is

$$\begin{aligned}\langle \theta_{lm}\theta^*_{l'm'}\rangle &= \delta_{l\,l'}\delta_{mm'}C_l + \sum_{LM} f_{LM}[C_l + C_{l'}] \int d\Omega_{\mathbf{n}}\ Y^*_{lm}(\hat{\mathbf{n}})\ Y_{l'm'}(\hat{\mathbf{n}})\ Y_{LM}(\hat{\mathbf{n}}). \\ &= \delta_{l\,l'}\delta_{mm'}C_l + \sum_{LM} f_{LM}\ [C_l + C_{l'}]\ \mathcal{G}^{l\,l'\,L}_{-mm'M}. \end{aligned} \tag{B.4}$$

The symbol $\mathcal{G}^{l\,l'\,L}_{-mm'M}$ represent the integral over three spherical harmonics. Its explicit expression in term of the Wigner 3-j symbols is

$$\mathcal{G}^{l\,l'\,L}_{-mm'M} = (-1)^m \sqrt{\frac{(2l+1)(2l'+1)(2L+1)}{4\pi}} \begin{pmatrix} l & l' & L \\ 0 & 0 & 0 \end{pmatrix} \begin{pmatrix} l & l' & L \\ -m & m' & M \end{pmatrix}. \tag{B.5}$$

The 3-j symbols entail that $\mathcal{G}^{l\,l'\,L}_{-mm'M}$ if $l + l' + L$ is even, $m' - m + M = 0$ and that $|l - l' \leq L \leq l + l'$.

If we assume the modulated field (4.1), then f_{LM} is non vanish only if $L = 1$, then eq(B.4) rewrites as

$$\langle \theta_{lm} \theta^*_{l'm'} \rangle = \delta_{ll'} \delta_{mm'} C_l + \sum_{M=-1}^{1} f_{1M} \, [C_l + C_{l'}] \, \mathcal{G}^{ll'1}_{-mm'1}, \tag{B.6}$$

where the f_{1M} coefficients are the spherical expansion of the term $A\hat{\mathbf{p}} \cdot \hat{\mathbf{n}}$.

B.2 Explicit calculation of $P_\zeta^{mod}(k)$

In presence of a background super-horizon perturbation $\zeta(\mathbf{k_l})$, the 2-point correlation function change. Its expression in Fourier space is (4.21). Its inverse Fourier transform gives the correlation function in real space

$$\langle \zeta(\mathbf{x})_2 \zeta(\mathbf{x})_3 \rangle_B = \int \frac{d^3k_2}{(2\pi)^3} \frac{d^3k_3}{(2\pi)^3} e^{i(\mathbf{k_2 x_2} + \mathbf{k_3 x_3})} \langle \zeta(\mathbf{k_2}) \zeta(\mathbf{k_3}) \rangle_B. \tag{B.7}$$

The first term of eq(4.21) gives the usual term $\int \frac{d^3k_S}{(2\pi)^3} e^{i\mathbf{k_s x_s}} P_\zeta(k_s)$, where $\mathbf{k_s}$ is a sub-horizon mode and $\mathbf{x_s}$ is defined as $\mathbf{x_s} := \mathbf{x_2} - \mathbf{x_3}$. To compute the second the term proportional to the bispectrum, we change the variables of integration defining $\mathbf{k_l} := \mathbf{k_2} + \mathbf{k_3}$ and $\mathbf{k_s} := (\mathbf{k_2} - \mathbf{k_3})/2$. The Jacobian determinant of the transformation is $|J| = 1$, then the integral reads

$$f_{NL} \int \frac{d^3k_l}{(2\pi)^3} \frac{d^3k_s}{(2\pi)^3} e^{i(\mathbf{k_s x_s} + \mathbf{k_l x_+})} \frac{\mathcal{B}_\zeta(k_l, |\mathbf{k_s} + \frac{\mathbf{k_l}}{2}|, |-\mathbf{k_s} + \frac{\mathbf{k_l}}{2}|)}{P_\zeta(k_l)} \zeta(\mathbf{k_l}), \tag{B.8}$$

where $\mathbf{x_+}$ is the middle point $\mathbf{x_+} := (\mathbf{x_2} + \mathbf{x_3})/2$. In conclusion the modulated correlation function in real space is

$$\begin{aligned} \langle \zeta(\mathbf{x})_2 \zeta(\mathbf{x})_3 \rangle_B \quad = \quad & \int \frac{d^3k_s}{(2\pi)^3} e^{i\mathbf{k_s x_s}} [P_\zeta(k_s) + f_{NL} \\ & \times \int \frac{d^3k_l}{(2\pi)^3} e^{i\mathbf{k_l x_+}} \frac{\mathcal{B}_\zeta(k_l, |\mathbf{k_s} + \frac{\mathbf{k_l}}{2}|, |-\mathbf{k_s} + \frac{\mathbf{k_l}}{2}|)}{P_\zeta(k_l)} \zeta(\mathbf{k_l})]. \end{aligned} \tag{B.9}$$

Remembering the general definition of the modulated power spectrum (4.10), $\langle \zeta(\mathbf{x_2}) \zeta(\mathbf{x_3}) \rangle = \int \frac{d^3k}{(2\pi)^3} e^{i\mathbf{k}(\mathbf{x_2} - \mathbf{x_3})} P_\zeta(k)$, from eq(B.8) we get the modulated power spectrum (4.23).

B.3 Computation of the local bispectrum

Let us assume the local model (4.24) for the curvature field. The Fourier transform of $\zeta(\mathbf{x})$ is

$$\zeta(\mathbf{k}) = \zeta_G(\mathbf{k}) + f_{NL} \int \frac{d^3k'}{(2\pi)^3} \zeta_G(\mathbf{k'}) \zeta_G(\mathbf{k} - \mathbf{k'}). \tag{B.10}$$

Therefore the 3-point correlation function, in Fourier space, is, at first order in f_{NL}

$$\begin{aligned}\langle\zeta(\mathbf{k_1})\zeta(\mathbf{k_2})\zeta(\mathbf{k_3})\rangle &= 2f_{NL}\int\frac{d^3k'}{(2\pi)^3}\left[\langle\zeta(\mathbf{k'})\zeta(\mathbf{k_1}-\mathbf{k'})\zeta(\mathbf{k_2})\zeta(\mathbf{k_3})\rangle + cyclic\right]= \\ &= 2f_{NL}\int\frac{d^3k'}{(2\pi)^3}(2\pi)^6[\delta^3(\mathbf{k'}+\mathbf{k_2})\delta^3(\mathbf{k_1}-\mathbf{k'}+\mathbf{k_3}) \\ &\quad +\delta^3(\mathbf{k'}+\mathbf{k_3})\delta^3(\mathbf{k_1}-\mathbf{k'}+\mathbf{k_2})]P(k_2)P(k_3) + cyclic = \\ &= 4\ f_{NL}(2\pi)^3\delta^3\left(\mathbf{k_1}+\mathbf{k_2}+\mathbf{k_3}\right) \\ &\quad \times\left[P(k_1)P(k_2)+P(k_1)P(k_3)+P(k_2)P(k_3)\right].\end{aligned} \tag{B.11}$$

In conclusion the bispectrum is

$$\mathcal{B}_\zeta(k_1,k_2,k_3) = 2\left[P(k_1)P(k_2)+P(k_1)P(k_3)+P(k_2)P(k_3)\right]+\vartheta(f_{NL}^2). \tag{B.12}$$

Now, from observations we know that the power spectrum peaks in the long scale limit, thus when $k\to 0$. Therefore, in the squeezed limit, when $k_1 \ll k_2, k_3$ we get that $Pa(k_1)P_\zeta(k_2) \sim P_\zeta(k_1)P_\zeta(k_3) \gg P_\zeta(k_2)P_\zeta(k_3)$. Therefore in the squeezed limit the bispectrum becomes

$$\mathcal{B}_\zeta(k_1,k_2,k_3) \approx 4(2\pi)^3P(k_1)P(k_s)+\vartheta\left(f_{NL}^2,(k_l/k)^2\right). \tag{B.13}$$

where again $\mathbf{k_s} = (\mathbf{k_2}-\mathbf{k_3})/2$.

B.4 Modulation in the non-local model

Let us compute now the modulated power spectrum $P_\Phi^{mod}(k_s)$ in the context of a non-local model of non-gaussianity, when the f_{NL} vary with the scale. The most general expression preserving these hypothesises is given by (4.39) where the kernel $W(\mathbf{y},\mathbf{z})$ is a function symmetric in their two arguments. In Fourier space it reads:

$$\widetilde{W}(\mathbf{k_1},\mathbf{k_2}) = \int d^3y\ d^3z\ e^{i(\mathbf{k_2}\mathbf{y}+\mathbf{k_3}\mathbf{z})}\ W(\mathbf{y},\mathbf{z}). \tag{B.14}$$

Because of statistical homogeneity eq(B.14) can be only a function of k_2, k_3, $\mathbf{k_2}\cdot\mathbf{k_3}$. It can thus alternatively be written as a function $\widetilde{W}(k_2,k_3,|\mathbf{k_2}+\mathbf{k_3}|)$ of the magnitude of the third side of the triangle constructed from $\mathbf{k_2}$ and $\mathbf{k_3}$. The Fourier transform of eq(4.39) is give by (4.41). Because of non-gaussianity of $\zeta(\mathbf{x})$, the long wavelength modes couples with short wavelength ones and this introduce a modulation in the power spectrum. We call this bias $\Delta P_\zeta(\mathbf{k_s})$. Therefore the 2-point correlation function is given by

$$\langle\zeta(\mathbf{x_2})\zeta(\mathbf{x_3})\rangle = \int\frac{d^3k_s}{(2\pi)^3}\ e^{-i\mathbf{k_s}(\mathbf{x}-\mathbf{x'})}[P(k_s)+\Delta P(\mathbf{k_s})] \tag{B.15}$$

To compute the modulation $\Delta P(k_s)$, we split the fields $\zeta(\mathbf{x})$ and $\zeta_{G,s}(\mathbf{x})$ into a short and a long wavelength pieces. With long modes we mean the modes such that $k_l < H_0$ and with short the ones such that $k_s \geq H_0$. Therefore eq(4.39) rewrites as

$$\zeta(\mathbf{x}) = \zeta_{G,s}(\mathbf{x}) + \zeta_{G,l}(\mathbf{x}) + f'_{NL} \int d^3y\, d^3z\, W(\mathbf{y},\mathbf{z})[\zeta_{G,s}(\mathbf{x}+\mathbf{y}) + \zeta_{G,l}(\mathbf{x}+\mathbf{y})] \times[\zeta_{G,s}(\mathbf{x}+\mathbf{z}) + \zeta_{G,l}(\mathbf{x}+\mathbf{z})]. \tag{B.16}$$

As usually, we are interested in the non-Gaussian effects on small-scale

$$\zeta_s(\mathbf{x}) = \zeta_{G,s}(\mathbf{x}) + f'_{NL} \int d^3y\, d^3z\, W(\mathbf{y},\mathbf{z})\ [\zeta_{G,l}(\mathbf{x}+\mathbf{y})\zeta_{G,s}(\mathbf{x}+\mathbf{z})] \times[\zeta_{G,s}(\mathbf{x}+\mathbf{y})\zeta_{G,l}(\mathbf{x}+\mathbf{z})]. \tag{B.17}$$

Thus the two-point correlation function is

$$\begin{aligned}\langle\zeta_s(\mathbf{x_2})\zeta_s(\mathbf{x_3})\rangle \;&=\; \langle\zeta_{G,s}(\mathbf{x_2})\zeta_{G,s}(\mathbf{x_3}))\rangle + f'_{NL} \\ &\times \int d^3y\, d^3z\, W(\mathbf{y},\mathbf{z})\,[\langle\zeta_{G,l}(\mathbf{x_2}+\mathbf{y})\zeta_{G,s}(\mathbf{x_2}+\mathbf{z})\zeta_{G,s}(\mathbf{x_3})\rangle \\ &+ \langle\zeta_{G,l}(\mathbf{x_2}+\mathbf{z})\zeta_{G,s}(\mathbf{x_2}+\mathbf{y})\zeta_{G,s}(\mathbf{x_3})\rangle + \text{"}\mathbf{x_2}\leftrightarrow\mathbf{x_3}\text{"}].\end{aligned} \tag{B.18}$$

The brakets "$\langle\ ,\ \rangle$" denotes the operation of average in the Hubble volume. Thus when we make this operation ζ_l does not average. For simplicity we compute only the first term of eq(B.18), the other terms are similar [1].

$$\langle\zeta_{G,l}(\mathbf{x_2}+\mathbf{y}))\zeta_{G,s}(\mathbf{x_2}+\mathbf{z}))\zeta_{G,s}(\mathbf{x'_3}))\rangle = \zeta_{G,l}(\mathbf{x_2}+\mathbf{y})\langle\zeta_{G,s}(\mathbf{x_2}+\mathbf{z})\zeta_{G,s}(\mathbf{x_3})\rangle \tag{B.19}$$

Now we use the fact that $\langle\zeta_{G,s}(\mathbf{x_2})\zeta_{G,s}(\mathbf{x_3})\rangle = \int \frac{d^3k_s}{(2\pi)^3} e^{i\mathbf{k_s}(\mathbf{x_2}-\mathbf{x_3})} P_\zeta(k_s)$ and we write $\zeta_{G,l}(\mathbf{x_2}+\mathbf{y})$ in Fourier space, obtaining

$$\begin{aligned}&\int \frac{d^3k_l}{(2\pi)^3} e^{-i\mathbf{k_l}(\mathbf{x}+\mathbf{y})}\zeta(\mathbf{k_l}) \int \frac{d^3k_s}{(2\pi)^3} e^{-i\mathbf{k_s}(\mathbf{x_2}+\mathbf{z}-\mathbf{x_3})} P_\zeta(k_s) = \\ =\ &\int \frac{d^3k_l}{(2\pi)^3}\frac{d^3k_s}{(2\pi)^3} e^{-i[\mathbf{k_l}(\mathbf{x_2}+\mathbf{y})+\mathbf{k_s}(\mathbf{x_2}+\mathbf{z}-\mathbf{x_3})} P_\zeta(k_s)\zeta(\mathbf{k_l}).\end{aligned} \tag{B.20}$$

[1] Notice that here, with k_s and k_l we mean the integration respectively over the short and long wavelength modes.

We plug this expression and eq(B.14) inside the integral in eq(B.18) getting

$$\begin{aligned}
&\int d^3y\ d^3z\ W(\mathbf{y},\mathbf{z})\ \langle\zeta_{G,l}(\mathbf{x_2}+\mathbf{y}))\zeta_{G,s}(\mathbf{x_2}+\mathbf{z}))\zeta_{G,s}(\mathbf{x_3})\rangle = \\
&= \int\frac{d^3y\,d^3z\,d^3k_l d^3k_s d^3k_1 d^3k_2}{(2\pi)^{12}} e^{-i[\mathbf{k_l}(\mathbf{x_2}+\mathbf{y})+\mathbf{k_s}(\mathbf{x_2}+\mathbf{z}-\mathbf{x_3})+\mathbf{k_1}\mathbf{y}+\mathbf{k_2}\mathbf{z}]} \\
&\qquad\qquad \times\widetilde{W}(\mathbf{k_1},\mathbf{k_2})P_\zeta(k_s)\zeta_{G,l}(\mathbf{k_l}) = \\
&= \int\frac{d^3k_l d^3k_s d^3k_1 d^3k_2}{(2\pi)^6} e^{-i[\mathbf{k_l}\mathbf{x_2}+\mathbf{k_s}(\mathbf{x_2}-\mathbf{x_3})]}\delta^3(\mathbf{k_l}+\mathbf{k_1})\delta^3(\mathbf{k_s}+\mathbf{k_2}) \\
&\qquad\qquad \times\widetilde{W}(\mathbf{k_1},\mathbf{k_2})P_\zeta(k_s)\zeta_{G,l}(\mathbf{k_l}) = \\
&= \int\frac{d^3k_s}{(2\pi)^3}e^{-i\mathbf{k_s}(\mathbf{x_2}-\mathbf{x_3})}\int\frac{d^3k_l}{(2\pi)^3}e^{-i\mathbf{k_l}\mathbf{x_2}}\widetilde{W}(\mathbf{k_l},\mathbf{k_s})P_\zeta(k_s)\zeta_{G,l}(\mathbf{k_l}).
\end{aligned} \tag{B.21}$$

In conclusion, considering all the others terms of eq(B.18) we get

$$\Delta P(k_s) = 4\ f'_{NL}\int\frac{d^3k_l}{(2\pi)^3}e^{-i\frac{\mathbf{k_l}}{2}(\mathbf{x_2}+\mathbf{x_3})}\ \widetilde{W}(\mathbf{k_l},\mathbf{k_s})P_\zeta(k_s)\zeta_{G,l}(\mathbf{k_l}) + \vartheta(f_{NL}^2). \tag{B.22}$$

This result is expressed as function of the kernel $\widetilde{W}$ and of the power spectrum. We want to write it in terms of the bispectrum $\mathcal{B}_\zeta(k_1,k_2,k_3)$.

Computation of the Bispectrum From eq(4.41) one gets:

$$\begin{aligned}
\langle\zeta(\mathbf{k_1})\zeta(\mathbf{k_2})\zeta(\mathbf{k_3})\rangle &= f'_{NL}\int\frac{d^3k_l}{(2\pi)^3}[\widetilde{W}(\mathbf{k_l},\mathbf{k}-\mathbf{k_l})\langle\zeta_G(\mathbf{k_l})\zeta_G(\mathbf{k_1}-\mathbf{k_l}) \\
&\qquad\qquad \times\zeta_G(\mathbf{k_2})\zeta_G(\mathbf{k_3})\rangle + \text{"}cyclic\text{"}] = \\
&= (2\pi)^3 f'_{NL}\int d^3k_l[\widetilde{W}(\mathbf{k_l},\mathbf{k}-\mathbf{k_l})\delta^3(\mathbf{k_l}+\mathbf{k_2})\delta^3(\mathbf{k_1}-\mathbf{k_l}+\mathbf{k_3}) \\
&\qquad\qquad \times P_\zeta(k_l)P_\zeta(|\mathbf{k_1}-\mathbf{k_l}|) + \delta^3(\mathbf{k_l}+\mathbf{k_3})\delta^3(\mathbf{k_1}-\mathbf{k_l}+\mathbf{k_2}) \\
&\qquad\qquad \times P_\zeta(k_l)P_\zeta(|\mathbf{k_1}-\mathbf{k_l}|) + \text{"}cyclic\text{"}] = \\
&\equiv 2(2\pi)^3\ f_{NL}(k_1,k_2,k_3)\delta^3(\mathbf{k_1}+\mathbf{k_2}+\mathbf{k_3}) \\
&\quad \times\left[P_\zeta(k_1)P_\zeta(k_2) + P_\zeta(k_1)P_\zeta(k_3) + P_\zeta(k_2)P_\zeta(k_3)\right].
\end{aligned} \tag{B.23}$$

Finally we find

$$f_{NL}(k_1,k_2,k_3) = f'_{NL}\ \widetilde{W}(k_1,k_2,k_3), \tag{B.24}$$

$$\mathcal{B}_\zeta(k_1,k_2,k_3) = 2\left[P_\zeta(k_1)P_\zeta(k_2) + \text{"}cyclic\text{"}\right]. \tag{B.25}$$

that they reduce in the squeezed limit to

$$f_{NL}(k_l, k_s, k_s) \approx f'_{NL}\, \widetilde{W}(k_l, k_s, k_s), \tag{B.26}$$

$$\mathcal{B}_\zeta(k_l, |k_s + \frac{\mathbf{k_l}}{2}|, |-k_s + \frac{\mathbf{k_l}}{2}|) \approx 4 P_\zeta(k_l) P_\zeta(k_s). \tag{B.27}$$

In conclusion the modulated part of power spectrum (B.22) is

$$\Delta P(k_s) = f'_{NL} \int \frac{d^3k_l}{(2\pi)^3} e^{-i\mathbf{k_l}\mathbf{x}_+} \frac{\mathcal{B}_\zeta(k_l, |k_s + \frac{\mathbf{k_l}}{2}|, |-k_s + \frac{\mathbf{k_l}}{2}|)}{P_\zeta(k_l)} \zeta_{G,l}(\mathbf{k_l}), \tag{B.28}$$

where $\mathbf{x}_+ := (\mathbf{x_2} + \mathbf{x_3})/2$. With this expression the derivation of the diolar amplitude (4.43) due to the single mode (4.34) is straightforward.

B.5 Modulation in spherical harmonics using the method of Sec.4.3

Starting from eq(4.59) we will try to get eq(4.62). As we showed in Chap.3 the multipoles θ_{lm} are related to the Bardeen potential Φ through

$$\theta_{lm} = \int \frac{d^3k}{(2\pi)^3} (-i)^l \Phi(\mathbf{k}) \Delta_l(k) Y^*_{lm}(\hat{\mathbf{k}}). \tag{B.29}$$

Therefore the covariant matrix is

$$\begin{aligned} \langle \theta_{lm} \theta^*_{l'm'} \rangle \;=\; & (4\pi)^2 \int \frac{d^3k}{(2\pi)^3} \frac{d^3k'}{(2\pi)^3} (-i)^{l-l'} \langle \Phi(\mathbf{k}) \Phi(\mathbf{k}') \rangle \Delta_l(k) \Delta^*_{l'}(k') \\ & \times Y^*_{lm}(\hat{\mathbf{k}}) Y_{l'm'}(\hat{\mathbf{k}}'). \end{aligned} \tag{B.30}$$

Now we plug the Taylor expanded power spectrum into the above equation. The first term of eq(4.60) gives the usual term $\delta_{l\,l'} \delta_{mm'} C_l$, while the second term results

$$\begin{aligned} & (4\pi)^2 \int \frac{d^3k}{(2\pi)^3} \frac{d^3k'}{(2\pi)^3} (-i)^{l-l'} \Delta_l(k) \Delta^*_{l'}(k') Y^*_{lm}(\hat{\mathbf{k}}) Y_{l'm'}(\hat{\mathbf{k}}') \\ & \qquad \times (2\pi)^3 \delta(\mathbf{k} - \mathbf{k}') \times \int \frac{d^3k_l}{(2\pi)^3} P_\Phi(k) G(\mathbf{k}, \mathbf{k_l}) \Phi(\mathbf{k_l}) = \\ = \quad & (4\pi)^2 \int \frac{d^3k}{(2\pi)^3} (-i)^{l-l'} \Delta_l(k) \Delta^*_{l'}(k) Y^*_{lm}(\hat{\mathbf{k}}) Y_{l'm'}(\hat{\mathbf{k}}) \\ & \qquad \times \int \frac{d^3k_l}{(2\pi)^3} P_\Phi(k) G(\mathbf{k}, \mathbf{k_l}) \Phi(\mathbf{k_l}). \end{aligned} \tag{B.31}$$

Now we expand the kernel $G(\mathbf{k}, \mathbf{k_l})$ into a sum of spherical harmonics:

$$G(\mathbf{k}, \mathbf{k_l}) = \sum_{LM} G_L(k, k_l) Y^*_{LM}(\hat{\mathbf{k}_l}) Y_{LM}(\hat{\mathbf{k}}), \tag{B.32}$$

and we define the coefficients $\Phi_{LM}(k_l)$ as

$$d\Omega_{\mathbf{k_l}}\Phi(\mathbf{k_l})Y^*_{LM}(\hat{\mathbf{k}}_\mathbf{l}) \equiv \Phi_{LM}(k_l), \tag{B.33}$$

that are the coefficients of the spherical expansion of the super-horizon realization $\Phi(\mathbf{k_l})$. Then Eq(B.30) rewrites as

$$\begin{aligned}
& (4\pi)^2(i)^{l-l'}\int\frac{d^3k}{(2\pi)^3}\frac{d^3k_l}{(2\pi)^3}\sum_{LM}G_L(k,k_l)\Phi(\mathbf{k_l})Y^*_{LM}(\hat{\mathbf{k}}_\mathbf{l})Y^*_{lm}(\hat{\mathbf{k}}) \\
& \qquad\qquad \times Y_{l'm'}(\hat{\mathbf{k}})Y_{LM}(\hat{\mathbf{k}}) = \\
= \quad & (4\pi)^2(i)^{l-l'}\int\frac{d^3k}{(2\pi)^3}dk_l\,k_l^2\sum_{LM}G_L(k,k_l)\Phi_{LM}k_lY^*_{lm}(\hat{\mathbf{k}})Y_{l'm'}(\hat{\mathbf{k}})Y_{LM}(\hat{\mathbf{k}}) = \\
= \quad & \int\frac{k_l^2dk_l}{(2\pi)^2}\sum_{LM}C_{l\,l'}(k_l)\;\Phi_{LM}(k_l)\;\mathcal{G}^{l\,l'\,L}_{-mm'M},
\end{aligned} \tag{B.34}$$

where in last step we integrated over $d\Omega_\mathbf{k}$ obtaining the $\mathcal{G}^{l\,l'\,L}_{-mm'M}$ symbol, and we defined the $C_{l\,l'}$ coefficients as

$$C_{l\,l'}(k_l) = \frac{1}{\pi}\int k^2dk[\Delta_l(k)\Delta^*_{l'}(k)+\Delta^*_l(k)\Delta_{l'}(k)]G_L(k,k_l)P_\Phi(k). \tag{B.35}$$

Appendix C

Dipolar amplitude in the curvaton model

In this appendix we explicitly extends the formalism of Chap.4 to the curvaton model. Our purpose consists in finding an explicit expression for the amplitude of a dipolar modulation across the sky of the field $\theta(\hat{\mathbf{n}})$, due to a super horizon quantum fluctuation $\Delta\sigma$. For sake of simplicity we will a consider the model in which the curvaton decays without generating isocurvature perturbations.

In the same hypotheses made in Sec.5.2, the final curvature perturbations are given by eq(2.79):

$$\zeta \simeq N_\varphi \delta\varphi + N_\sigma \delta\sigma + N_{\sigma\sigma}\delta\sigma^2. \tag{C.1}$$

Notice that we can split the total curvature perturbation ζ in a sum of two terms: the inflaton contribution, $\zeta_{|\,\varphi}$ and the curvatn one, $\zeta_{|\,\sigma}$. Only the latter term has a non-gaussian component, and hence mode coupling can rises only between different Fourier modes $\zeta_{|\,\sigma}(\mathbf{k})$; furthermore the super-horizon fluctuation $\Delta\sigma$ contributes only in $\zeta_{|\,\sigma}$. Taking in mind these facts we recalculate the 2-point correlation function for ζ, in presence of a background super-horizon mode, following the procedure made in Sec.4.1.1. We get:

$$\langle\zeta(\mathbf{x_2})\zeta(\mathbf{x_3})\rangle_B \simeq \langle\zeta\zeta\rangle + \zeta_{|\,\sigma}(\mathbf{x}_+)\frac{d\ \langle\zeta_{|\,\sigma}\,\zeta_{|\,\sigma}\rangle}{d\zeta_B}. \tag{C.2}$$

Notice that in the second term on the right is involved only the curvaton contribute to ζ. However, since the super-horizon ζ_B leaves untouched the inflaton part of ζ we can replace $d\langle\zeta_{|\,\sigma}\zeta_{|\,\sigma}\rangle/d\zeta_B$ with $d\langle\zeta\zeta\rangle/d\zeta_B$. Then eq.(C.2) in Fourier space reads

$$\langle\zeta(\mathbf{k_2})\zeta(\mathbf{k_3})\rangle \simeq (2\pi)^3\ \delta^3(\mathbf{k_2}+\mathbf{k_3})\ P_\zeta(k_s) + 2f_{_{NL}}\ \zeta_{|\,\sigma}(\mathbf{k_l})\ P_\zeta(k_s) \tag{C.3}$$

where $\mathbf{k_2} := (\mathbf{k_2}-\mathbf{k_3})/2$, $\mathbf{k_l} := \mathbf{k_2}+\mathbf{k_3}$ and $P_{\zeta_{|\,\sigma}}(k) = N_\sigma^2\, P_{\delta\sigma}$. Now we compute the bispectrum, adding the Fourier mode $\zeta(\mathbf{k_1})$ and averaging in all the volume:

$$\begin{aligned}\langle\zeta(\mathbf{k_1})\zeta(\mathbf{k_2})\zeta(\mathbf{k_3})\rangle &= \langle\zeta(\mathbf{k_1})\ \langle\zeta\zeta\rangle_B(|\mathbf{k_2}-\mathbf{k_3}|)\ \rangle = \\ &= 2f_{_{NL}}\ \langle\zeta_{|\,\sigma}(\mathbf{k_1})\zeta_{|\,\sigma}(\mathbf{k_l})\rangle\ P_\zeta(k_s) = \\ &= 2f_{_{NL}}\ P_{\zeta_{|\,\sigma}}(k_l)\ P_\zeta(k_s) = \end{aligned} \tag{C.4}$$

Finally plugging the explicit expression of the bispectrum into the 2-point correlation function in Fourier space (C.3), we get an expression similar to to eq(4.21),

$$\begin{aligned}\langle\zeta(\mathbf{k_2})\zeta(\mathbf{k_3})\rangle_B \;\simeq\; & (2\pi)^3\delta^3(\mathbf{k_2}+\mathbf{k_3})P_\zeta(k_s) \\ & -2f_{_{NL}}\frac{\mathcal{B}_\zeta(k_l,|\mathbf{k_s}+\frac{\mathbf{k_l}}{2}|,|-\mathbf{k_s}+\frac{\mathbf{k_l}}{2}|)}{P_{\zeta_{|\,\sigma}}(k_l)}\zeta(\mathbf{k_l}),\end{aligned} \tag{C.5}$$

where we wrote $P_{\zeta_{|\,\sigma}}(k_l)$ in place of $P_\zeta(k_l)$. Now, $P_{\zeta_{|\,\sigma}}(k_l)/P_\zeta(k_l)\equiv\xi$, the fraction of the curvaton contribute to the power spectrum. Following the same steps made in Sec.4.1.1 we then obtain the following modulated power spectrum:

$$P_\zeta^{mod}(\mathbf{k_s},\mathbf{x})\simeq P_\zeta(k_s)-2f_{_{NL}}\int\frac{d^3k_l}{(2\pi)^3}\,e^{i\mathbf{k_l}\mathbf{x}_+}\,\frac{\mathcal{B}_\zeta(k_l,|\mathbf{k_s}+\frac{\mathbf{k_l}}{2}|,|-\mathbf{k_s}+\frac{\mathbf{k_l}}{2}|)}{\xi\;P_\zeta(k_l)}\,\zeta(\mathbf{k_l}). \tag{C.6}$$

This, in turn, lead to a dipolar modulation with amplitude

$$A=4\,\frac{f_{_{NL}}\Delta\zeta}{\xi}, \tag{C.7}$$

where $\Delta\zeta$ is the super-horizon perturbation.

Bibliography

[1] L.F. Abbott, M. B. Wise, Nuclear Physics **B244**, 541-548 (1984).

[2] A. A. Abolhasani, S. Baghram, H. Firouzjahi and M. H. Namjoo, Phys.Rev. **D 89**, 063511 (2014).

[3] V. Acquaviva, N. Bartolo, S. Matarrese and A. Riotto, Nucl. Phys. B **667**, 119 (2003), [astro-ph/0209156].

[4] P.A.R. Ade, et all, Phys. Rev **112** 241101 (2014), ArXiv:1403.3985.

[5] A. J. Albrecht and P. J. Steinhardt, Phys. Rev. Lett. **48**, 1220 (1982).

[6] B. Audren, D. G. Figueroa and T. Tram, arXiv:1405.1390 [astro-ph.CO].

[7] J. M. Bardeen, Phys. Rev. D **22**, 1882 (1980).

[8] N. Bartolo and A. R. Liddle, Phys.Rev. **D65**, 121301 (2002), arXiv:astro-ph/0203076.

[9] N. Bartolo, S. Matarrese and A. Riotto Phys.Rev. **D69**, 043503 (2003), arXiv:hep-ph/0309033.

[10] N. Bartolo, E. Komatsu, S. Matarrese and A. Riotto, Phys.Rept. **402**, 103 (2004), arXiv:0406398 [astro-ph].

[11] C. L. Bennett et all, Astrophys.J.Suppl. **192**, 17 (2011), arXiv:1001.4758v2 [astro-ph.CO].

[12] C. L. Bennett et all, Astrophys.J.Suppl. **208**, 20 (2013), arXiv:1212.5225v3 [astro-ph.CO].

[13] J. Bramante, J. Kumar,E. Nelson and S. Shandera JCAP **1311**, 021 (2013), arXiv:1307.5083.

[14] M. Bruni, S. Matarrese, S. Mollerach and S. Sonego, Class.Quant.Grav. **14**, 2585 (1997), arXiv:gr-qc/9609040v2.

[15] X. Chen, Adv.Astron. **2010**, 638979 (2010), arXiv:1002.1416v3 [astro-ph].

[16] C. Cheung, A. L. Fitzpatrick, J. Kaplan and L. Senatore, *On the consistency relation of the 3-point function in single field inflation* JCAP **0802**, 21(2008), arXiv:0709.0295v2.

[17] J. Chluba, L. Dai, D. Jeong, M. Kamionkowski and A. Yoho, *Linking the BICEP2 result and the hemispherical power asymmetry through spatial variation of r*, (2014), arXiv:1404.2798.

[18] C. R. Contaldi, M. Peloso, L. Sorbo JCAP **1407**, 014 (2014), arXiv: 1403.4596

[19] E. J. Copeland, M. Sami and S. Tsujikawa, Int. J. Mod. Phys. **D 15**, 1753 (2006) [hep-th/0603057].

[20] P.Creminelli, JCAP **0310**, 003 (2003), arXiv:astro-ph/0306122.

[21] P. Creminelli, G. D'Amico, M. Musso, Jorge Noreña, JCAP **1111**, 038 (2011), arXiv:1106.1462v2.

[22] G. D'Amico, R. Gobbetti, M. Kleban and M. Schillo JCAP **1311**, 013 (2013), arXiv:1306.6872 [astro-ph.CO].

[23] L. Dai, D. Jeong, M. Kamionkowski and J. Chluba, Phys.Rev. **D87**, 123005 (2013), arXiv: 1303.6949v1 [astro-ph.CO].

[24] S. Dodelson, *Modern Cosmology*, Academic Press (2003).

[25] C. Dvorkin, H. V. Peiris and W. Hu Phys.Rev. **D77**, 063008 (2008), arXiv:0711.2321v2.

[26] G. Efstathiou, Mon. Not. Roy. Astron. Soc. **348**, 885 (2004) [arXiv:astro-ph/0310207].

[27] A. L. Erickcek, M. Kamionkowski, and S. M. Carroll, Phys.Rev. **D78**, 123520 (2008), arXiv:0806.0377v3.

[28] A. L. Erickcek, M. Hirata and M. Kamionkowski, Phys.Rev. **D80**, 083507 (2009), arXiv:0907/0705

[29] H. Firouzjahi, J. -O. Gong and M. H. Namjoo, arXiv:1405.0159 [astro-ph.CO].

[30] C. Gordon, W. Hu, D. Huterer, and T. Crawford, Phys.Rev.**D**, 72, (2005), arXiv:astro-ph/0509301.

[31] A. Guth, Phys. Rev. **D 23**, 347 (1981).

[32] D. Hanson and A. Lewis, Phys.Rev. **D80**, 063004 (2012), arXiv:0908.0963.

[33] S. W. Hawking, Phys. Lett. **B 115** 295 (1982).

[34] C. M. Hirata, JCAP **0909**, 011 (2009), arXiv:0907.0703, [astro-ph.CO].

[35] H. M. Hodges, G. R. Blumenthal, L. A. Kofman and J. R. Primack, Nucl. Phys. **B 335**, 197 (1990).

[36] W. T.Hu, *Wandering in the Background: A CMB Explorer* (1995), arXiv:astro-ph/9508126.

[37] W. Hu, S. Dodelson, Ann.Rev.Astron.Astrophys **40**, 171 (2002), arXiv:0110414 [astro-ph].

[38] M. Kamionkowski, L. Dai and D. Jeong, Phys.Rev. **D 89**, 107302 (2014) arXiv:1404.3730.

[39] S. Kanno, M. Sasaki and T. Tanaka PTEP **11**, 111E01 2013 arXiv:1309.1350 [atro-ph].

[40] H. Kodama and M. Sasaki, Prog. Theor. Phys. Suppl. **78**, 1 (1984).

[41] L.A. Kofman, G. R. Blumenthal, H. Hodges and J. R. Primack, *Large-Scale Structures and Peculiar Motions in the Universe*, ASP Conference Series, Vol. **15**, D. W. Latham and L. N. daCosta, Eds., p. 339 (1991).

[42] E. W. Kolb and M. S. Turner, *The Early Universe*, Addison-Wesley Publishing Company (1990).

[43] S.Kundu, JCAP **1404**, 016 (2014), arXiv:1311.1575.

[44] M. Liguori, E. Sefusatti, J.R. Fergusson and E.P.S. Shellard, Adv.Astron. **2010**, 980523 (2010), arXiv:1001.4707.

[45] A. D. Linde, Phys. Lett. **B 108**, 389 (1982).

[46] A. Linde and V. Mukhanov, Phys.Rev. **D56**, 535 (1997), arXiv:astro-ph/9610219v2.

[47] D. H. Lyth and D. Wands, Phys.Lett. **B524**, 5 (2002), arXiv:hep-ph/0110002.

[48] D. H. Lyth, C. Ungarelli and D. Wands, Phys.Rev. **D67**, 023503 (2002), arXiv:astro-ph/0208055.

[49] D. Lyth and Y. Rodriguez, Phys.Rev.Lett. **95**, 121302 (2005), arXiv:astro-ph/0504045.

[50] D. H. Lyth JCAP **0606**, 015 (2006), arXiv:astro-ph/0602285.

[51] D. Lyth and A. Liddle, *The primordial density perturbation*, Cambridge (2009).

[52] D. H. Lyth, JCAP **1308** 007 (2013), arXiv:1304.1270v5.

[53] D. H. Lyth, *Generating* f_{NL} *at* $l \lesssim 60$, (2014), arXiv:1405.3562

[54] C. P. Ma and E. Bertschinger, Astrophysical Journal **455**, 7 (1995).

[55] J. Maldacena, JHEP **5**, 13 (2003) arXiv:0210603 [astro-ph].

[56] K. A. Malik and D. Wands, JCAP **0502**, 007 (2005), arXiv:astro-ph/0411703v2.

[57] K. A. Malik and D. Wands, Phys.Rept. **475**, 1 (2009), arXiv:0809.4944v2 [astro-ph].

[58] S. Matarrese, S. Mollerach and M. Bruni, Phys.Rev. **D58**, 043504 (1998), arXiv:astro-ph/9707278v2.

[59] Mather et all, Astrophys.J. **354**, L37 (1990).

[60] Mollerach, Phys.Rev. **D42**, 313 (1990)

[61] V. F. Mukhanov and G. V. Chibisov, JETP Lett. **33** 532 (1981).

[62] M. H. Namjoo, S. Baghram and H. Firouzjahi,Phys.Rev. **D88**, 083527 (2013), arXiv:1305.0813v2 [astro-ph].

[63] M. H. Namjoo, A. A. Abolhasani, S Baghram and H. Firouzjahi, JCAP **1408**, 002 (2014), ArXiv:1405.7317.

[64] E. Nelson and S. Shandera, Phys.Rev.Lett. **13**, 131301 (2013), arXiv:1212.4550.

[65] Planck Collaboration,*Planck 2013 results. I. Overview of products and scientific results*, arXiv:1303.5062 [astro-ph.CO].

[66] Planck collaboration, *Planck 2013 results. XXII. Constraints on inflation* (2013), arXiv:1303.5082v2 [astro-ph.CO].

[67] Planck collaboration, *Planck 2013 results. XXIII. Isotropy and statistics of the CMB* (2014), arXiv:1303.5083v3 [astro-ph.CO].

[68] Planck collaboration, *Planck 2013 results. XXIV. Constraints on primordial non-Gaussianity* (2013), arXiv:1303.5084 [astro-ph.CO].

[69] Planck collaboration, *Planck 2013 results. XVI. Cosmological parameters* (2013), arXiv:1303.5076v3 [astro-ph.CO].

[70] T. Falk, R. Rangarajan and M. Srednicki, Astrophys. J. **403** (1993) L1.

[71] D. S. Salopek, J. R. Bond, Phys.Rev. **D42**, 3936 (1990).

[72] F. Schmidt and M. Kamionkowski, Phys.Rev. **D82**, 103002 (2012), arXiv:1008.0638.

[73] F. Schmidt and L. Hui, Phys.Rev.Lett. **110**, 011301 (2012), arXiv:1210.2965

[74] R. Scoccimarro, L. Hui M. Manera and K. C. Chan, Phys.Rev. **D85**, 083002 (2012), arXiv:1108.5512.

[75] D. Scott and G. F. Smoot, Physics Letters, B.**592**, 1 (2004).

[76] M. S. Turner and L.M. Widrow, Phys. Rev. **D37**, 2743 (1988).